HHS Public Access

Author manuscript

J Med Chem. Author manuscript; available in PMC 2023 October 27.

Published in final edited form as:

J Med Chem. 2022 October 27; 65(20): 14144–14179. doi:10.1021/acs.jmedchem.2c01349.

Structure–Uptake Relationship Studies of Oxazolidinones in Gram-Negative ESKAPE Pathogens

Ziwei Hu[‖],
Department of Medicinal Chemistry, College of Pharmacy, University of Minnesota, Minneapolis, Minnesota 55414, United States

Inga V. Leus[‖],
Department of Chemistry & Biochemistry, University of Oklahoma, Stephenson Life Sciences Research Center, Norman, Oklahoma 73019, United States

Brinda Chandar[‖],
Department of Chemistry & Biochemistry, University of Oklahoma, Stephenson Life Sciences Research Center, Norman, Oklahoma 73019, United States

Bradley S. Sherborne,
Merck & Co., Inc., Rahway, New Jersey 07065, United States

Quentin P. Avila,
Department of Chemistry & Biochemistry, University of Oklahoma, Stephenson Life Sciences Research Center, Norman, Oklahoma 73019, United States

Valentin V. Rybenkov,
Department of Chemistry & Biochemistry, University of Oklahoma, Stephenson Life Sciences Research Center, Norman, Oklahoma 73019, United States

Helen I. Zgurskaya,
Department of Chemistry & Biochemistry, University of Oklahoma, Stephenson Life Sciences Research Center, Norman, Oklahoma 73019, United States

Corresponding Authors: **Helen I. Zgurskaya** – *Department of Chemistry & Biochemistry, University of Oklahoma, Stephenson Life Sciences Research Center, Norman, Oklahoma 73019, United States*; Phone: (405) 325–1678; elenaz@ou.edu; **Adam S. Duerfeldt** – *Department of Medicinal Chemistry, College of Pharmacy, University of Minnesota, Minneapolis, Minnesota 55414, United States*; Phone: (612) 624–6184; aduerfel@umn.edu.

[‖]Author Contributions

Z.H., I.V.L., and B.C. contributed equally. All authors contributed to the writing of the manuscript and have approved its content. Z.H. and Q.P.A. designed, synthesized, purified, and characterized all analogues. I.V.L. and B.C. measured antibacterial activities. V.V.R. carried out the PCA analysis. H.I.Z. designed and supervised the microbiological studies and antibacterial analyses. A.S.D. provided the design and synthetic insight into the library development and analogue synthesis. A.S.D., H.I.Z., and V.V.R. interpreted structure–activity and structure–uptake relationships.

Supporting Information

The Supporting Information is available free of charge at https://pubs.acs.org/doi/10.1021/acs.jmedchem.2c01349.

Table with PC decomposition, MIC values, ratio tables for each species, and comparative activity tables (XLSX)

Library design approach, representative HPLC traces, H^1 and C^{13} NMR spectra for final compounds, bacterial strains, table with PC decomposition, MIC values, ratio tables for each species, comparative activity tables, and molecular formula strings (PDF)

Molecular formula strings (CSV)

Complete contact information is available at: https://pubs.acs.org/10.1021/acs.jmedchem.2c01349

The authors declare no competing financial interest.

Adam S. Duerfeldt
Department of Medicinal Chemistry, College of Pharmacy, University of Minnesota, Minneapolis, Minnesota 55414, United States

Abstract

The clinical success of linezolid for treating Grampositive infections paired with the high conservation of bacterial ribosomes predicts that if oxazolidinones were engineered to accumulate in Gram-negative bacteria, then this pharmacological class would find broad utility in eradicating infections. Here, we report an investigative study of a strategically designed library of oxazolidinones to determine the effects of molecular structure on accumulation and biological activity. *Escherichia coli, Acinetobacter baumannii*, and *Pseudomonas aeruginosa* strains with varying degrees of compromise (in efflux and outer membrane) were used to identify motifs that hinder permeation across the outer membrane and/or enhance efflux susceptibility broadly and specifically between species. The results illustrate that small changes in molecular structure are enough to overcome the efflux and/or permeation issues of this scaffold. Three oxazolidinone analogues (**3e**, **8d**, and **8o**) were identified that exhibit activity against all three pathogens assessed, a biological profile not observed for linezolid.

Graphical Abstract

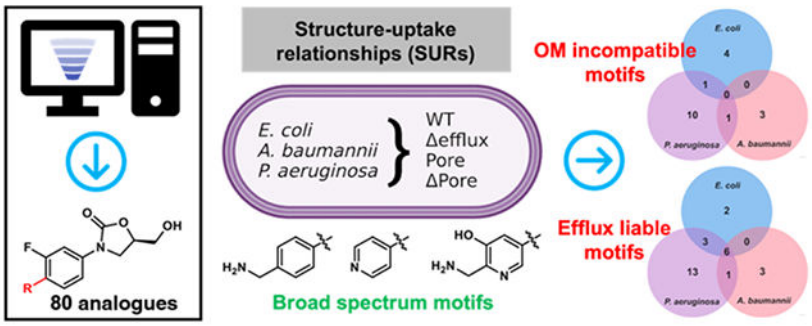

INTRODUCTION

The emergence and widespread prevalence of multidrug-resistant (MDR) bacteria pose a great threat to society.[1,2] A 2019 report from the Centers for Disease Control and Prevention estimates that >2.8 million MDR infections occur annually in the United States, giving rise to >35,000 deaths.[3] MDR Gram-negative bacteria (GNB) have been pinpointed as the most urgent threats.[1,4,5] In fact, four (*Klebsiella pneumoniae, Acinetobacter baumannii, Pseudomonas aeruginosa*, and *Enterobacter spp.*) of the six leading contributors to hospital-acquired infections are GNB.[6]

It is well established that the encapsulation of the hydrophobic inner membrane by an asymmetric outer membrane (OM) presents a formidable barrier to small-molecule permeation in GNB. Molecules must either be amphipathic enough to permeate these antithetic membranes or capitalize on porin-mediated entry. Additionally, after a compound successfully crosses the outer or both membranes, it is subject to highly promiscuous efflux

pumps.[7,8] As a result, while potent biochemical inhibitors can often be identified for new targets, developing them into compounds with whole-cell antibacterial activity has proven challenging.[9–11]

Two approaches are typically taken to enhance the accumulation of molecules in GNB: (1) cotreatment with OM permeabilizing agents or (2) strategic structural modification. Sensitization of the OM upon cotreatment with permeabilizing agents (e.g., polymyxin B nonapeptide (PMBN)) provides a workaround for OM permeation issues.[12] Unfortunately, these permeabilization agents fail to address efflux issues and have demonstrated dose-limiting toxicities in the clinic. However, new PMBN analogues (e.g., NAB7061, SPR741/NAB741)[12] and permeabilizing chemotypes (e.g., tridecaptin A_1, teixobactin)[13,14] continue to provide inspiration for interrogating this strategy to broaden the spectrum of select agents. The second and more direct approach to improving compound accumulation is to rationally engineer the antibacterial molecule itself to render it capable of membrane penetration and efflux avoidance. Our poor understanding, however, of the structural features that correlate with small-molecule GNB permeation and accumulation persists as a major roadblock to this approach.

Retrospective efforts to summarize the physicochemical properties that coincide with Gram-negative activity[9,11,15] have inspired initial efforts to enhance Gram-negative compatibility of compounds in a more prospective manner. In fact, predictive models for chemical modification to impart activity against *Escherichia coli* through porin-mediated interactions have been achieved[16,17] and employed for diverse chemotypes.[18–26] For the deoxynybomycins and Debio-1452 series, lessons learned from *E. coli* have even proven useful in gaining antibacterial activity against *A. baumannii* and *K. pneumoniae*.[17,26] However, although the basic envelope composition is relatively conserved across GNB, significant variation exists between species and strains,[27] which often limits the generalization and extension of physicochemical predictors determined for *E. coli* permeation to other pathogens. As such, it is crucial to analyze compound behavior across not only species but also strains to gain insight into generally applicable “rules” versus those that are more organism-specific for each chemotype.

While novel antibacterial scaffolds are desperately needed, critical information remains to be learned from well-interrogated compound families, as the technology now exists to deconvolute permeation and efflux liabilities that lacked during the original period of chemotype development. Oxazolidinones, for example, were rationally developed in the 1990s as a new class of synthetic antibiotics that exert their activity by binding to the 23S rRNA of the 50S ribosomal subunit and inhibiting the initiation step of bacterial protein synthesis.[28] The clinical success of linezolid (LZD; Figure 1), yet susceptibility to resistance, has inspired pharmaceutical companies and academic groups to develop next-generation oxazolidinones.[29–31] Thus far, studies have focused mainly on overcoming target-driven LZD resistance,[32–34] exploring the utility in infections of the central nervous system,[35] and reducing toxic side effects.[36] However, the potential of this chemotype for broad-spectrum activity has been underexplored due to the Gram-positive specific activity and inability, thus far, to rationally design GNB-active derivatives.[37–40] High conservation of bacterial ribosomes, however, predicts that if oxazolidinones were engineered to accumulate

in GNB, then this pharmacological class would find great utility in eradicating infections.[40] These reasons, paired with the knowledge that the biological activity of this chemotype can be maintained through broad C-ring diversification (Figure 1), establish the oxazolidinones as a seminal class to interrogate the effect of motif variation on GNB accumulation.

To expand the understanding of how specific motifs influence GNB accumulation and efflux susceptibility, we report the design, synthesis, and evaluation of oxazolidinones distinctly functionalized at the C-ring. Activity against wild-type *E. coli*, *P. aeruginosa*, and *A. baumannii*, and corresponding strains with varying degrees of the outer membrane and/or efflux pump efficiencies, was employed to allow for the deconvolution of structure–activity and structure–uptake relationships (SAR and SURs). Assessment in a ribosomal translation inhibition assay and against *Staphylococcus aureus* and LZD-resistant *E. coli* was used to verify the on-target activity of representative analogues. Motifs that prove problematic to OM permeation and/or efflux for each species were revealed. Three LZD analogues were identified that exhibit broad-spectrum activity against all three Gram-negative pathogens.

RESULTS AND DISCUSSION

Molecular Design.

An oxazolidinone A-ring containing an (*S*) C-5 methylene-linked acetamide and an *N*-aryl substituent (B-ring) comprises the bulk of the scaffold required for target engagement (Figure 1). A third ring system (C-ring) is appended to the para-position of the B-ring. Previous studies clearly demonstrate that the C-ring is the most amenable to modification and that the C-5 acetamide can be replaced with a more synthetically tractable hydroxyl group (Figure 1).[41] As such, we aimed to design a library capable of leveraging known chemistry to provide common intermediates that could be exposed to reactants exhibiting diverse physicochemical attributes.

The design of the library was dictated by four factors: (1) the chemistry accessible from key synthetic intermediates, (2) reactant availability, (3) reagent compatibility with other libraries of interest, and (4) clustering-driven reagent selection. To begin the library design (Figure S1), we decided to use a single vendor, Enamine, which maintains a catalog of ~210 million building blocks. To narrow the focus, the catalog was filtered to provide building blocks with ≥250 mg of availability. These building blocks were then classified based on the molecular functionality present (e.g., amines, boronates, carboxylic acids, acid chlorides, alkyl halides, etc.), helping to identify available chemistries. Within these classifications, reagents with heavy atom counts ≥15 were removed to provide an inclusive list of reagents available for library generation. Because the targeted key intermediates (**2a**, **6**, and **7**; Scheme 1) used to synthesize the library congeners would be an aryl halide (or boronic acid/ester), we settled on Suzuki–Miyaura- and Sonogashira–Hagihara-compatible reactants and filtered the reagents to eliminate any noncompatible compositions. This narrowed the reagent classifications to alkynes, aryl boronic acids/esters, and aryl bromides. The remaining reagents were filtered to exclude structural alerts. At this point, protecting group compatibility was also considered for additional libraries we were targeting. Lastly, reagents were merged and clustered based on fingerprints comprised of the A log *P* atom type, with clusters being defined as a group of compounds exhibiting a ≥0.6 Tanimoto score.

Samples within each cluster were sorted by increasing the size, and the smallest reagent was generally selected to represent each cluster. If, for any reason, the top priority compound was unavailable or otherwise triaged, the next smallest reagent within a cluster was chosen as the representative.

Synthesis.

As mentioned, reagents resulting from the design workflow were amenable to Suzuki–Miyaura or Sonogashira–Hagihara coupling conditions to provide aryl–aryl- or alkynyl-linked compounds, respectively. For ease of discussion, we have classified the library into four series: phenyl, pyridyl, pyridinyl, and alkynyl (Figure 2).

Phenyl Series.—Analogues **3a–x** were synthesized according to Scheme 1. Treatment of 4-bromo-3-fluoroaniline or 3-fluoroaniline with benzyl chloroformate under mildly basic conditions afforded intermediate **1**, which reacted with (*R*)-(–)-glycidyl butyrate to generate the corresponding oxazolidinone **2**. With the exception of **3f**, analogues **3a–o** were obtained following a Suzuki cross-coupling between **2a** and various aryl boronic acids/esters. Compound **3f** was obtained by guanidinylation of compound **3e** followed by deprotection of the resulting di-Bocguanidine to reveal the free guanidinium salt.

To synthesize analogues **3p–r**, the hydroxy group of **2** was protected prior to the Suzuki coupling for purification purposes. Briefly, the primary hydroxy group of oxazolidinone **2a** was protected as the methoxymethyl ether to give **4**, which was coupled with select aryl boronic acids to provide the protected products **5a–c**. Deprotection of **5a–c** under typical acidic conditions yielded analogues **3p–r**, respectively. To obtain analogues **3s–x**, commercially available aryl bromides were utilized as the Suzuki coupling partner instead of aryl boronic acids/esters. Regioselective iodination of **2b** by treatment with *N*-iodosuccinimide provided intermediate **6**, which was subsequently transformed into boronic ester **7** through a palladium-catalyzed borylation reaction. Suzuki coupling between boronic ester **7** and select aryl bromides yielded compounds **3s–w**. Removal of the Boc protecting group on **3w** under acidic conditions yielded analogue **3x**.

Pyridyl Series.—The general synthetic approach for pyridyl C-ring derivatives **8a–o** is presented in Scheme 2. Analogues **8a,b** were obtained following a Suzuki cross-coupling between **2a** and the requisite boronic esters. Saponification of compound **8b** generated carboxylic acid **8c**. Suzuki coupling between boronic ester **7** and select aryl bromides yielded compounds **8d–m**. Compound **8n** was generated through a modified Suzuki reaction from the iodo-oxazolidinone **6**. Additionally, the pendant hydroxyl group on **7** could be protected as the methoxymethyl ether to afford **9**, which upon exposure to typical Suzuki conditions yielded the cyano pyridine **10**. Attempts to isolate the free amine **8o** after nitrile reduction proved problematic. Thus, we resorted to a strategy of trapping the free amine as the *t*-butylcarbamate for purification purposes. Once isolated, the resulting compound could be exposed to acidic conditions to simultaneously cleave the carbamate, methoxymethyl ether, and *t*-butyl group to reveal compound **8o**.

Pyridinium Series.—The general synthetic route for substituted pyridinium C-ring derivatives **12a–1** is shown in Scheme 3. A Suzuki reaction between intermediate **9** and a corresponding heterocyclic bromide provided **11a–h**, which were then reacted with a haloalkane of choice to form the *N*-alkylated pyridiniums. Removal of the methoxymethyl ether afforded final compounds **12a–1**.

Alkynyl Series.—For the last cohort of analogues, substituted alkynyl derivatives **13** were generated from **6** through a Sonogashira reaction with select coupling partners, as depicted in Scheme 4. In many cases, the resulting products were manipulated further to afford additional derivatives. For example, saponification of **13m** provided alcohol **13n** and hydrochloride salts **13t**, **13v**, **13x**, **13z**, and **13ab** were obtained after Boc removal from **13s**, **13u**, **13w**, **13y**, and **13aa** with trifluoroacetic acid followed by salt exchange, respectively.

Overview of Library Antibacterial Activity.

We next analyzed the activities of each compound series in three GNB, *E. coli, P. aeruginosa*, and *A. baumannii*. For all three species, wild-type and isogenic mutants lacking efflux pumps (Δ) and/or producing a large recombinant OM pore (Pore) were used to separate the contributions of active efflux and the OM permeability barriers on the activities of compounds.[42] The MIC (Table S2) and IC_{50} values (Tables 1–4) were determined first in the defined M9-MOPS medium, a better model (than nutrient-rich conditions) for bacterial growth observed *in vivo* during certain infections.[43–45] The dominant number of compounds had no activity in the wild-type strains of GNB (Tables 1–4 and S2). In contrast, at least half of the compounds inhibited the growth of the double-compromised (Δ+Pore) strains. Compounds **3e**, **8d**, and **8o** exhibited activity against all three Gram-negative pathogens.

With some exceptions, these compounds were active across species, including *S. aureus* (Table 5), suggesting that species-specific differences in binding to ribosomes are only minor factors in their activities. This was a bit surprising as interrogation of existing crystal structures reveals that while the cocrystal structure of LZD bound to the *S. aureus* 50S (SA50Slin) subunit indicates binding at the peptidyl transferase center (PTC), blocking the A-site in an orientation similar to that observed in other ribosome LZD complexes, a noteworthy difference is apparent. In the SA50Slin complex, the flexible nucleotide U2585 undergoes significant rotation and forms a hydrogen bond with the oxygen of the LZD morpholine ring, leading to a nonproductive conformation of the PTC.[46] This is different from other ribosome LZD complexes including *Deinococcus radiodurans* 50S, the whole ribosome of *Thermus thermophilus*, as well as the *E. coli* 70S structure. Hence, we anticipated that the alteration of the C-ring could affect target engagement and, by extension, antibacterial activity of LZD derivatives in a species-specific manner.

Structure–Activity Relationships.

E. coli is the best characterized, and we will first focus on SAR in this species and then identify species-specific differences for *A. baumannii* and *P. aeruginosa*.

Phenyl Series.—Among group **3** with substituted phenyl variants (Scheme 1), 16/24 analogues exhibited activity against ECWT (Table 1) at the concentrations tested (up to

100 μM). Within this series, 16/24 derivatives exhibited near-equal or better activity than LZD against the double-compromised ECΔPore strain. Compounds **3k**, **3f**, **3m**, **3w**, and **3x** exhibited >4-fold less activity than LZD in the ECΔPore strain, suggesting that the motifs associated with these molecules are likely detrimental to target engagement. Inspection of the corresponding motifs reveals no obvious functionality or trend that may explain target engagement issues. Compounds **3d** and **3u** are interesting in that they exhibited improved activity against the ECΔPore strain but were inactive against ECWT. Efflux susceptibility seems to be the main issue for **3d**, whereas **3u** exhibits issues with both OM permeation and efflux susceptibility.

Activity of this series against ABWT decreased to include only 7/24 compounds, with **3j**, **3k**, **3l**, and **3n–s** dropping out from the series that was active against ECWT (Table 1). Seven compounds (**3a–c**, **3e**, **3g**, **3h**, and **3v**) exhibited activity against ECWT and ABWT. Contrary to activity against ECΔPore, only 7/24 analogues exhibited equal or better activity than LZD against the ABΔPore strain. In addition to the analogues identified as problematic for target engagement against *E. coli*, **3i**, **3j** and **3o** also proved detrimental in *A. baumannii*. The list of compounds that exhibited activity against the ΔPore strain but not against the WT grew for *A. baumannii* to include **3l** and **3n–s**. This suggests that the OM and efflux proficiency of *A. baumannii* supersede that of *E. coli* for this chemotype.

Against *P. aeruginosa*, **3e** was the only compound that exhibited activity against the WT strain (Table 1). Within this series, 5/24 compounds performed better than LZD against the PAΔPore strain, fewer than both *E. coli* and *A. baumannii*. In addition to the motifs identified that decreased the target engagement efficiency against *E. coli* and *A. baumannii*, **3h**, **3j**, and **3l**, and **3u** are included in the list of compounds exhibiting a >5-fold decreased activity than LZD against the ΔPore strain. Compound **3c** is interesting to note, as it provided very good potency (20 nM) against PAΔPore, perhaps suggesting additional mechanisms of action. This is a reasonable hypothesis given the presence of a reactive aldehyde.

In summary, from this series, only **3e** exhibited pan activity against *E. coli, A. baumannii*, and *P. aeruginosa* WT. No members of this subset that were inactive against ECWT exhibited activity against ABWT or PAWT. SAR trends observed in this series clearly indicate that barrier stringency exhibited between these species can be summarized as *P. aeruginosa* > *A. baumannii* > *E. coli*. Likewise, although the 23S rRNA target of the oxazolidinones is known to be highly conserved and the activity of analogues is mostly consistent across species, the observation that the list of motifs proving detrimental to target engagement increases from *E. coli* to *A. baumannii* to *P. aeruginosa* highlights that discernible differences in the target exist and can potentially be exploited for narrowing or broadening the activity.

Pyridyl Series.—Within this series, only 3/15 derivatives (**8d**, **8o**, and **8m**) were active against ECWT and 5/15 exhibited near-equal or better activity than LZD against the ECΔPore strain (Table 2). The list of compounds that exhibited >5-fold worse activity against ECΔPore than LZD includes (**8f** and **8h–m**). It is worth noting that within this group that exhibits less efficient target engagement, motifs include extended pyridyls, comprising

both rotatable (**8k–m**) and fused (**8i** and **8j**) extensions. All analogues of this series that were nearly equal or more potent than LZD against ECΔPore exhibited weak/no activity against ECWT. Thus, while pyridyls may improve target engagement, they still pose OM permeation and efflux liabilities.

Against *A. baumannii*, 6/15 compounds were active against the WT strain, with four exhibiting equal or better activity than LZD. However, only 3/15 compounds exhibited near-equal or better activity than LZD against ABΔPore. Contrary to *E. coli*, compounds **8k** and **8i** exhibited good activity against ABΔPore. Compound **8l** also exhibited activity against ABΔPore, whereas it was inactive against ECΔPore. These three analogues once again highlight the discernible differences in target engagement between the species. Against *A. baumannii*, in addition to **8f**, **8h**, **8j**, **8l**, and **8m** identified in *E. coli*, derivatives **8a**, **8c**, and **8n** proved to be detrimental to on-target activity.

This series produced two compounds active against PAWT (**8d** and **8o**) and three that exhibited better activity than LZD in PAΔPore (**8o**, **8k**, and **8j**). Compound **8j** is especially interesting, as it is inactive against ECΔPore and ABΔPore. This suggests either a secondary mechanism of action in *P. aeruginosa* or a special feature of the 23S rRNA binding pocket that can be selectively exploited. LZD exhibits activity against Pore and Δ6 strains, whereas most pyridyl analogues are inactive. This suggests that pyridyls succumb to additive/synergistic properties of OM permeation and efflux.

In summary, this series produced two analogues with pan WT activity (**8d** and **8o**) and an additional compound (**8m**) that exhibited activity against ECWT and ABWT. Contrary to the substituted phenyl series, ECWT activity is not a preliminary qualifier for ABWT activity, as three compounds (**8a**, **8b**, and **8e**) exhibited activity against ABWT but were inactive against ECWT. For this series, the barrier stringency seems to be summarized as *P. aeruginosa* > *E. coli* > *A. baumannii*, thus highlighting that motif properties can influence species response.

Pyridinium Series.—Compound series **12** was comprised of various pyridinium motifs. From this series, 9/12 analogues were active against ECWT (Table 3). Only two derivatives (**12c** and **12b**) were >5-fold less active than LZD against ECΔPore, indicating good complementarity of a pyridinium functionality with the 23S rRNA target. Comparison of the IC_{50} values across all four strains reveals this series to be less of an issue for OM permeation and efflux susceptibility. This is consistent with previous observations that positively charged motifs may improve the accumulation of small molecules due to porin uptake mechanisms.

Against *A. baumannii*, only two compounds were active against ABWT (**12a** and **12k**), but both were less active than LZD. In addition, **12b–d**, **12i**, and **12k** exhibited a >5-fold lower activity than LZD against ABΔPore. This suggests that the pyridinium motif may not be as complementary to target binding site as it is for *E. coli*. In fact, most analogues in this series are less active than LZD against any of the *A. baumannii* strains.

For *P. aeruginosa*, no analogues within this series were active against WT. In addition to motifs identified for being detrimental to target engagement in *E. coli* and *A. baumannii*,

all compounds except **12l** and **12h** can be added to this list for *P. aeruginosa*. This further highlights the decrease in susceptibility of *P. aeruginosa* to modification of the oxazolidinone scaffold for 23S rRNA inhibition.

In summary, no pyridinium analogues were identified that exhibited a broad-spectrum activity against all three species. While this motif class seems rather beneficial for improving WT activity against *E. coli*, it is detrimental to whole-cell activity against *A. baumannii* and *P. aeruginosa*. The trend of motif SAR narrowing from *E. coli* to *A. baumannii* to *P. aeruginosa*, with *P. aeruginosa* being more stringent for allowable functionality, was consistent for this chemotype.

Alkynyl Series.—This series was the least active, with only 5/28 exhibiting activity against ECWT and no compounds active against ABWT of PAWT (Table 4). In fact, although 64% ofthe compounds in this series exhibited activity against ECΔPore, albeit with most having lower activity than LZD, only 21 and 14% were active against ABΔPore and PAΔPore, respectively. These results further suggest that the positioning and functionality at this location on the oxazolidinone chemotype are important for target engagement. The alkynyl attachment of this series likely extends beyond the binding pocket and is counterproductive to binding and by extension, activity. These results also confirm a trend of *E. coli* > *A. baumannii* > *P. aeruginosa* regarding compatibility with a broadened motif functionality.

Additional Trends from Cross-Series Comparisons.—While interrogation of each subset independently provided insight into each series, cross-series comparisons also provided interesting observations. For example, the comparison of IC_{50} values of **3a**, **8d–f**, and **12a–c**, elucidates the effect of pyridine inclusion, location, and conversion into a pyridinium on activity (Tables 1–3). This series demonstrates that activity against WT and ΔPore strains is relatively maintained against *E. coli* and *A. baumannii* after the incorporation of a pyridine with the nitrogen at the *para*-position (**3a** compared to **8d**) and activity against PAWT is gained. Interestingly, if the position of the nitrogen is moved to the 3-position (**8e**) activity against ECWT and PAWT is lost, with both barriers now contributing to the loss of activity in *E. coli* and primarily efflux susceptibility becoming the main issue in *P. aeruginosa*. Conversion of the pyridine to the pyridinium, however, only improves WT activity against *E. coli*, further illustrating the potential limitation of the benefit that charge incorporation provides with general GNB activity. In fact, inherent charge incorporation was detrimental to ABWT and PAWT activities in every instance in this study.

When compounds **3a**, **8d**, **12a**, and **12i–l** are compared, IC_{50} values highlight the effect of alkyl size appended to the nitrogen in the pyridinium groups. As mentioned previously, the incorporation of a charged pyridinium results in a slight loss in EC–Pore activity but the drop in activity is not magnified upon continued increases in the alkyl size. However, the activity against WT seems to correlate negatively with size, as groups larger than a methyl demonstrated decreased ECWT activity. Against *A. baumannii* and *P. aeruginosa* smaller or larger substituents exhibited more activity against the ΔPore strains, however, WT activity decreased in both of these species following the incorporation of a pyridinium.

Target Verification.

The above results show that the generated compounds vary broadly in their potencies against GNB. We next compared the MICs of select compounds against "barrier-less" strains of *E. coli, A. baumannii*, and *P. aeruginosa* to those against *S. aureus*, all grown in the nutrient-rich LB medium. Our results show consistent differences in MICs between the Gram-negative strains as well as in comparison to *S. aureus* (Table 5), albeit compounds seem to be more potent against cells grown in the M9-MOPS medium. In general, *S. aureus* was at least 2–4-fold more susceptible to growth inhibition induced by tested compounds, including the antibiotic LZD (Table 5). The most potent across the species were substituted pyridyls **8d** and **8e** and the substituted benzyl derivative **3g**. Furthermore, these compounds were at least 4-fold more potent than LZD against *S. aureus*.

To confirm that the activities of compounds remain target-dependent, we analyzed the efficiency of the cell-free *E. coli* transcription–translation in the absence and presence of increasing concentrations of select compounds (Figure 3). We found that the apparent protein translation inhibition constant, K_I^{app}, of LZD is 2.8 μM (Figure 3A), which is in excellent agreement with K_I^{app} = 2.5 μM reported previously[47] and with the growth inhibition IC_{50} = 9.3 μM for ECΔPore cells. The on-target activities of **3h**, **8o**, **8d**, and **12f** were all comparable to that of LZD and were consistent with their respective growth inhibition IC_{50} values (Figure 3B).

We also determined MICs against the *E. coli* SQ110 and SQDTC (ΔTolC) strains carrying only one copy of the rRNA operon and against SQDTC derivatives producing the LZD-resistant 23S rRNA variants with G2032A or C2610A substitutions.[48] We found that the SQ110 strain was resistant to all tested compounds (Table 5). With a few exceptions, SQ110 DTC was more susceptible to compounds than ECΔPore strain, suggesting that 23S rRNA copy number contributes to differences in MICs. However, for all compounds, MICs were higher in LZD-resistant strains. Thus, the antibacterial activities of compounds remain dependent on 23S rRNA inhibition.

Structure–Uptake Relationships.

We next identified problematic motifs associated with general or species-specific efflux susceptibility and poor OM permeation. All compounds exhibiting measurable IC_{50} values against at least one double-compromised strain were included in the analysis. IC_{50} ratios for WT(Pore)/ΔEfflux(Pore) (efflux impact ratio, P/PE) and ΔEfflux/ ΔEfflux(Pore) (OM impact ratio, E/PE) were calculated for each species and strain. Any IC_{50} value >100 for a ΔEfflux or (Pore) strain was set to 100 to allow P/PE and E/PE ratios for each motif to be calculated. This approach ensures that, if anything, the ratios for compounds with >100 IC_{50} values are underestimated. Ratios exceeding an arbitrary threshold of ≥5 were classified as a motif exhibiting problematic behavior for the corresponding barrier. For example, an E/PE ratio of 10 for a given analogue in *E. coli* would identify the corresponding motif as problematic to *E. coli* OM permeation. This ratio analysis was completed for each analogue over each of the three species. Motifs associated with poor OM permeation and/or increased efflux susceptibility are shown in Figures 4 and 5, respectively. Interestingly, no motifs were identified that exhibited poor OM permeation across all three species but six motifs (**3c**, **3n**,

3p, **3r**, **3s**, and **3u**) increased efflux susceptibility across all three species. In accordance with previous studies that indicate *P. aeruginosa* to exhibit higher levels of OM and efflux barrier synergy, 7 of the 10 motifs identified as being problematic for OM permeation were also exposed as efflux liabilities (**3b**, **3t**, **8j**, **8o**, **12a**, **12h**, and **LZD**).

Principal Component Analysis.

Important to the objective of advancing to a point of the rational design of GNB-accumulating chemotypes is the development of computational models. In an effort to confirm if observations identified from manual structural mapping (i.e., human interpretation of activity data) could be recapitulated via bioinformatics, we subjected the data set to principal component analysis (PCA). Three IC_{50} ratios, WT/ΔEfflux(Pore) (total barrier ratio, *W*/PE), WT(Pore)/ΔEfflux(Pore) (efflux impact ratio, *P*/PE), and ΔEfflux/ΔEfflux(Pore) (OM impact ratio, *E*/PE), were analyzed by PCA to provide insight into the influence of each barrier (i.e., efflux and porination) on activity for each species. For this PCA, only the 26 compounds that showed a detectable IC_{50} in at least two barrier-variant strains across all three bacteria were used (Figure 6). The rest of the compounds had to be excluded from the comparative analysis because the effect of neither efflux nor porination could be quantified in at least one of the species.

In most cases for all three bacteria, the effect of efflux inactivation (*P*/PE ratio) dominated that of porination (*E*/PE ratio). Thus, any compound specificity observed for each species is primarily defined by the organism's repertoire of efflux pumps. We further noted that *A. baumannii* was much closer to *E. coli* than *P. aeruginosa*, according to PCA. For both efflux and porination, the first principal component (PC1) was defined by the difference between *P. aeruginosa* and the other two bacteria, whereas the second principal component (PC2) was aligned with the distinction between *E. coli* and *A. baumannii*. Inspection of PCs (Table S1) revealed that the PC1 and PC2 in the efflux impact ratio (*P*/PE) were dominated, respectively, by **8o** and **12l**, and by **3p**, **3r**, and **3n**. Thus, these compounds are the most reflective of the species-specific difference in the efficiency of their permeation barriers. In particular, both **8o** and **12l** were identified as efflux liabilities for *P. aeruginosa* but not for *E. coli* or *A. baumannii* (Figure 5). For the OM impact, most of the difference could be attributed to compounds **3c**, **8o**, and **LZD** (PC1) and **3m**, **3c**, **3e**, and **12g** (PC2). As seen in Figure 4, permeabilities of compounds **3c**, **8o**, and **LZD** were greatly affected by the presence of the pore for *P. aeruginosa* but not for *E. coli* or *A. baumannii*. Thus, the distinction of *P. aeruginosa* from two other bacteria is achieved through both the more efficient efflux and lower transmembrane diffusion. However, the two factors are differentially affected by compound structures. The PCA results are largely confirmatory of the observations ascertained through manual structural inspection, thus setting a foundation for more prospective designing of GNB-active compounds.

Growth Inhibition against Diverse Isolates.

To determine whether the trends established in the above experiments are applicable to other bacterial strains and species, we measured MICs for the select compounds with activities in the WT strains against multidrug-resistant *A. baumannii* (AYE and Ab5075), *P. aeruginosa* (BAA 2108 and BAA 2109, multidrug resistance ATCC panel), *K. pneumoniae*

(ATCC13883 and ATCC43816), and *K. aerogenes* ATCC13048 (Table 6). The MICs were measured in the ion-adjusted Mueller-Hinton broth (per recommendations of CLSI) and in M9-MOPS. None of the compounds inhibited *P. aeruginosa* growth in concentrations up to 200 μM. However, all compounds except LZD inhibited the growth of *K. pneumoniae* ATCC13883 and *K. aerogenes* ATCC13048, especially in M9-MOPS medium with **8o** having the lowest MIC = 12.5 μM against the ATCC13058 strain. In addition, compounds **3e** and **8o** inhibited the growth of *K. pneumoniae* ATCC43816 cells also grown in M9-MOPS. Compounds **3h**, **8e**, and **8d** inhibited the growth of both *A. baumannii* strains when grown in M9-MOPS with MICs = 100–200 μM (Table 6).

Thus, the uncovered trends can be applied to bacterial strains with diverse genetic backgrounds and could improve the activities of oxazolidinones and perhaps other antibiotics against Gram-negative pathogens. However, additional resistance mechanisms such as those present in MDR strains of *P. aeruginosa* require further studies.

CONCLUSIONS

In conclusion, we report the design, synthesis, and evaluation of a library of oxazolidinones against *E. coli, P. aeruginosa*, and *A. baumannii* and their isogenic strains with varying degrees of the outer membrane and/or efflux pump deficiencies. The data indicate that the evaluated permeation mechanisms do not account for all activity differences between organisms. This could suggest (1) secondary mechanisms of action or different off-target profiles for oxazolidinones in some species, (2) tangible differences in target engagement, and/or (3) involvement of additional permeation mechanisms such as alternative efflux pumps. While we do observe growth media-specific differences in activity, this was expected as growth and metabolic rates of bacteria differ in minimal versus nutrient-rich environments. It is important to note, however, that the overall trends of activity against certain species were not changed, suggesting that the growth medium does not contribute significantly to species-specific inhibitory differences.

The data clearly indicate that motif manipulation on a chemotype is enough to significantly modulate efflux and permeation. As such, the perception that the efflux and OM permeation issues are an inherent characteristic of the chemotype does not hold true for the oxazolidinone scaffold. Rather, the orientation, location, and composition of functional groups are the determinants of chemotype accumulation. In general, *P. aeruginosa* is more divergent from the other two bacteria and the least responsive to oxazolidinone treatment. It would be more challenging to engineer activity against *P. aeruginosa* for this chemotype, as efflux and OM barriers synergize strongly in this organism. *A. baumannii* and *E. coli* are more similar, with efflux being the major issue for this chemotype, with certain motifs also facing difficulties with OM permeation.

Determination of IC_{50} values revealed three analogues (**3e**, **8d**, and **8o**) with a broadened spectrum of activity to include WT *E. coli, A. baumannii*, and *P. aeruginosa*. While these three analogues were previously reported to exhibit activity against another ECWT strain (MG1655),[40] this is the first report of their broadened activity to include two other ESKAPE pathogens *A. baumannii* and *P. aeruginosa*. Of the 80 compounds presented in this study,

no single motif was identified that correlated with poor OM permeation across all three GNB species. On the contrary, six different motifs were identified that increased efflux susceptibility across all three species (**3c**, **3n**, **3p**, **3r**, **3s**, and **3u**). These observations provide compelling evidence that molecular features that dictate compound accumulation are likely to vary from one species to the next, with OM permeation being the most species-specific and efflux susceptibility exhibiting more overlap.

While generating overarching Lipinski-like rules or guidelines for compound accumulation in Gram-negative bacteria is an enticing goal, we postulate that a more feasible first step may be to identify motifs for several chemotypes that significantly affect accumulation (positively or negatively). Once this has been completed for a variety of chemotypes and across several bacterial species, a clearer picture of general versus chemotype-and species-specific trends is expected to emerge. One can then imagine eventually advancing to a point wherein hierarchical ranking of motifs can be organized to provide Topliss-like trees[49] and/or bioisostere-like classifications[50] to guide accumulation improvement efforts and rational design for Gram-negative active molecules.

EXPERIMENTAL SECTION

Chemistry.

Starting materials, ACS-grade methylene chloride (DCM), methanol (MeOH), hexanes, ethyl acetate (EtOAc), acetone, acetonitrile (CH_3CN), dimethyl formamide (DMF), anhydrous dimethyl sulfoxide (DMSO), dioxane, ethanol, formic acid, anhydrous tetrahydrofuran (THF), tetrahydrofuran (THF), toluene, and trifluoroacetic acid (TFA) were purchased from TCI Chemicals, Oakwood, Alfa Aesar, Fisher Scientific, Enamine, or Sigma-Aldrich. Deionized water was used for all experimental procedures where “water” is indicated. All reactions requiring anhydrous conditions were run under a nitrogen atmosphere. Analytical and preparative thin-layer chromatography (TLC) was performed on silica gel 60 F_{254} plates (Sigma-Aldrich 1.05715). Flash column chromatography was carried out on silica gel (70–230 mesh, SiliCycle). NMR data were collected on a 400, 500, and 600 MHz (specified below) Varian VNMRS Direct Drive spectrometer equipped with an indirect detection probe. NMR data were collected at 25 °C unless otherwise indicated. Pulse sequences were used as supplied by Varian VNMRJ 4.2 software. All NMR data were processed in MestReNova. High-resolution mass spectrometry was obtained from and analyzed by the Mass Spectrometry Facility at the University of Minnesota. All compounds evaluated in biological assays were >95% purity based on high-performance liquid chromatography (HPLC) and/or NMR.

Benzyl (4-Bromo-3-fluorophenyl)carbamate (1a).—

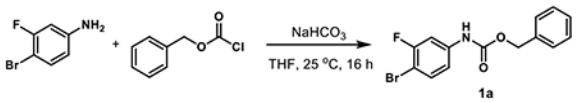

1a

To a solution of 4-bromo-3-fluoroaniline (3.8 g, 20 mmol) in THF (80 mL) was added sodium bicarbonate (3.36 g, 40 mmol) and the mixture was cooled to 0 °C. Benzyl chloroformate (4.23 mL, 30 mmol) was added dropwise with a syringe. The reaction

mixture was stirred at 25 °C. After the reaction was judged to be completed by TLC (16 h), it was quenched with water and extracted with EtOAc three times. The combined organic layers were washed with water and concentrated under reduced pressure by rotary evaporation. The crude residue was purified by flash column chromatography (SiO_2, eluent gradient 0–20% EtOAc in hexanes) to give compound **1a** as a yellow amorphous solid (5.90 g, 91%). ^{1}H NMR (300 MHz, chloroform-*d*) δ 7.71–7.31 (m, 7H), 6.93 (dd, J = 8.7, 2.5 Hz, 1H), 6.75 (s, 1H), 5.20 (s, 2H).

Benzyl (3-Fluorophenyl)carbamate (1b).—

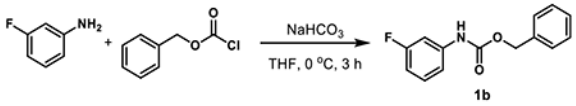

1b

A mixture of 3-fluoroaniline (1.92 mL, 20 mmol) and sodium bicarbonate (3.36 g, 40 mmol) was suspended in THF (80 mL) and cooled to 0 °C. Benzyl chloroformate (4.23 mL, 30 mmol) was added dropwise with a syringe. The reaction mixture was stirred at 0 °C. After the reaction was judged to be completed by TLC (3 h), it was quenched with water and extracted with EtOAc three times. The combined organic layers were washed with water and concentrated under reduced pressure by rotary evaporation. The crude residue was purified by flash column chromatography (SiO_2, eluent gradient 0–15% EtOAc in hexanes) to give compound **1b** as a white amorphous solid (4.9 g, 99%). ^{1}H NMR (300 MHz, chloroform-*d*) δ 7.47–7.29 (m, 5H), 7.29–7.16 (m, 1H), 7.01 (ddd, J = 8.4, 2.1, 0.9 Hz, 1H), 6.83–6.66 (m, 2H), 5.21 (s, 2H).

(R)-3-(4-Bromo-3-fluorophenyl)-5-(hydroxymethyl)oxazolidin-2-one (2a).[38]—

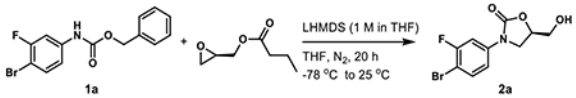

1a 2a

Compound **1a** (1.62 g, 5 mmol) was dissolved in anhydrous THF (25 mL) and cooled to −78 °C under a nitrogen atmosphere. Lithium bis(trimethylsilyl)amide solution (1 M in THF, 4.25 mL, 4.25 mmol) was added to the mixture slowly over a period of 40 min with a syringe. The mixture was stirred at −78 °C for 1 h under a nitrogen atmosphere followed by the addition of (*R*)-(–)-glycidyl butyrate (0.59 mL, 4.25 mmol) dropwise with a syringe at −78 °C. The mixture was stirred at this temperature for an additional 1 h and then gradually warmed to 25 °C. After the reaction was judged to be completed by TLC (20 h), it was quenched with water and extracted with EtOAc three times. The combined organic layers were washed with water and evaporated under reduced pressure by rotary evaporation. The crude residue was purified by flash column chromatography (SiO_2, eluent gradient 0–100% EtOAc in hexanes) to afford compound **2a** as a yellow amorphous solid (1.10 g, 76%). ^{1}H NMR (300 MHz, acetone-d_6) δ 7.74 (dd, J = 11.7, 2.7 Hz, 1H), 7.64 (dd, J = 8.9, 8.0 Hz, 1H), 7.36 (ddd, J = 8.9, 2.7, 1.0 Hz, 1H), 4.96–4.70 (m, 1H), 4.38 (dd, J = 6.2, 5.6 Hz, 1H), 4.20 (t, J = 8.8 Hz, 1H), 4.01 (dd, J = 8.8, 6.2 Hz, 1H), 3.90 (ddd, J = 12.3, 5.6, 3.4 Hz, 1H), 3.76 (ddd, J = 12.3, 6.2, 3.9 Hz, 1H).

(R)-3-(3-Fluorophenyl)-5-(hydroxymethyl)oxazolidin-2-one (2b).—

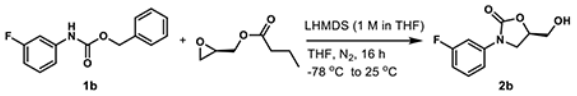

Compound **1b** (4.73 g, 19.27 mmol) was dissolved in anhydrous THF (100 mL) and cooled to −78 °C under a nitrogen atmosphere. Lithium bis(trimethylsilyl)amide solution (1 M in THF, 16.38 mL, 16.38 mmol) was added to the mixture slowly over a period of 1 h with a syringe. The mixture was stirred at −78 °C for 1 h under a nitrogen atmosphere followed by the addition of (*R*)-(–)-glycidyl butyrate (2.23 mL, 16.38 mmol) dropwise with a syringe at −78 °C. The mixture was stirred at this temperature for an additional 1 h and then gradually warmed to 25 °C. After the reaction was judged to be completed by TLC (16 h), it was quenched with water and evaporated under reduced pressure by rotary evaporation to remove most of THF. The mixture was diluted with water and extracted with EtOAc three times. The combined organic layers were washed with water and evaporated under reduced pressure by rotary evaporation. The crude residue was purified by flash column chromatography (SiO_2, eluent gradient 0–67% EtOAc in hexanes) to afford compound **2b** as a white amorphous solid (2.86 g, 70%). ^{1}H NMR (400 MHz, acetone-d_6) δ 7.67–7.51 (m, 1H), 7.47–7.26 (m, 2H), 6.96–6.76 (m, 1H), 4.87–4.70 (m, 1H), 4.39 (t, J = 5.7 Hz, 1H), 4.25–4.09 (m, 1H), 4.04–3.95 (m, 1H), 3.94–3.83 (m, 1H), 3.81–3.71 (m, 1H).

General Procedure 1: Synthesis of Heterocyclic Oxazolidinone Analogues 3a–3o.[40]

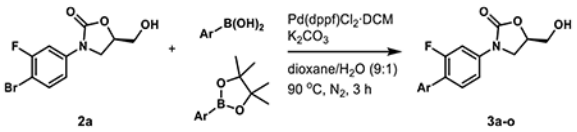

A mixture of compound **2a** (29 mg, 0.1 mmol), aryl boronic acid or ester (0.12 mmol), potassium carbonate (55 mg, 0.4 mmol), and [1,1′-bis(diphenylphosphino)ferrocene]dichloropalladium(II) complex with dichloromethane (8.2 mg, 0.01 mmol) in dioxane/H_2O (v/v = 9:1, 0.5 mL) was stirred at 90 °C under a nitrogen atmosphere for 3 h. The reaction mixture was cooled to room temperature, diluted with EtOAc, washed with water, and concentrated under reduced pressure by rotary evaporation. The crude residue was purified by flash column chromatography (SiO_2) using an appropriate eluent as described below to afford compounds **3a–o** and **8a,b**. Various derivatives deviated slightly from this procedure, and full descriptions are included as needed for **3a–o** and **8a,b**.

(R)-3-(2-Fluoro-[1,1′-biphenyl]-4-yl)-5-(hydroxymethyl)-oxazolidin-2-one (3a).—

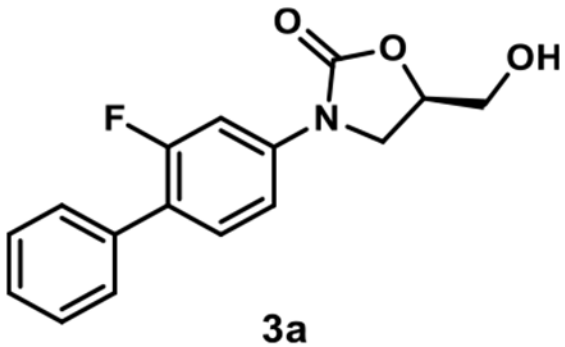

3a

Using general procedure 1, employing phenylboronic acid (15 mg, 0.12 mmol), compound **3a** was obtained after flash column chromatography (SiO_2, eluent gradient 0–100% EtOAc in hexanes) as a white amorphous solid (20 mg, 70%). ^{1}H NMR (400 MHz, acetone-d_6) δ 7.70 (dd, J = 13.7, 2.3 Hz, 1H), 7.62–7.50 (m, 3H), 7.50–7.42 (m, 3H), 7.42–7.35 (m, 1H), 4.90–4.77 (m, 1H), 4.41 (t, J = 5.9 Hz, 1H), 4.24 (t, J = 8.8 Hz, 1H), 4.05 (dd, J = 8.8, 6.3 Hz, 1H), 3.91 (ddd, J = 12.3 5.9, 3.4 Hz, 1H), 3.78 (ddd, J = 12.3, 5.9, 3.9 Hz, 1H). ^{13}C NMR (101 MHz, acetone-d_6) δ 160.5 (d, J = 244.5 Hz), 155.3, 140.9 (d, J = 11.3 Hz), 136.2 (d, J = 1.6 Hz), 131.7 (d, J = 5.0 Hz), 129.6 (d, J = 3.1 Hz, 2C), 129.4 (2C), 128.4, 124.1 (d, J = 14.0 Hz), 114.3 (d, J = 3.3 Hz), 106.2 (d, J = 29.3 Hz), 74.3, 63.2, 46.9.

(R)-3-(2-Fluoro-4′-((trifluoromethyl)thio)-[1,1′-biphenyl]-4-yl)-5-(hydroxymethyl)oxazolidin-2-one (3b).—

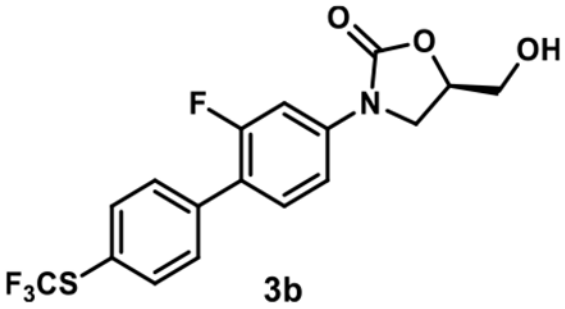

3b

Using general procedure 1, employing 4,4,5,5-tetramethyl-2-(4-((trifluoromethyl)thio)phenyl)-1,3,2-dioxaborolane (37 mg, 0.12 mmol), compound **3b** was obtained after flash column chromatography (SiO_2, eluent gradient 0–100% EtOAc in hexanes) as a yellow amorphous solid (26 mg, 67%). ^{1}H NMR (400 MHz, acetone-d_6) δ 7.82 (d, J = 8.1 Hz, 2H), 7.77–7.69 (m, 3H), 7.61 (t, J = 8.7 Hz, 1H), 7.50 (dd, J = 8.7, 2.3 Hz, 1H), 4.95–4.71 (m, 1H), 4.41 (s, 1H), 4.25 (t, J = 8.8 Hz, 1H), 4.06 (dd, J = 8.8, 6.2 Hz, 1H), 3.92 (dd, J = 12.6, 3.6 Hz, 1H), 3.83–3.70 (m, 1H). ^{13}C NMR (101 MHz, acetone-d_6) δ 160.7 (d, J = 245.7 Hz), 155.4, 141.9 (d, J = 11.3 Hz), 139.5, 137.4 (2C), 131.8 (d, J = 4.6 Hz), 131.0 (d, J = 3.4 Hz, 2C), 130.9 (q, J = 306.9 Hz), 123.6, 122.5 (d, J = 13.3 Hz), 114.6 (d, J = 3.1 Hz), 106.4 (d, J = 29.1 Hz), 74.5, 63.3, 47.0.

(R)-2′-Fluoro-4′-(5-(hydroxymethyl)-2-oxooxazolidin-3-yl)-[1,1′-biphenyl]-4-carbaldehyde (3c).—

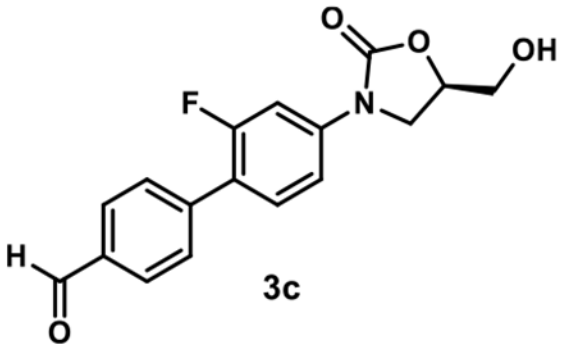

3c

A mixture of compound **2a** (58 mg, 0.2 mmol), 4-formylphenylboronic acid (36 mg, 0.24 mmol), potassium carbonate (110 mg, 0.8 mmol), and [1,1′-bis(diphenylphosphino)ferrocene]dichloropalladium(II) complex with dichloromethane (16 mg, 0.02 mmol) in dioxane/H_2O (v/v = 9:1, 0.5 mL) was stirred at 90 °C under a nitrogen atmosphere. After the reaction was judged to be completed by TLC (3 h), it was cooled to room temperature, diluted with EtOAc, washed with water, and concentrated under reduced pressure by rotary evaporation. The crude residue was purified by flash column chromatography (SiO_2, eluent gradient 0–100% EtOAc in hexanes) to afford compound **3c** as a yellow amorphous solid (40 mg, 56%). ^{1}H NMR (500 MHz, acetone-d_6) δ 10.09 (s, 1H), 8.01 (d, J = 8.3 Hz, 2H), 7.80 (d, J = 8.3 Hz, 2H), 7.74 (dd, J = 13.8, 2.3 Hz, 1H), 7.63 (t, J = 8.8 Hz, 1H), 7.51 (dd, J = 8.8, 2.3 Hz, 1H), 4.87–4.78 (m, 1H), 4.40 (t, J = 5.9 Hz, 1H), 4.25 (t, J = 8.9 Hz, 1H), 4.07 (dd, J = 8.9, 6.2 Hz, 1H), 3.96–3.87 (m, 1H), 3.82–3.74 (m, 1H). ^{13}C NMR (126 MHz, acetone-d_6) δ 192.5, 160.6 (d, J = 246.0 Hz), 155.3, 142.1 (d, J = 1.7 Hz), 141.9 (d, J = 11.4 Hz), 136.6, 131.8 (d, J = 4.7 Hz), 130.5 (2C), 130.2 (d, J = 3.7 Hz, 2C), 122.8 (d, J = 13.3 Hz), 114.5 (d, J = 3.2 Hz), 106.3 (d, J = 29.3 Hz), 74.4, 63.2, 47.0.

(R)-3-(2-Fluoro-4′-hydroxy-[1,1′-biphenyl]-4-yl)-5-(hydroxymethyl)oxazolidin-2-one (3d).—

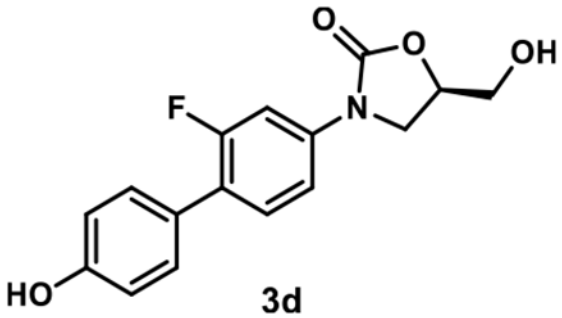

3d

A mixture of compound **2a** (58 mg, 0.2 mmol), 4-hydroxyphenylboronic acid (33 mg, 0.24 mmol), potassium carbonate (110 mg, 0.8 mmol), and [1,1′-bis(diphenylphosphino)ferrocene]-dichloropalladium(II) complex with dichloromethane (16 mg, 0.02 mmol) in dioxane/H_2O (v/v = 9:1, 0.5 mL) was stirred at 90 °C under a nitrogen atmosphere. After the reaction was judged to be completed by TLC (3 h), it was cooled to room temperature, diluted with EtOAc, washed with water, and concentrated under

reduced pressure by rotary evaporation. The crude residue was purified by flash column chromatography (SiO_2, eluent gradient 0–100% EtOAc in hexanes) to afford compound **3d** as a yellow amorphous solid (7 mg, 11%). ^{1}H NMR (400 MHz, acetone-d_6) δ 8.48 (s, 1H), 7.66 (dd, J = 13.7, 2.3 Hz, 1H), 7.47 (t, J = 8.7 Hz, 1H), 7.44–7.39 (m, 3H), 6.96–6.91 (m, 2H), 4.86–4.76 (m, 1H), 4.36 (t, J = 5.9 Hz, 1H), 4.22 (t, J = 8.8 Hz, 1H), 4.03 (dd, J = 8.8, 6.2 Hz, 1H), 3.95–3.86 (m, 1H), 3.82–3.74 (m, 1H). ^{13}C NMR (101 MHz, acetone-d_6) δ 160.5 (d, J = 245.4 Hz), 158.1, 155.4, 140.3, 131.4 (d, J = 5.1 Hz), 130.9 (d, J = 4.0 Hz, 2C), 127.5 (d, J = 2.0 Hz), 124.4 (d, J = 14.1 Hz), 116.4 (2C), 116.3, 114.5 (d, J = 4.0 Hz), 106.4 (d, J = 29.3 Hz), 74.4, 63.4, 47.1.

(R)-3-(4′-(Aminomethyl)-2-fluoro-[1,1′-biphenyl]-4-yl)-5-(hydroxymethyl)oxazolidin-2-one Hydrochloride (3e).—

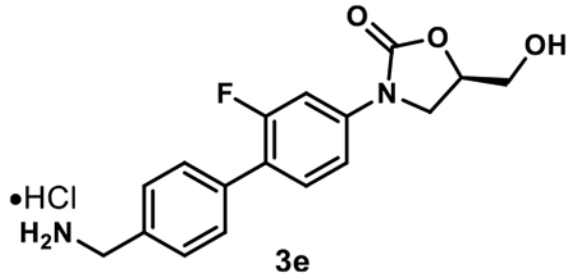

3e

A mixture of compound **2a** (29 mg, 0.1 mmol), 4-aminomethylphenylboronic acid hydrochloride (23 mg, 0.12 mmol), potassium carbonate (55 mg, 0.4 mmol), and [1,1′-bis(diphenylphosphino)-ferrocene]dichloropalladium(II) complex with dichloromethane (8 mg, 0.01 mmol) in dioxane/H_2O (v/v = 9:1, 0.5 mL) was stirred at 90 °C under a nitrogen atmosphere. After the reaction was judged to be completed by TLC (3 h), it was cooled to room temperature and concentrated under reduced pressure with a rotary evaporator. The crude residue was purified by flash column chromatography (SiO_2, eluent gradient 0–20% MeOH in DCM with 1% ammonia). The appropriate fractions were collected and evaporated under reduced pressure with a rotary evaporator. The resulting residue was dissolved in MeOH (1 mL), charged with the addition of HCl/dioxane (4 M, 50 μL), and concentrated under reduced pressure with a rotary evaporator. The resulting hydrochloride salt was washed with acetone (1 mL) and dried under high vacuum to afford compound **3e** as a white amorphous solid (26 mg, 82%). ^{1}H NMR (400 MHz, DMSO-d_6) δ 8.73 (s, 3H), 7.76–7.36 (m, 7H), 5.39 (t, J = 5.6 Hz, 1H), 4.80–4.65 (m, 1H), 4.12 (t, J = 8.9 Hz, 1H), 4.04 (s, 2H), 3.92 (dd, J = 8.9, 6.0 Hz, 1H), 3.75–3.64 (m, 1H), 3.61–3.50 (m, 1H). ^{13}C NMR (101 MHz, DMSO-d_6) δ 159.1 (d, J = 244.7 Hz), 154.4, 139.6 (d, J = 11.1 Hz), 134.7, 133.6, 130.9 (d, J = 4.6 Hz), 129.4 (2C), 128.7 (d, J = 3.0 Hz, 2C), 122.1 (d, J = 13.4 Hz), 113.9 (d, J = 2.0 Hz), 105.4 (d, J = 28.8 Hz), 73.5, 61.5, 46.1, 41.8. MSESI m/z: 339.1125 ($C_{17}H_{17}FN_2O_3$ + Na^+ requires 339.1115).

Bis-boc-(R)-1-((2′-fluoro-4′-(5-(hydroxymethyl)-2-oxooxazolidin-3-yl)-[1,′-biphenyl]-4-yl)methyl)guanidine (3ea).—

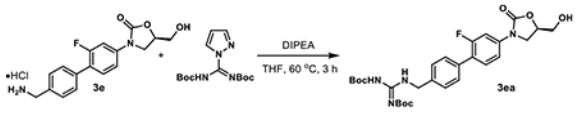

A mixture of compound **3e** (182 mg, 0.51 mmol), *N,N*′-di-boc-1*H*-pyrazole-1-carboxamidine (240 mg, 0.77 mmol), and *N,N*-diisopropylethylamine (266 μL, 1.53 mmol) in THF (10 mL) was stirred at 60 °C. After the reaction was judged to be completed by TLC (3 h), it was cooled to room temperature, diluted with EtOAc, washed with water, and concentrated under reduced pressure with rotary evaporation. The crude residue was purified by flash column chromatography (SiO_2, eluent gradient 0–75% EtOAc in hexanes) to afford compound **3ea** as a white amorphous solid (74 mg, 26%). ^{1}H NMR (400 MHz, acetone-d_6) δ 11.71 (s, 1H), 8.71 (s, 1H), 7.70 (dd, J = 13.7, 2.3 Hz, 1H), 7.59–7.42 (m, 6H), 4.86–4.76 (m, 1H), 4.70 (d, J = 5.8 Hz, 2H), 4.42 (s, 1H), 4.23 (t, J = 8.9 Hz, 1H), 4.05 (dd, J = 8.9, 6.2 Hz, 1H), 3.96–3.85 (m, 1H), 3.82–3.73 (m, 1H), 1.51 (s, 9H), 1.44 (s, 9H). ^{13}C NMR (101 MHz, acetone-d_6) δ 164.6, 160.5 (d, J = 244.5 Hz), 157.0, 155.3, 153.8, 140.9 (d, J = 11.2 Hz), 138.8, 135.2 (d, J = 1.5 Hz), 131.6 (d, J = 5.0 Hz), 129.8 (d, J = 3.1 Hz, 2C), 128.7 (2C), 123.8 (d, J = 13.8 Hz), 114.3 (d, J = 3.2 Hz), 106.2 (d, J = 29.2 Hz), 83.8, 78.9, 74.3, 63.2, 46.9, 44.5, 28.4, 28.1.

(R)-1-((2′-Fluoro-4′-(5-(hydroxymethyl)-2-oxooxazolidin-3-yl)-[1,1′-biphenyl]-4-yl)methyl)guanidine Hydrochloride (3f).—

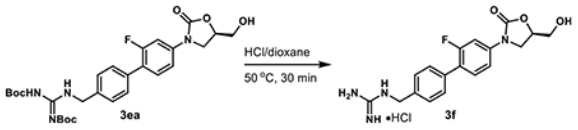

A mixture of **3ea** (28 mg, 0.05 mmol) in HCl/dioxane (4 M, 1 mL) was stirred at 50 °C. After the reaction was judged to be completed by TLC (30 min), its solvent was removed under reduced pressure with rotary evaporation. The residue was washed with acetone (1 mL) and dried under high vacuum to give compound **3f** as a white amorphous solid (11 mg, 56%). ^{1}H NMR (400 MHz, DMSO-d_6) δ 8.31 (t, J = 6.2 Hz, 1H), 7.63 (dd, J = 13.5, 2.3 Hz, 1H), 7.60–7.49 (m, 3H), 7.48–7.35 (m, 3H), 5.31 (t, J = 5.6 Hz, 1H), 4.79–4.69 (m, 1H), 4.45 (d, J = 6.2 Hz, 2H), 4.13 (t, J = 9.0 Hz, 1H), 3.90 (dd, J = 9.0, 6.1 Hz, 1H), 3.69 (ddd, J = 12.4, 5.6, 3.3 Hz, 1H), 3.57 (ddd, J = 12.4, 5.6, 3.9 Hz, 1H). ^{13}C NMR (101 MHz, DMSO-d_6) δ 159.1 (d, J = 243.9 Hz), 157.2, 154.4, 139.5 (d, J = 11.1 Hz), 136.8, 133.9, 130.9 (d, J = 4.4 Hz), 128.8 (2C), 127.5 (2C), 122.3 (d, J = 12.9 Hz), 113.8, 105.4 (d, J = 28.9 Hz), 73.4, 61.6, 46.0, 43.6. MSESI *m/z*: 359.1532 ($C_{18}H_{19}FN_4O_3$ + H^+ requires 359.1514).

(R)-3-(2-Fluoro-4′-(hydroxymethyl)-[1,1′-biphenyl]-4-yl)-5-(hydroxymethyl)oxazolidin-2-one (3g).—

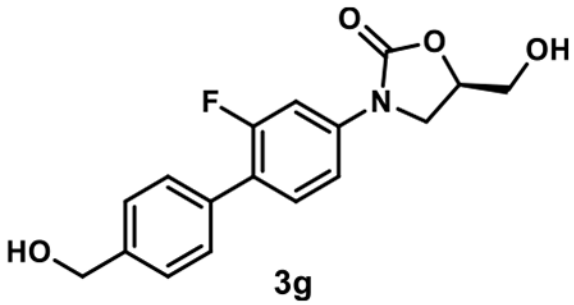

3g

Using general procedure 1, employing 4-(hydroxymethyl)-benzeneboronic acid (18 mg, 0.12 mmol), compound **3g** was obtained after flash column chromatography (SiO_2, eluent gradient 0–10% MeOH in DCM) as a yellow amorphous solid (10 mg, 32%). ^{1}H NMR (500 MHz, DMSO-d_6) δ 7.62 (dd, J = 13.6, 2.2 Hz, 1H), 7.55 (t, J = 8.6 Hz, 1H), 7.52–7.48 (m, 2H), 7.44 (dd, J = 8.6, 2.2 Hz, 1H), 7.41 (d, J = 8.0 Hz, 2H), 5.29–5.09 (m, 2H), 4.81–4.70 (m, 1H), 4.54 (d, J = 5.3 Hz, 2H), 4.13 (t, J = 8.9 Hz, 1H), 3.88 (dd, J = 8.9, 6.1 Hz, 1H), 3.74–3.65 (m, 1H), 3.63–3.54 (m, 1H). ^{13}C NMR (101 MHz, DMSO-d_6) δ 159.0 (d, J = 244.3 Hz), 154.3, 142.0, 139.2 (d, J = 11.1 Hz), 133.0, 130.8 (d, J = 4.8 Hz), 128.3 (d, J = 3.0 Hz, 2C), 126.7 (2C), 122.7 (d, J = 13.5 Hz), 113.8 (d, J = 3.1 Hz), 105.3 (d, J = 29.0 Hz), 73.4, 62.6, 61.6, 46.0. MSESI m/z: 340.0949 ($C_{17}H_{16}FNO_4$ + Na^+ requires 340.0956).

(R)-3-(2-Fluoro-3′-(hydroxymethyl)-[1,1′-biphenyl]-4-yl)-5-(hydroxymethyl)oxazolidin-2-one (3h).—

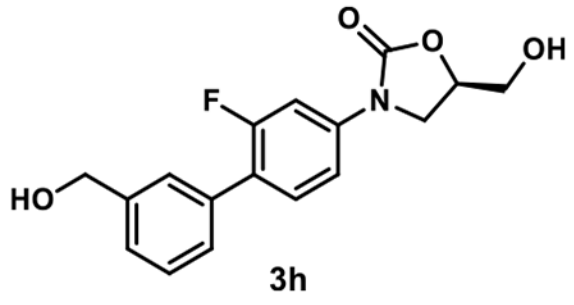

3h

A mixture of compound **2a** (58 mg, 0.2 mmol), 3-(hydroxymethyl)-phenylboronic acid (36 mg, 0.24 mmol), potassium carbonate (110 mg, 0.8 mmol), and [1,1′-bis(diphenylphosphino)ferrocene]-dichloropalladium(II) complex with dichloromethane (16 mg, 0.02 mmol) in dioxane/H_2O (v/v = 9:1, 0.5 mL) was stirred at 90 °C under a nitrogen atmosphere. After the reaction was judged to be completed by TLC (3 h), it was cooled to room temperature, diluted with EtOAc, washed with water, and concentrated under reduced pressure by rotary evaporation. The crude residue was purified by flash column chromatography (SiO_2, eluent gradient 0–10% MeOH in DCM) to afford compound **3h** as a brown amorphous solid (55 mg, 87%). ^{1}HNMR (400 MHz, methanol-d_4) δ 7.63 (dd, J = 13.3, 2.3 Hz, 1H), 7.54–7.47 (m, 2H), 7.44–7.33 (m, 4H), 4.81–4.73 (m, 1H), 4.66 (s, 2H), 4.16 (t, J = 9.0 Hz, 1H), 3.97 (dd, J = 9.0, 6.4 Hz, 1H), 3.87 (dd, J = 12.6, 3.2 Hz, 1H), 3.71 (dd, J = 12.6, 4.0 Hz, 1H). ^{13}C NMR (101 MHz, methanol-d_4) δ 161.0 (d, J = 246.4 Hz), 156.9, 143.1, 140.6 (d, J = 11.1 Hz), 136.7 (d, J = 1.0 Hz), 132.0 (d, J = 5.1 Hz), 129.6,

128.8 (d, J = 3.0 Hz), 128.4 (d, J = 3.0 Hz), 127.2, 125.5 (d, J = 13.1 Hz), 115.0 (d, J = 3.0 Hz), 107.2 (J = 29,3 Hz), 75.2, 65.1, 63.3, 47.6.

(R)-3-(2-Fluoro-3′-((trifluoromethyl)sulfonyl)-[1,1′-biphenyl]-4-yl)-5-(hydroxymethyl)oxazolidin-2-one (3i).—

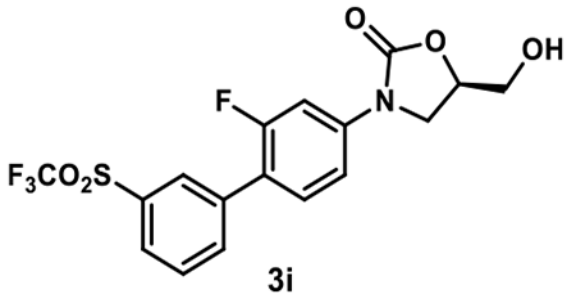

3i

Using general procedure 1, employing 4,4,5,5-tetramethyl-2-(3-trifluoromethanesulfonylphenyl)-1,3,2-dioxaborolane (40 mg, 0.12 mmol), compound **3i** was obtained after flash column chromatography (SiO_2, eluent gradient 0–100% EtOAc in hexanes) as a foamy yellow amorphous solid (34 mg, 81%). ^{1}H NMR (400 MHz, acetone-d_6) δ 8.26 (s, 1H), 8.22 (d, J = 7.9 Hz, 1H), 8.14 (d, J = 7.9 Hz, 1H), 7.98 (t, J = 7.9 Hz, 1H), 7.78 (dd, J = 13.9, 2.3 Hz, 1H), 7.69 (t, J = 8.8 Hz, 1H), 7.55 (dd, J = 8.8, 2.3 Hz, 1H), 4.93–4.74 (m, 1H), 4.44 (s, 1H), 4.26 (t, J = 8.9 Hz, 1H), 4.08 (dd, J = 8.9, 6.2 Hz, 1H), 3.92 (dd, J = 12.4, 3.3 Hz, 1H), 3.79 (dd, J = 12.4, 3.8 Hz, 1H). ^{13}C NMR (101 MHz, acetone-d_6) δ 159.7 (d, J = 245.7 Hz), 154.4, 141.4 (d, J = 11.4 Hz), 137.7 (d, J = 1.6 Hz), 137.3 (d, J = 3.0 Hz), 131.3 (d, J = 1.6 Hz), 130.9, 130.9, 130.3 (d, J = 4.2 Hz), 129.5, 120.2 (d, J = 13.3 Hz), 119.9 (q, J = 325.3 Hz), 113.8 (d, J = 3.1 Hz), 105.4 (d, J = 29.0 Hz), 73.5, 62.2, 46.1.

(R)-3-(2-Fluoro-2′-(trifluoromethoxy)-[1,1’-biphenyl]-4-yl)-5-(hydroxymethyl)oxazolidin-2-one (3j).—

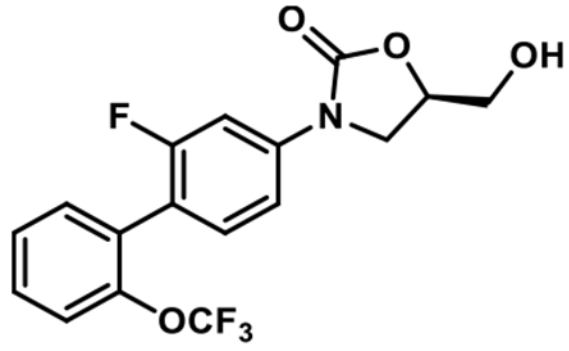

3j

Using general procedure 1, employing 2-(trifluoromethoxy)-phenylboronic acid (25 mg, 0.12 mmol), compound **3j** was obtained after flash column chromatography (SiO_2, eluent gradient 0–100% EtOAc in hexanes) as a yellow oil (32 mg, 86%). ^{1}H NMR (400 MHz, acetone-d_6) δ 7.72 (dd, J = 12.8, 2.2 Hz, 1H), 7.59–7.44 (m, 5H), 7.41 (t, J = 8.4 Hz, 1H),

4.98–4.75 (m, 1H), 4.44 (t, J = 5.9 Hz, 1H), 4.24 (t, J = 8.9 Hz, 1H), 4.06 (dd, J = 8.9, 6.2 Hz, 1H), 3.99–3.86 (m, 1H), 3.84–3.73 (m, 1H). ^{13}C NMR (101 MHz, acetone-d_6) δ 160.4 (d, J = 244.8 Hz), 155.3, 147.5, 141.8 (d, J = 11.2 Hz), 133.1, 132.6 (d, J = 4.6 Hz), 130.7, 129.9, 128.2, 121.7 (d, J = 1.6 Hz), 121.3 (q, J = 256.3 Hz), 119.4 (d, J = 16.4 Hz), 113.9 (d, J = 3.2 Hz), 105.6 (d, J = 28.7 Hz), 74.3, 63.2, 46.9.

Methyl (R)-2′-Fluoro-4′-(5-(hydroxymethyl)-2-oxooxazolidin-3-yl)-[1,1′-biphenyl]-2-carboxylate (3k).—

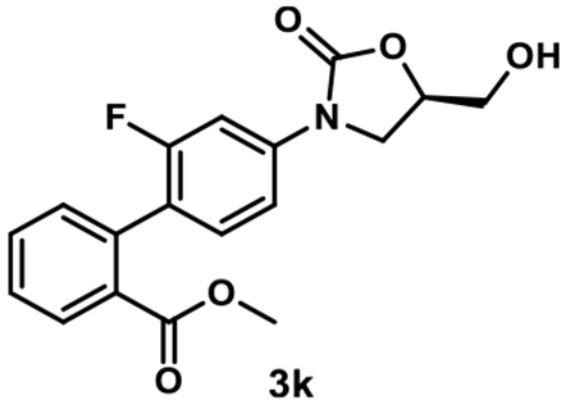

Using general procedure 1, employing 2-methoxycarbonylphenylboronic acid (22 mg, 0.12 mmol), compound **3k** was obtained after flash column chromatography (SiO_2, eluent gradient 0–100% EtOAc in hexanes) followed by preparative TLC (eluent 100% EtOAc) as a yellow oil (33 mg, 94%). ^{1}H NMR (400 MHz, acetone) δ 7.93 (d, J = 7.6 Hz, 1H), 7.74–7.59 (m, 2H), 7.52 (t, J = 7.6 Hz, 1H), 7.45–7.31 (m, 3H), 4.89–4.77 (m, 1H), 4.46 (s, 1H), 4.23 (t, J = 8.8 Hz, 1H), 4.04 (dd, J = 8.8, 6.2 Hz, 1H), 3.91 (dd, J = 12.4, 3.3 Hz, 1H), 3.79 (dd, J = 12.4, 3.8 Hz, 1H), 3.68 (s, 3H). ^{13}C NMR (101 MHz, acetone-d_6) δ 168.2, 160.3 (d, J = 242.6 Hz), 155.3, 141.0 (d, J = 11.1 Hz), 136.7, 132.7, 132.3, 132.1, 131.5 (d, J = 5.0 Hz), 130.7, 128.7, 124.3 (d, J = 16.1 Hz), 113.7 (d, J = 3.1 Hz), 105.2 (d, J = 28.9 Hz), 74.3, 63.2, 52.2, 46.9.

(R)-3-(2-Fluoro-2′,4′-diisopropyl-[1,1′-biphenyl]-4-yl)-5-(hydroxymethyl)oxazolidin-2-one (3l).—

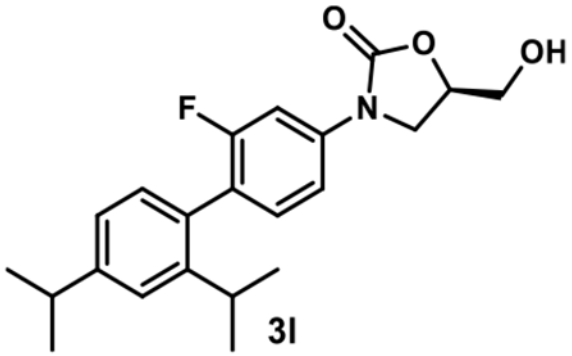

Using general procedure 1, employing [2,4-bis(propan-2-yl)phenyl]-boronic acid (25 mg, 0.12 mmol), compound **3l** was obtained after flash column chromatography (SiO_2, eluent gradient 0–100% EtOAc in hexanes) as a white amorphous solid (33 mg, 89%). ^{1}H NMR (400 MHz, acetone-d_6) δ 7.67 (dd, J = 12.3, 2.3 Hz, 1H), 7.43 (dd, J = 8.5, 2.3 Hz, 1H), 7.32 (s, 1H), 7.27 (t, J = 8.5 Hz, 1H), 7.13 (d, J = 7.9, 1H), 7.6 (d, J = 7.9 Hz, 1H), 4.91–4.71 (m, 1H), 4.40 (t, J = 5.9 Hz, 1H), 4.24 (t, J = 8.8 Hz, 1H), 4.05 (dd, J = 8.8, 6.2 Hz, 1H), 3.92 (ddd, J = 12.4, 5.9, 3.5 Hz, 1H), 3.79 (ddd, J = 12.4, 5.9, 4.0 Hz, 1H), 2.96 (p, J = 7.0 Hz, 1H), 2.82–2.78 (m, 1H), 1.28 (d, J = 7.0 Hz, 6H), 1.25–1.01 (m, 6H). ^{1}H NMR (400 MHz, acetone) δ 7.67 (dd, J = 12.3, 2.3 Hz, 1H), 7.43 (dd, J = 8.5, 2.2 Hz, 1H), 7.32 (d, J = 1.9 Hz, 1H), 7.27 (t, J = 8.5 Hz, 1H), 7.13 (dd, J = 7.8, 1.8 Hz, 1H), 7.06 (d, J = 7.8 Hz, 1H), 4.89–4.75 (m, 1H), 4.40 (t, J = 5.9 Hz, 1H), 4.24 (t, J = 8.8 Hz, 1H), 4.5 (dd, J = 8.8, 6.2 Hz, 1H), 3.92 (ddd, J = 12.4, 5.9, 3.5 Hz, 1H), 3.79 (ddd, J = 12.4, 5.9, 4.0 Hz, 1H), 2.96 (p, J = 6.9 Hz, 1H), 2.84–2.77 (m, 1H), 1.28 (d, J = 6.9 Hz, 6H), 1.22–1.05 (m, 6H). ^{13}C NMR (101 MHz, acetone-d_6) δ 160.6 (d, J = 241.5 Hz), 155.4, 149.8, 148.0, 140.9 (d, J = 10.7 Hz), 132.9 (d, J = 5.0 Hz), 132.5, 131.2, 124.6 (d, J = 17.6 Hz), 124.4 (d, J = 5.2 Hz), 113.9 (d, J = 3.2 Hz), 105.7 (d, J = 29.1 Hz), 74.3, 63.3, 47.1, 35.0, 31.1, 24.5.

(R)-5-(Hydroxymethyl)-3-(2,3′,5′-trifluoro-[1,1′-biphenyl]-4-yl)-oxazolidin-2-one (3m).—

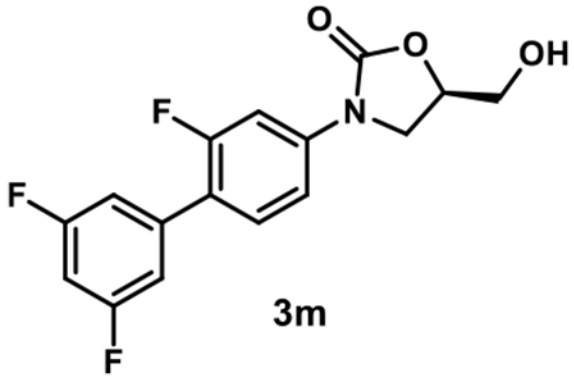

3m

A mixture of compound **2a** (58 mg, 0.2 mmol), 3,5-difluorophenylboronic acid (38 mg, 0.24 mmol), potassium carbonate (110 mg, 0.8 mmol), and [1,1′-bis(diphenylphosphino)ferrocene]-dichloropalladium(II) complex with dichloromethane (16 mg, 0.02 mmol) in dioxane/H_2O (v/v = 9:1, 0.5 mL) was stirred at 90 °C under a nitrogen atmosphere. After the reaction was judged to be completed by TLC (3 h), it was cooled to room temperature, diluted with EtOAc, washed with water, and concentrated under reduced pressure by rotary evaporation. The crude residue was purified by flash column chromatography (SiO_2, eluent gradient 0–100% EtOAc in hexanes) to afford compound **3m** as a yellow amorphous solid (48 mg, 66%). ^{1}H NMR (300 MHz, acetone) δ 7.73 (dd, J = 13.9, 2.3 Hz, 1H), 7.62 (t, J = 8.8 Hz, 1H), 7.53–7.44 (m, 1H), 7.34–7.18 (m, 2H), 7.05 (tt, J = 9.2, 2.3 Hz, 1H), 4.95–4.71 (m, 1H), 4.47–4.37 (m, 1H), 4.25 (t, J = 8.8 Hz, 1H), 4.06 (dd, J = 8.8, 6.2 Hz, 1H), 3.99–3.85 (m, 1H), 3.84–3.67 (m, 1H). ^{13}C NMR (101 MHz, acetone-d_6) δ 163.9 (dd, J = 246.4, 13.1 Hz, 2C), 160.5 (d, J = 246.4 Hz), 155.3, 142.0 (d, J = 12.1 Hz), 139. 7 (td, J = 10.1, 1.0 Hz), 131.6 (d, J = 5.1 Hz), 114.5 (d, J = 3.0 Hz), 112.5

(dd, J = 26.3, 3.0 Hz, 2C), 112.5 (d, J = 12.1, 3.0 Hz), 106.3 (d, J = 29.3 Hz), 103.5 (t, J = 26.3 Hz), 74.4, 63.2, 47.0.

(R)-3-(4-(Benzo[d][1,3]dioxol-5-yl)-3-fluorophenyl)-5-(hydroxymethyl)oxazolidin-2-one (3n).—

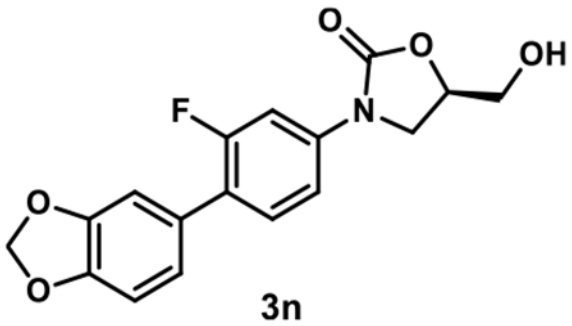

3n

A mixture of compound **2a** (58 mg, 0.2 mmol), 3,4-(methylenedioxy)-phenylboronic acid (40 mg, 0.24 mmol), potassium carbonate (110 mg, 0.8 mmol), and [1,1′-bis(diphenylphosphino)ferrocene]-dichloropalladium(II) complex with dichloromethane (16 mg, 0.02 mmol) in dioxane/H_2O (v/v = 9:1, 0.5 mL) was stirred at 90 °C under a nitrogen atmosphere. After the reaction was judged to be completed by TLC (3 h), it was cooled to room temperature, diluted with EtOAc, washed with water, and concentrated under reduced pressure by rotary evaporation. The crude residue was purified by flash column chromatography (SiO_2, eluent gradient 0–67% EtOAc in hexanes) to afford compound **3n** as a brown amorphous solid (48 mg, 64%). ^{1}H NMR (300 MHz, acetone-d_6) δ 7.67 (dd, J = 13.7, 2.2 Hz, 1H), 7.55–7.35 (m, 2H), 7.12–7.01 (m, 2H), 6.99–6.83 (m, 1H), 6.05 (s, 2H), 4.93–4.68 (m, 1H), 4.39 (t, J = 5.9 Hz, 1H), 4.22 (t, J = 8.9 Hz, 1H), 4.3 (dd, J = 8.9, 6.2 Hz, 1H), 3.91 (ddd, J = 12.3, 5.9, 3.4 Hz, 1H), 3.78 (ddd, J = 12.3, 5.9, 3.9 Hz, 1H). ^{13}C NMR (101 MHz, acetone-d_6) δ 160.5 (d, J = 245.4 Hz), 155.4, 148.9, 148.3, 140.7 (d, J = 11.1 Hz), 131.6 (d, J = 5.1 Hz), 130.1 (d, J = 1.0 Hz), 124.1 (d, J = 14.1 Hz), 123.4 (d, J = 3.0 Hz), 114.4 (d, J = 3.0 Hz), 110.0 (d, J = 4.0 Hz), 109.3, 106.4 (d, J = 29.3 Hz), 102.4, 74.4, 63.3, 47.1.

(R)-3-(3-Fluoro-4-(1H-indol-7-yl)phenyl)-5-(hydroxymethyl)-oxazolidin-2-one (3o).—

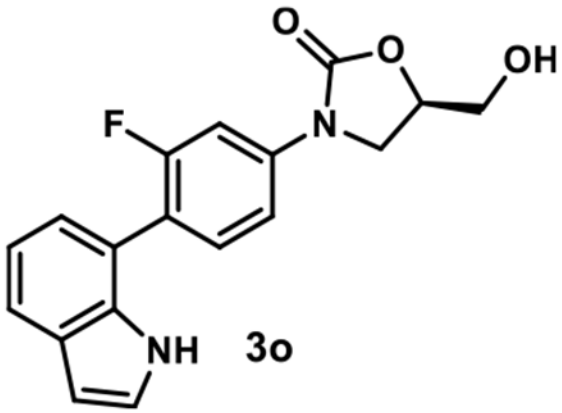

Using general procedure 1, employing 7-(4,4,5,5-tetramethyl-1,3,2-dioxaborolan-2-yl)-1*H*-indole (29 mg, 0.12 mmol), compound **3o** was obtained after flash column chromatography (SiO_2, eluent gradient 0–100% EtOAc in hexanes) as a brown amorphous solid (25 mg, 76%). ^{1}H NMR (400 MHz, acetone-d_6) δ 10.16 (s, 1H), 7.74 (dd, J = 13.0, 2.2 Hz, 1H), 7.63 (t, J = 4.5 Hz, 1H), 7.55 (t, J = 8.4 Hz, 1H), 7.45 (dd, J = 8.4, 2.2 Hz, 1H), 7.34 (t, J = 2.6 Hz, 1H), 7.19–6.98 (m, 2H), 6.56 (t, J = 2.6 Hz, 1H), 5.04–4.75 (m, 1H), 4.44 (s, 1H), 4.25 (t, J = 8.8 Hz, 1H), 4.07 (dd, J = 8.8, 6.1 Hz, 1H), 3.93 (dd, J = 12.4, 3.3 Hz, 1H), 3.79 (dd, J = 12.4, 3.8 Hz, 1H). ^{13}C NMR (101 MHz, acetone-d_6) δ 160.8 (d, J = 244.3 Hz), 155.4, 141.0 (d, J = 11.0 Hz), 135.3, 132.6 (d, J = 5.6 Hz), 129.6, 126.1, 123.4, 122.1 (d, J = 16.4 Hz), 121.1, 120.2, 120.2, 114.4 (d, J = 3.1 Hz), 106.3 (d, J = 28.8 Hz), 102.7, 74.3, 63.2, 47.1.

(R)-3-(3-Fluoro-4-(2-(pyrrolidin-1-yl)pyridin-4-yl)phenyl)-5-(hydroxymethyl)oxazolidin-2-one (8a).—

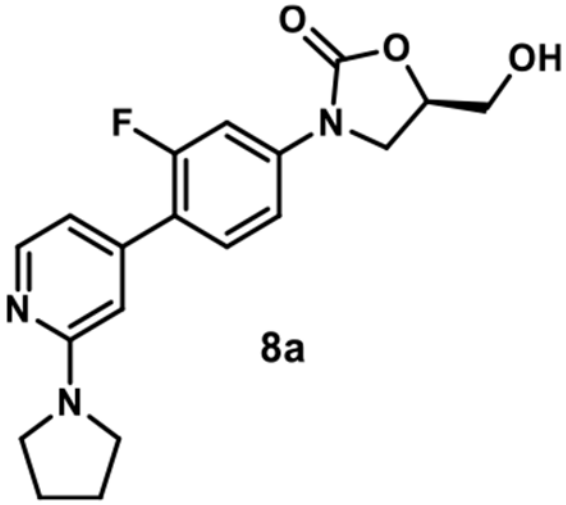

Using general procedure 1, employing 2-(pyrrolidino)pyridine-4-boronic acid pinacol ester (33 mg, 0.12 mmol), compound **8a** was obtained after flash column chromatography (SiO_2, eluent gradient 0–10% MeOH in DCM) followed by washing with acetone (1 mL) as a gray amorphous solid (29 mg, 81%). 1H NMR (600 MHz, acetone-d6) δ 8.12 (d, J = 5.2 Hz, 1H),

7.70 (dd, J = 13.7, 2.2 Hz, 1H),7.60 (t, J = 8.7 Hz, 1H), 7.51–7.44 (m, 1H), 6.70 (d, J = 5.2 Hz, 1H), 6.55 (s, 1H), 4.91–4.75 (m, 1H), 4.39 (t, J = 5.9 Hz, 1H), 4.24 (t, J = 8.7 Hz, 1H), 4.3 (dd, J = 8.7, 6.2 Hz, 1H), 3.95–3.85 (m, 1H), 3.82–3.72 (m, 1H), 3.63–3.37 (m, 4H), 2.02–1.88 (m, 4H). ^{13}C NMR (101 MHz, acetone-d_6) δ 160.9 (d, J = 246.0 Hz), 158.9, 155.4, 149.3, 144.6 (d, J = 1.0 Hz), 141.8 (d, J = 11.4 Hz), 131.6 (d, J = 4.9 Hz), 122.9 (d, J = 13.2 Hz), 114.5 (d, J = 3.1 Hz), 112.1 (d, J = 3.4 Hz), 106.6, 106.4 (d, J = 26.9 Hz), 74.5, 63.3, 47.4, 47.1, 26.3. MSESI m/z: 358.1572 ($C_{19}H_{20}FN_3O_3$ + H^+ requires 358.1561).

Methyl (R)-5-(2-Fluoro-4-(5-(hydroxymethyl)-2-oxooxazolidin-3-yl)phenyl)nicotinate (8b).—

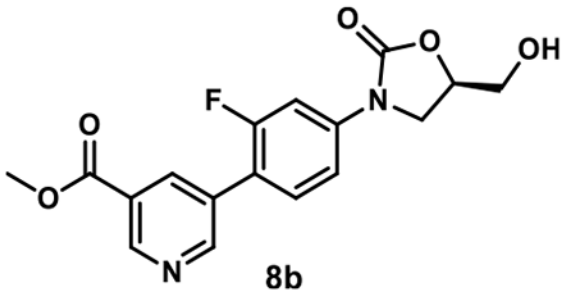

8b

Using general procedure 1, employing methyl 5-(4,4,5,5-tetramethyl-1,3,2-dioxaborolan-2-yl)nicotinate (32 mg, 0.12 mmol), compound **8b** was obtained after flash column chromatography (SiO_2, eluent gradient 0–10% MeOH in DCM) as a yellow amorphous solid (27 mg, 77%). ^{1}H NMR (600 MHz, acetone-d_6) δ 9.11 (d, J = 1.9 Hz, 1H), 8.99 (d, J = 1.9 Hz, 1H), 8.46 (s, 1H), 7.79 (dd, J = 13.7, 2.3 Hz, 1H), 7.69 (t, J = 8.7 Hz, 1H), 7.55 (dd, J = 8.7, 2.3 Hz, 1H), 4.90–4.75 (m, 1H), 4.40 (t, J = 5.9 Hz, 1H), 4.27 (t, J = 8.8 Hz, 1H), 4.08 (dd, J = 8.8, 6.1 Hz, 1H), 3.96 (s, 3H), 3.95–3.89 (m, 1H), 3.82–3.73 (m, 1H). ^{13}C NMR (151 MHz, acetone-d_6) δ 166.3, 160.9 (d, J = 245.6 Hz), 155.4, 154.0 (d, J = 3.6 Hz), 150.1, 142.4 (d, J = 11.3 Hz), 137.3 (d, J = 3.5 Hz), 132.2 (d, J = 1.5 Hz), 131.9 (d, J = 4.2 Hz), 127.0, 119.8 (d, J = 13.9 Hz), 114.9 (d, J = 3.4 Hz), 106.5 (d, J = 28.8 Hz), 74.6, 63.3, 53.0, 47.2. MSESI m/z: 369.0856 ($C_{17}H_{15}FN_2O_5$ + Na^+ requires 369.0857).

(R)-5-(2-Fluoro-4-(5-(hydroxymethyl)-2-oxooxazolidin-3-yl)-phenyl)nicotinic Acid (8c).—

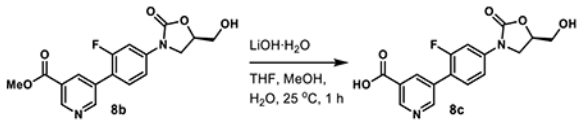

Lithium hydroxide monohydrate (42 mg, 1 mmol) was added to a solution of **8b** (35 mg, 0.1 mmol) in THF (1.5 mL), MeOH (0.5 mL), and H_2O (0.5 mL). The mixture was stirred at 25 °C. After the reaction was judged to be completed by TLC (1 h), it was acidified to pH = 1 with the addition of formic acid and concentrated under reduced pressure by rotary evaporation. The crude residue was purified by flash column chromatography (SiO_2, eluent 10% MeOH in DCM and then 10% MeOH in DCM with 1% formic acid) to give compound **8c** as a yellow amorphous solid (19 mg, 56%). ^{1}H NMR (400 MHz, DMSO-d_6) δ 9.05 (s, 1H), 8.92 (s, 1H), 8.37 (s, 1H), 8.21 (s, 1H), 7.79–7.63 (m, 2H), 7.55–7.41 (m, 1H),

4.81–4.70 (m, 1H), 4.15 (t, J = 8.9 Hz, 1H), 3.90 (dd, J = 8.9, 5.9 Hz, 1H), 3.70 (dd, J = 12.4, 3.2 Hz, 1H), 3.58 (dd, J = 12.4, 3.9 Hz, 1H). ^{13}C NMR (101 MHz, DMSO-d_6) δ 163.5, 159.3 (d, J = 245.2 Hz), 154.4, 151.9 (d, J = 3.6 Hz), 149.2, 140.5 (d, J = 11.4 Hz), 136.3, 131.0 (d, J = 4.1 Hz), 130.3, 128.1, 118.6 (d, J = 13.4 Hz), 114.0 (d, J = 3.0 Hz), 105.3 (d, J = 28.4 Hz), 73.5, 61.7, 46.0. MSESI m/z: 355.0733 ($C_{16}H_{13}FN_2O_5$ + Na^+ requires 355.0701).

(R)-3-(4-Bromo-3-fluorophenyl)-5-((methoxymethoxy)methyl)-oxazolidin-2-one (4).—

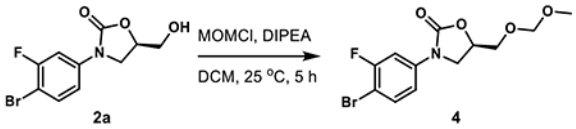

To a solution of compound **2a** (300 mg, 1.04 mmol) in DCM (5 mL), *N,N*-diisopropylethylamine (0.54 mL, 3.11 mmol) and methyl chloromethyl ether (0.24 mL, 3.11 mmol) were added. The reaction mixture was stirred at 25 °C. After the reaction was judged to be completed by TLC (5 h), it was diluted with EtOAc, washed with water, and concentrated under reduced pressure by rotary evaporation. The crude residue was purified by flash column chromatography (SiO_2, eluent gradient 0–67% EtOAc in hexanes) to afford compound **4** as a white amorphous solid (296 mg, 85%). ^{1}H NMR (300 MHz, acetone-d_6) δ 7.74 (dd, J = 11.6, 2.6 Hz, 1H), 7.64 (dd, J = 8.9, 8.0 Hz, 1H), 7.37 (ddd, J = 8.9, 2.6, 1.0 Hz, 1H), 4.95 (dddd, J = 9.0, 6.2, 4.4, 3.5 Hz, 1H), 4.66 (s, 2H), 4.26 (t, J = 9.0 Hz, 1H), 4.00 (dd, J = 9.0, 6.2 Hz, 1H), 3.86 (dd, J = 11.3, 3.5 Hz, 1H), 3.80 (dd, J = 11.3, 4.4 Hz, 1H), 3.32 (s, 3H). ^{13}C NMR (101 MHz, acetone-d_6) δ 159.7 (d, J = 243.1 Hz), 155.0, 141.2 (d, J = 10.0 Hz), 134.3 (d, J = 1.8 Hz), 115.6 (d, J = 3.4 Hz), 106.9 (d, J = 28.2 Hz), 102.1 (d, J = 21.1 Hz), 97.3, 72.7, 68.6, 55.4, 47.4.

General Procedure 2: Synthesis of Heterocyclic Oxazolidinone Analogues 3p–r.

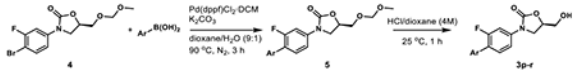

A mixture of compound **4** (67 mg, 0.2 mmol), aryl boronic acid (0.24 mmol), potassium carbonate (110 mg, 0.8 mmol), and [1,1′-bis(diphenylphosphino)ferrocene]dichloropalladium(II) complex with dichloromethane (16 mg, 0.02 mmol) in dioxane/H_2O (v/v = 9:1, 0.5 mL) was stirred at 90 °C under a nitrogen atmosphere. After the reaction was judged to be completed by TLC (3 h), it was cooled to room temperature, diluted with EtOAc, washed with water, and concentrated under reduced pressure by rotary evaporation. The crude residue was purified by flash column chromatography (SiO_2, eluent gradient 0–40% EtOAc in hexanes) to afford compound **5**. Compound **5** (25 mg) was added to HCl/dioxane (4 M, 1 mL), and the mixture was stirred at 25 °C. After the reaction was judged to be completed by TLC (1 h), its solvent was evaporated (the residue was purified by flash column chromatography (SiO_2) if necessary) to afford compounds **3p–r**.

(R)-3-(2-Fluoro-4′-methyl-[1,1′-biphenyl]-4-yl)-5-((methoxymethoxy)methyl)oxazolidin-2-one (5a).—

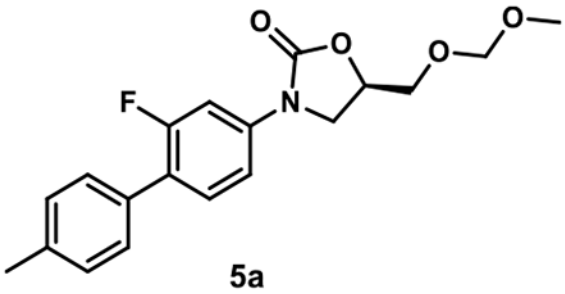

5a

Using general procedure 2, employing 4-methylphenylboronic acid (33 mg, 0.24 mmol), compound **5a** was obtained as a yellow amorphous solid (68 mg, 98%). ^{1}H NMR (300 MHz, chloroform-*d*) δ 7.51 (dd, J = 12.8, 2.3 Hz, 1H), 7.47–7.38 (m, 3H), 7.34 (dd, J = 8.6, 2.3 Hz, 1H), 7.28–7.21 (m, 2H), 4.92–4.74 (m, 1H), 4.69 (s, 2H), 4.33–4.04 (m, 1H), 3.96 (dd, J = 8.7, 6.2 Hz, 1H), 3.85 (dd, J = 11.1, 4.2 Hz, 1H), 3.78 (dd, J = 11.1, 4.1 Hz, 1H), 3.39 (s, 3H), 2.40 (s, 3H).

(R)-3-(2-Fluoro-4′-methyl-[1,1′-biphenyl]-4-yl)-5-(hydroxymethyl)oxazolidin-2-one (3p).—

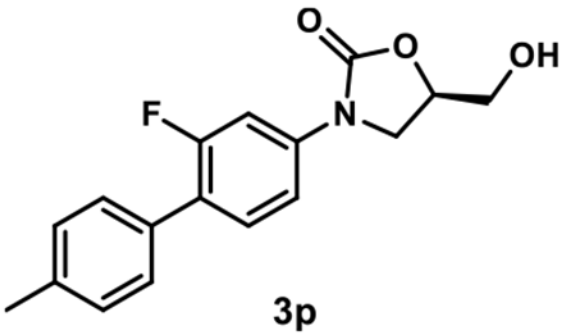

3p

Using general procedure 2, employing **5a** (25 mg, 0.072 mmol), compound **3p** was obtained (without flash column chromatography) as a yellow amorphous solid (22 mg, 100%). ^{1}H NMR (300 MHz, methanol-d_4) δ 7.61 (dd, J = 13.4, 2.2 Hz, 1H), 7.50–7.32 (m, 4H), 7.25 (d, J = 7.9 Hz, 2H), 4.83–4.71 (m, 1H), 4.16 (t, J = 8.9 Hz, 1H), 3.96 (dd, J = 8.9, 6.4 Hz, 1H), 3.87 (dd, J = 12.5, 3.2 Hz, 1H), 3.71 (dd, J = 12.5, 4.0 Hz, 1H), 2.38 (s, 3H). ^{13}C NMR (101 MHz, methanol-d_4) δ 161.0 (d, J = 245.2 Hz), 156.9, 140.3 (d, J = 11.0 Hz), 138.5, 133.7, 131.8 (d, J = 5.0 Hz), 130.2 (2C), 129.7 (d, J = 3.2 Hz, 2C), 125.5 (d, J = 13.8 Hz), 115.0 (d, J = 3.4 Hz), 107.2 (d, J = 29.3 Hz), 75.2, 63.3, 47.6, 21.2.

(R)-3-(2,4′-Difluoro-[1,1′-biphenyl]-4-yl)-5-((methoxymethoxy)-methyl)oxazolidin-2-one (5b).—

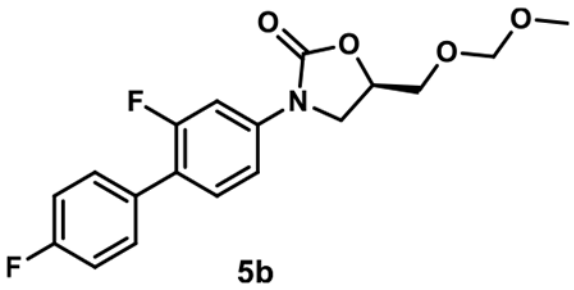

5b

A mixture of compound **4** (50 mg, 0.15 mmol), 4-fluorophenylboronic acid (25 mg, 0.18 mmol), potassium carbonate (83 mg, 0.6 mmol), and [1,1'-bis(diphenylphosphino)ferrocene]dichloropalladium(II) complex with dichloromethane (12 mg, 0.015 mmol) in dioxane/H_2O (v/v = 9:1, 0.4 mL) was stirred at 90 °C under a nitrogen atmosphere for 2 h. The mixture was cooled to room temperature, diluted with EtOAc, washed with water, and concentrated under reduced pressure by rotary evaporation. The crude residue was purified by flash column chromatography (SiO_2, eluent gradient 0–40% EtOAc in hexanes) to afford compound **5b** as a yellow amorphous solid (45 mg, 85%). ^{1}H NMR (300 MHz, $CDCl_3$) δ 7.63–7.32 (m, 5H), 7.21–7.08 (m, 2H), 4.93–4.76 (m, 1H), 4.69 (s, 2H), 4.10 (t, J = 8.8 Hz, 1H), 3.97 (dd, J = 8.8, 6.2 Hz, 1H), 3.91–3.73 (m, 2H), 3.39 (s, 3H).

(R)-3-(2,4′-Difluoro-[1,1′-biphenyl]-4-yl)-5-(hydroxymethyl-oxazolidin-2-one (3q).—

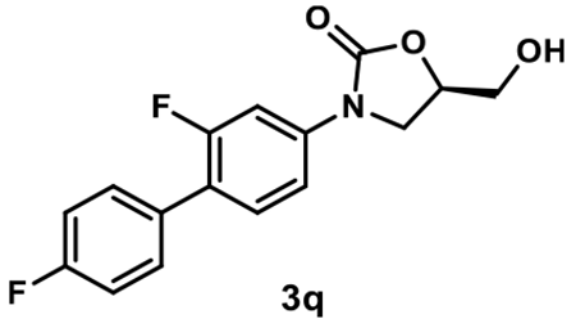

3q

Using general procedure 2, employing **5b** (25 mg, 0.072 mmol), compound **3q** was obtained after flash column chromatography (SiO_2, eluent gradient 0–100% EtOAc in hexanes) as a white amorphous solid (11 mg, 50%). ^{1}H NMR (400 MHz, acetone-d_6) δ 7.70 (dd, J = 13.7, 2.2 Hz, 1H), 7.65–7.57 (m, 2H), 7.57–7.50 (m, 1H), 7.46 (dd, J = 8.6, 2.2 Hz, 1H), 7.35–7.11 (m, 2H), 4.93–4.76 (m, 1H), 4.52–4.31 (m, 1H), 4.23 (t, J = 9.0 Hz, 1H), 4.11–3.98 (m, 1H), 3.96–3.85 (m, 1H), 3.82–3.71 (m, 1H). ^{13}C NMR (101 MHz, acetone-d_6) δ 163.2 (d, J = 245.2 Hz), 160.4 (d, J = 244.2 Hz), 155.3, 141.1 (d, J = 11.1 Hz), 132. 5 (dd, J = 3.0, 1.0 Hz), 131.6 (d, J = 3.8 Hz, 2C), 131.5 (d, J = 3.1 Hz), 123. 1 (d, J = 13.9 Hz), 116.2 (d, J = 21.6 Hz, 2C), 114.4 (d, J = 3.2 Hz), 106.3 (d, J = 29.1 Hz), 74.3, 63.2, 47.0.

(R)-3-(2-Fluoro-4′-methoxy-[1,1′-biphenyl]-4-yl)-5-((methoxymethoxy)methyl)oxazolidin-2-one (5c).—

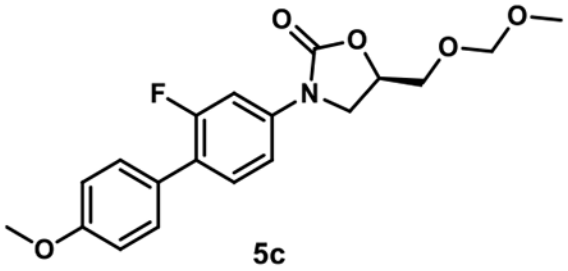

5c

Using general procedure 2, employing 4-methoxyphenylboronic acid (36 mg, 0.24 mmol), compound **5c** was obtained as a yellow amorphous solid (66 mg, 90%). ^{1}H NMR (300 MHz, chloroform-*d*) δ 7.57–7.30 (m, 5H), 6.98 (d, *J* = 8.7 Hz, 2H), 4.83 (ddt, *J* = 8.6, 6.2, 4.2 Hz, 1H), 4.69 (s, 2H), 4.10 (t, *J* = 8.6 Hz, 1H), 3.96 (dd, *J* = 8.6, 6.2 Hz, 1H), 3.93–3.63 (m, 5H), 3.39 (s, 3H).

(R)-3-(2-Fluoro-4′-methoxy-[1,1′-biphenyl]-4-yl)-5-(hydroxymethyl)oxazolidin-2-one (3r).—

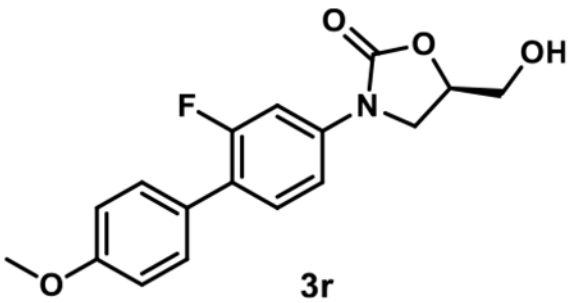

3r

Using general procedure 2, employing **5c** (25 mg, 0.069 mmol), compound **3r** was obtained (without flash column chromatography) as a yellow amorphous solid (22 mg, 100%). ^{1}H NMR (300 MHz, acetone-d_6) δ 7.67 (dd, *J* = 13.7, 2.3 Hz, 1H), 7.55–7.38 (m, 4H), 7.09–6.98 (m, 2H), 4.91–4.72 (m, 1H), 4.39 (dd, *J* = 6.2, 5.6 Hz, 1H), 4.22 (t, *J* = 8.9 Hz, 1H), 4.03 (dd, *J* = 8.9, 6.3 Hz, 1H), 3.95–3.87 (m, 1H), 3.84 (s, 3H), 3.83–3.73 (m, 1H). ^{13}C NMR (101 MHz, acetone-d_6) δ 160.4 (d, *J* = 245.4 Hz), 160.3, 155.3, 140.4 (d, *J* = 11.1 Hz), 131.4 (d, *J* = 5.0 Hz), 130.7 (d, *J* = 3.1 Hz, 2C), 128.4 (d, *J* = 1.3 Hz), 124.0 (d, *J* = 13.7 Hz), 114.9 (2C), 114.4 (d, *J* = 3.3 Hz), 106.3 (d, *J* = 29.3 Hz), 74.3, 63.2, 55.6, 47.0. MSESI *m/z*: 340.0943 ($C_{17}H_{16}FNO_4$ + Na^+ requires 340.0956).

(R)-3-(3-Fluoro-4-iodophenyl)-5-(hydroxymethyl)oxazolidin-2-one (6).[38]—

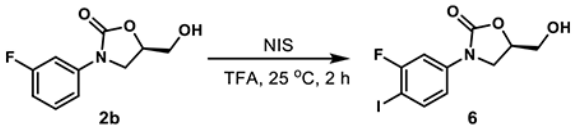

2b 6

N-Iodosuccinimide (6.31 g, 28.0 mmol) was added to a solution of compound **2b** (5.64 g, 26.7 mmol) in TFA (130 mL). The mixture was stirred at 25 °C. After the reaction was judged to be completed by TLC (2 h), it was concentrated under reduced pressure by rotary evaporation. The residue was dissolved in EtOAc and washed with saturated aqueous

sodium carbonate until the aqueous phase was basic. The organic layer was evaporated under reduced pressure by rotary evaporation, and the residue was purified by flash column chromatography (SiO_2, eluent gradient 0–100% EtOAc in hexanes) to afford compound **6** as a gray amorphous solid (6.9 g, 77%). ^{1}H NMR (400 MHz, acetone-d_6) δ 7.87 (dd, J = 8.8, 7.4 Hz, 1H), 7.67 (dd, J = 11.0, 2.5 Hz, 1H), 7.27 (ddd, J = 8.8, 2.5, 0.7 Hz, 1H), 4.80 (dddd, J = 9.3, 6.2, 4.1, 3.3 Hz, 1H), 4.13 (t, J = 9.3 Hz, 1H), 4.03–3.84 (m, 2H), 3.80–3.70 (m, 1H), 3.33 (t, J = 5.9 Hz, 1H).

(R)-3-(3-Fluoro-4-(4,4,5,5-tetramethyl-1,3,2-dioxaborolan-2-yl)-phenyl)-5-(hydroxymethyl)oxazolidin-2-one (7).[38]—

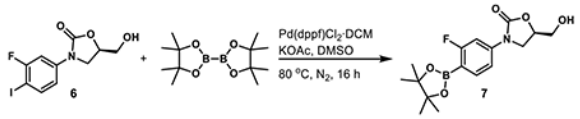

To a solution of compound **6** (3.37 g, 10 mmol) in anhydrous DMSO (40 mL), [1,1′-bis(diphenylphosphino)ferrocene]dichloropalladium-(II) complex with dichloromethane (408 mg, 0.5 mmol), potassium acetate (4.91 g, 50 mmol), and bis(pinacolato)diboron (5.08 g, 20 mmol) were added. The reaction mixture was stirred at 80 °C under a nitrogen atmosphere. After the reaction was judged to be completed by TLC (16 h), it was cooled to room temperature, treated with the addition of MeOH (20 mL), and filtered through celite. The filtrate was concentrated under reduced pressure by rotary evaporation to remove MeOH, dissolved in EtOAc, washed with water, and evaporated under reduced pressure by rotary evaporation. The crude residue was purified by flash column chromatography (SiO_2, eluent gradient 0–100% EtOAc in hexanes) to afford compound **7** as a yellow amorphous solid (1.64 g, 49%). ^{1}H NMR (400 MHz, acetone-d_6) δ 7.75–7.67 (m, 1H), 7.55 (dd, J = 12.2, 2.0 Hz, 1H), 7.37 (dd, J = 8.3, 2.0 Hz, 1H), 4.91–4.74 (m, 1H), 4.40 (t, J = 5.9 Hz, 1H), 4.20 (t, J = 8.9 Hz, 1H), 4.01 (dd, J = 8.9, 6.2 Hz, 1H), 3.90 (ddd, J = 12.3, 5.9, 3.3 Hz, 1H), 3.76 (ddd, J = 12.3, 5.9, 4.0 Hz, 1H), 1.33 (s, 12H).

General Procedure 3: Synthesis of Heterocyclic Oxazolidinone Analogues 3s–x, 8d–m.

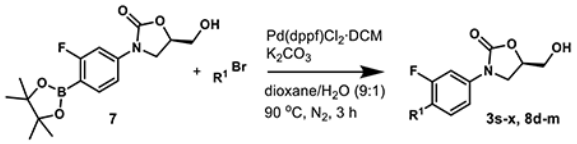

A mixture of compound **7** (34 mg, 0.1 mmol), heterocyclic bromide, potassium carbonate (55 mg, 0.4 mmol), and [1,1′-bis-(diphenylphosphino)ferrocene]dichloropalladium(II) complex with dichloromethane (8.2 mg, 0.01 mmol) in dioxane/H_2O (v/v = 9:1, 0.5 mL) was stirred at 90 °C under a nitrogen atmosphere for 3 h. The reaction mixture was cooled to room temperature, diluted with EtOAc, washed with water, and concentrated under reduced pressure by rotary evaporation. The crude residue was purified by flash column chromatography (SiO_2, eluent gradient 0–10% MeOH in DCM) to afford compound **3s–x** and **8d–m**. If not pure, compounds **3s–x** and **8d–m** were further purified by washing with EtOAc (1 mL).

(R)-3-(2-Fluoro-4′-(trifluoromethyl)-[1,1′-biphenyl]-4-yl)-5-(hydroxymethyl)oxazolidin-2-one (3s).—

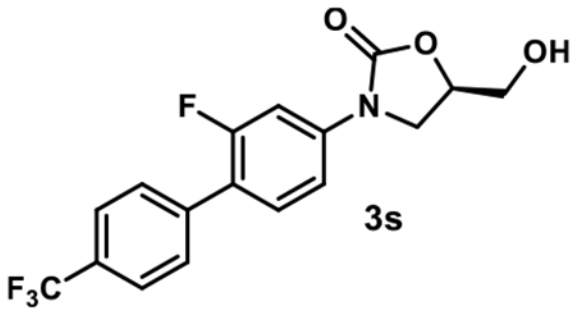

Using general procedure 3, employing 1-bromo-4-(trifluoromethyl)-benzene (45 mg, 0.2 mmol), compound **3s** was obtained by flash column chromatography (SiO_2, eluent gradient 0–100% EtOAc in hexanes) as a white amorphous solid (16 mg, 45%). ^{1}H NMR (400 MHz, acetone-d_6) δ 7.81 (s, 4H), 7.75 (dd, J = 13.8, 2.2 Hz, 1H), 7.62 (t, J = 8.6 Hz, 1H), 7.51 (dd, J = 8.6, 2.3 Hz, 1H), 4.91–4.75 (m, 1H), 4.41 (s, 1H), 4.25 (t, J = 8.9 Hz, 1H), 4.07 (dd, J = 8.9, 6.2 Hz, 1H), 3.95–3.88 (m, 1H), 3.84–3.74 (m, 1H). ^{13}C NMR (101 MHz, acetone-d_6) δ 160.6 (d, J = 245.5 Hz), 155.3, 141.8 (d, J = 11.4 Hz), 140.3, 131.8 (d, J = 4.5 Hz), 130.3 (d, J = 3.4 Hz, 2C), 129.7 (d, J = 32.2 Hz), 126.3 (q, J = 3.9 Hz, 2C), 125.2 (q, J = 253.6 Hz), 122.5 (d, J = 13.4 Hz), 114.5 (d, J = 3.3 Hz), 106.3 (d, J = 29.1 Hz), 74.4, 63.2, 47.0. MSESI m/z: 356.0900 ($C_{17}H_{13}F_4NO_3$ + H^+ requires 356.0904).

(R)-3-(2-Fluoro-4′-(trifluoromethoxy)-[1,1′-biphenyl]-4-yl)-5-(hydroxymethyl)oxazolidin-2-one (3t).—

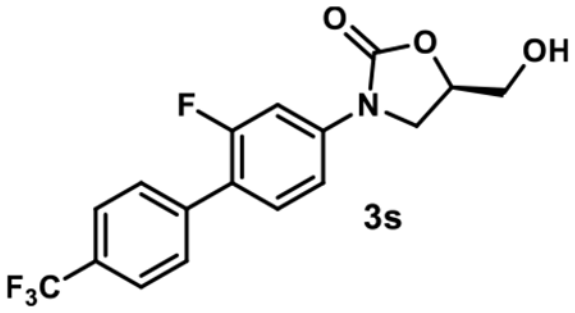

Using general procedure 3, employing 1-bromo-4-(trifluoromethoxy)-benzene (48 mg, 0.2 mmol), compound **3t** was obtained by flash column chromatography (SiO_2, eluent gradient 0–100% EtOAc in hexanes) as a white amorphous solid (17 mg, 46%). ^{1}H NMR (400 MHz, acetone-d_6) δ 7.78–7.65 (m, 3H), 7.57 (t, J = 8.7 Hz, 1H), 7.48 (dd, J = 8.7, 2.3 Hz, 1H), 7.46–7.40 (m, 2H), 4.93–4.73 (m, 1H), 4.40 (s, 1H), 4.24 (t, J = 8.9 Hz, 1H), 4.06 (dd, J = 8.9, 6.2 Hz, 1H), 3.95–3.87 (m, 1H), 3.81–3.75 (m, 1H). ^{13}C NMR (101 MHz, acetone-d_6) δ 160.6 (d, J = 245.0 Hz), 155.4, 149.4 (d, J = 1.9 Hz), 141.5 (d, J = 11.2 Hz), 135.6 (d, J = 1.6 Hz), 131.8 (d, J = 4.6 Hz), 131.5 (d, J = 3.3 Hz, 2C), 122.7 (d, J = 13.7 Hz), 122.1 (2C), 121.6 (q, J = 255.6 Hz), 114.6 (d, J = 3.2 Hz), 106.4 (d, J = 29.0 Hz), 74.5, 63.3, 47.1. MSEI m/z: 371.0775 ($C_{17}H_{13}F_4NO_3$ (M^+) requires 371.0781).

(R)-2′-Fluoro-4′-(5-(hydroxymethyl)-2-oxooxazolidin-3-yl)-[1,1′-biphenyl]-4-carboxylic Acid (3u).—

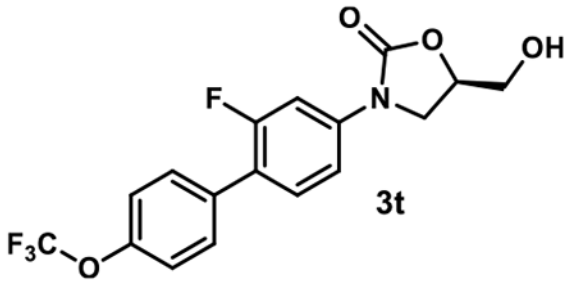

A mixture of compound 7 (40 mg, 0.12 mmol), 4-bromobenzoic acid (20 mg, 0.1 mmol), potassium carbonate (55 mg, 0.4 mmol), and [1,1′-bis(diphenylphosphino)ferrocene]dichloropalladium(II) complex with dichloromethane (8.2 mg, 0.01 mmol) in dioxane/H_2O (v/v = 9:1, 0.5 mL) was stirred at 90 °C under a nitrogen atmosphere. After the reaction was judged to be completed by TLC (3 h), formic acid (1 mL) was added to acidify the reaction. The mixture was concentrated under reduced pressure by rotary evaporation. The crude residue was purified by flash column chromatography (SiO_2, eluent gradient 0–15% MeOH in DCM with 1% formic acid). The appropriate fractions were concentrated under reduced pressure by rotary evaporation, and the resulting residue was washed with MeOH (2 mL) to give compound **3u** as a white amorphous solid (10 mg, 30%). ^{1}H NMR (400 MHz, DMSO-d_6) δ 8.03 (d, J = 8.4 Hz, 2H), 7.74–7.59 (m, 4H), 7.49 (dd, J = 8.6, 2.3 Hz, 1H), 5.27 (s, 1H), 4.86–4.68 (m, 1H), 4.14 (t, J = 8.9 Hz, 1H), 3.89 (dd, J = 8.9, 6.1 Hz, 1H), 3.70 (dd, J = 12.4, 3.3 Hz, 1H), 3.57 (dd, J = 12.4, 3.9 Hz, 1H). ^{13}C NMR (101 MHz, DMSO-d_6) δ 167.1, 159.1 (d, J = 245.4 Hz), 154.4, 140.1 (d, J = 11.2 Hz), 139.0, 131.0 (d, J = 4.5 Hz), 129.8, 129.7 (2C), 128.8 (d, J = 3.3 Hz, 2C), 121.6 (d, J = 13.0 Hz), 113.9 (d, J = 3.0 Hz), 105.4 (d, J = 28.6 Hz), 73.5, 61.6, 46.0. MSESI *m/z*: 330.0766 ($C_{17}H_{13}FNO_5^-$ requires 330.0783).

(R)-2′-Fluoro-N′-hydroxy-4′-(5-(hydroxymethyl)-2-oxooxazolidin-3-yl)-[1,1′-biphenyl]-4-carboximidamide (3v).—

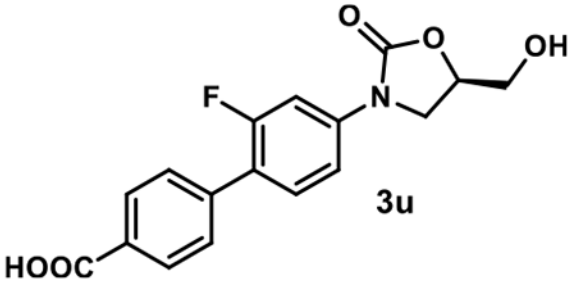

A mixture of compound **7** (40 mg, 0.12 mmol), compound **14** (22 mg, 0.1 mmol), potassium carbonate (55 mg, 0.4 mmol), and [1,1′-bis(diphenylphosphino)ferrocene]dichloropalladium(II) complex with dichloromethane (8.2 mg, 0.01 mmol) in dioxane/H_2O (v/v = 9:1, 0.5 mL) was stirred at 90 °C under a nitrogen atmosphere. After the reaction was judged to be completed by TLC (3 h), it was concentrated under reduced pressure by rotary evaporation. The crude residue was

purified by flash column chromatography (SiO_2, eluent gradient 0–20% MeOH in DCM) and preparative TLC (eluent, 15% MeOH in DCM) to give compound **3v** as a yellow amorphous solid (17 mg, 49%). ^{1}H NMR (300 MHz, DMSO-d_6) δ 9.71 (s, 1H), 7.85–7.72 (m, 2H), 7.68–7.52 (m, 4H), 7.46 (dd, J = 8.6, 2.2 Hz, 1H), 5.87 (s, 2H), 5.25 (t, J = 5.6 Hz, 1H), 4.80–4.68 (m, 1H), 4.14 (t, J = 9.0 Hz, 1H), 3.88 (dd, J = 9.0, 6.1 Hz, 1H), 3.70 (ddd, J = 12.3, 5.6, 3.3 Hz, 1H), 3.57 (ddd, J = 12.3, 5.6, 4.0 Hz, 1H). ^{13}C NMR (101 MHz, DMSO-d_6) δ 159.1 (d, J = 244.8 Hz), 154.4, 150.5, 139.6 (d, J = 11.2 Hz), 135.1 (d, J = 1.7 Hz), 132.6, 130.8 (d, J = 5.0 Hz), 128.3 (d, J = 3.3 Hz, 2C), 125.6 (2C), 122.1 (d, J = 13.3 Hz), 113.8 (d, J = 3.1 Hz), 105.4 (d, J = 28.8 Hz), 73.4, 61.6, 46.0. MSESI *m/z*: 346.1187 ($C_{17}H_{16}FN_3O_4$ + H^+ requires 346.1198).

(S)-2-((tert-Butoxycarbonyl)amino)-3-(2′-fluoro-4′-((R)-5-(hydroxymethyl)-2-oxooxazolidin-3-yl)-[1,1′-biphenyl]-3-yl)propanoic Acid (3w).—

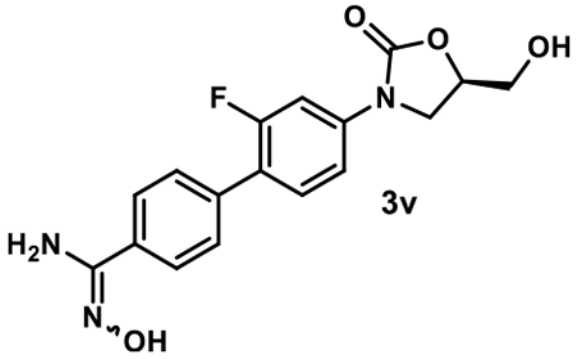

A mixture of compound **7** (80 mg, 0.24 mmol), (*S*)-*N*-boc-3-bromophenylalanine (69 mg, 0.2 mmol), potassium carbonate (110 mg, 0.8 mmol), and [1,1′-bis(diphenylphosphino)ferrocene]-dichloropalladium(II), complex with dichloromethane (16 mg, 0.02 mmol) in dioxane/H_2O (v/v = 9:1, 1.0 mL) was stirred at 90 °C under a nitrogen atmosphere. After the reaction was judged to be completed by TLC (3 h), it was cooled to room temperature, diluted with EtOAc, washed with water, and concentrated under reduced pressure by rotary evaporation. The crude residue was purified by flash column chromatography (SiO_2, eluent gradient 0–10% MeOH in DCM with 1% formic acid) to afford compound **3w** as a yellow amorphous solid (34 mg, 36%). ^{1}H NMR (400 MHz, acetone-d_6) δ 7.70 (dd, J = 13.6, 2.3 Hz, 1H), 7.55 (t, J = 8.7 Hz, 1H), 7.50–7.42 (m, 3H), 7.39 (t, J = 7.5 Hz, 1H), 7.30 (d, J = 7.5 Hz, 1H), 6.11 (d, J = 8.4 Hz, 1H), 4.95–4.71 (m, 1H), 4.57–4.42 (m, 1H), 4.41–4.35 (m, 1H), 4.22 (t, J = 8.9 Hz, 1H), 4.04 (dd, J = 8.9, 6.2 Hz, 1H), 3.91 (dd, J = 12.3, 3.4 Hz, 1H), 3.78 (dd, J = 12.3, 3.9 Hz, 1H), 3.29 (dd, J = 13.8, 4.9 Hz, 1H), 3.08 (dd, J = 13.8, 8.8 Hz, 1H), 1.34 (s, 9H). ^{13}C NMR (101 MHz, acetone-d_6) δ 173.8, 160.5 (d, J = 245.0 Hz), 156.2, 155.3, 140.8 (d, J = 11.2 Hz), 138.9, 136.1, 131.7 (d, J = 5.0 Hz), 130.6 (d, J = 2.7 Hz), 129.4, 129.3, 127.9 (d, J = 3.6 Hz), 124.1 (d, J = 13.5 Hz), 114.3 (d, J = 3.4 Hz), 106.2 (d, J = 29.1 Hz), 79.2, 74.3, 63.1, 55.7, 46.9, 38.1, 28.5.

(S)-2-Amino-3-(2′-fluoro-4′-((R)-5-(hydroxymethyl)-2-oxooxazolidin-3-yl)-[1,1′-biphenyl]-3-yl)propanoic Acid Hydrochloride (3x).—

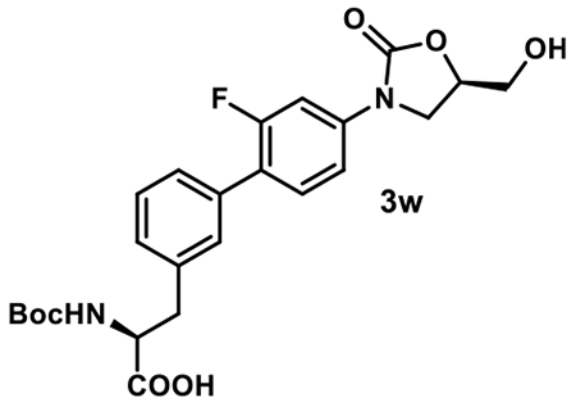

A mixture of compound **3w** (20 mg, 0.042 mmol) in HCl/dioxane (4 M, 1 mL) was stirred at 25 °C. After the reaction was judged to be completed by TLC (30 min), its solvent was removed under reduced pressure by rotary evaporation. The resulting residue was washed with acetone (1 mL) and dried under high vacuum to give **3x** as a yellow amorphous solid (16 mg, 91%). ^{1}H NMR (400 MHz, DMSO-d_6) δ 8.51 (s, 3H), 7.69–7.56 (m, 2H), 7.53–7.38 (m, 4H), 7.30 (d, J = 7.4 Hz, 1H), 5.33 (s, 1H), 4.81–4.67 (m, 1H), 4.22 (t, J = 6.1 Hz, 1H), 4.13 (t, J = 8.9 Hz, 1H), 3.91 (dd, J = 8.9, 6.0 Hz, 1H), 3.69 (dd, J = 12.3, 3.3 Hz, 1H), 3.62–3.52 (m, 1H), 3.21 (d, J = 6.1 Hz, 2H). ^{13}C NMR (101 MHz, DMSO-d_6) δ 170.4, 159.0 (d, J = 244.9 Hz), 154.4, 139.5 (d, J = 11.1 Hz), 135.5, 134.9, 131.0 (d, J = 4.8 Hz), 129.8, 128.9, 128.8, 127.6 (d, J = 3.2 Hz), 122.5 (d, J = 13.1 Hz), 113.8 (d, J = 2.5 Hz), 105.4 (d, J = 28.8 Hz), 73.4, 61.6, 53.1, 46.0, 35.6. MSESI *m/z*: 375.1360 ($C_{19}H_{19}FN_2O_5$ + H^+ requires 375.1351).

(R)-3-(3-Fluoro-4-(pyridin-4-yl)phenyl)-5-(hydroxymethyl)-oxazolidin-2-one (8d).—

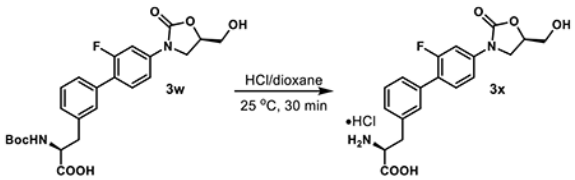

Using general procedure 3, employing 4-bromopyridine hydrochloride (25 mg, 0.13 mmol), compound **8d** was obtained as a brown amorphous solid (21 mg, 73%). ^{1}H NMR (400 MHz, DMSO-d_6) δ 8.65 (d, J = 5.0 Hz, 2H), 7.78–7.64 (m, 2H), 7.59 (d, J = 5.0 Hz, 2H), 7.54–7.47 (m, 1H), 5.27 (t, J = 5.5 Hz, 1H), 4.82–4.70 (m, 1H), 4.14 (t, J = 8.9 Hz, 1H), 3.89 (dd, J = 8.9, 6.1 Hz, 1H), 3.74–3.65 (m, 1H), 3.63–3.52 (m, 1H). ^{13}C NMR (101 MHz, DMSO-d_6) δ 159.4 (d, J = 247.0 Hz), 154.4, 150.0 (2C), 142.1, 140.9 (d, J = 11.4 Hz), 130.8 (d, J = 4.5 Hz), 123.1 (d, J = 3.8 Hz, 2C), 119.7 (d, J = 12.4 Hz), 113.9 (d, J = 3.0 Hz), 105.4 (d, J = 28.6 Hz), 73.5, 61.6, 46.0. MSESI *m/z*: 289.0965 ($C_{15}H_{13}FN_2O_3$ + H^+ requires 289.0983).

(R)-3-(3-Fluoro-4-(pyridin-3-yl)phenyl)-5-(hydroxymethyl)-oxazolidin-2-one (8e).—

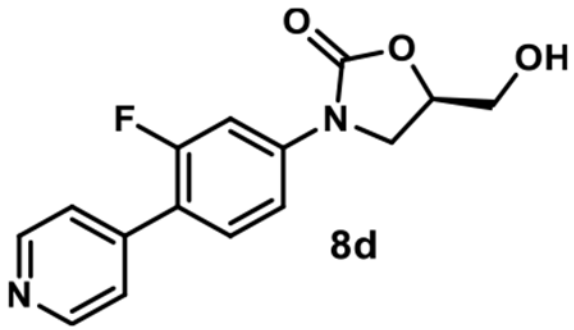

8d

Using general procedure 3, employing 3-bromopyridine (12.5 μL, 0.13 mmol), compound **8e** was obtained as a white amorphous solid (20 mg, 70%). ^{1}H NMR (300 MHz, DMSO-d_6) δ 8.76 (s, 1H), 8.63–8.53 (m, 1H), 7.97 (d, J = 7.9 Hz, 1H), 7.75–7.60 (m, 2H), 7.55–7.43 (m, 2H), 5.28 (s, 1H), 4.84–4.69 (m, 1H), 4.14 (t, J = 8.9 Hz, 1H), 3.89 (dd, J = 8.9, 6.1 Hz, 1H), 3.79–3.64 (m, 1H), 3.63–3.52 (m, 1H). ^{13}C NMR (101 MHz, DMSO-d_6) δ 159.2 (d, J = 245.0 Hz), 154.4, 149.0 (d, J = 3.7 Hz), 148.6, 140.2 (d, J = 11.3 Hz), 136.0 (d, J = 3.2 Hz), 131.0 (d, J = 4.5 Hz), 130.6, 123.7, 119.4 (d, J = 13.7 Hz), 114.0 (d, J = 3.1 Hz), 105.3 (d, J = 28.5 Hz), 73.5, 61.6, 46.0. MSESI *m/z*: 289.0965 ($C_{15}H_{13}FN_2O_3$ + H^+ requires 289.0983).

(R)-3-(3-Fluoro-4-(pyridin-2-yl)phenyl)-5-(hydroxymethyl)-oxazolidin-2-one (8f).—

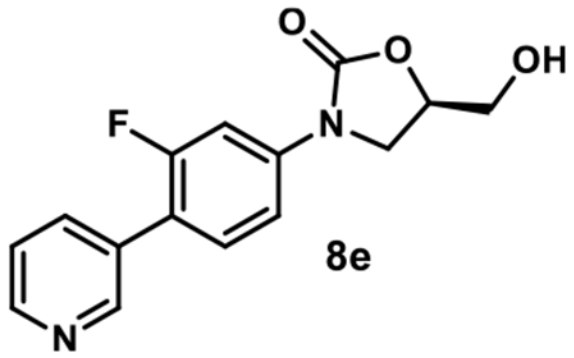

8e

Using general procedure 3, employing 2-bromopyridine (13.1 μL, 0.13 mmol), compound **8f** was obtained as a yellow amorphous solid (20 mg, 70%). ^{1}H NMR (400 MHz, DMSO-d_6) δ 8.70 (dd, J = 5.1, 1.8 Hz, 1H), 8.01 (t, J = 8.9 Hz, 1H), 7.96–7.85 (m, 1H), 7.83–7.75 (m, 1H), 7.65 (dd, J = 14.4, 2.2 Hz, 1H), 7.49 (dd, J = 8.7, 2.2 Hz, 1H), 7.46–7.35 (m, 1H), 5.28 (s, 1H), 4.84–4.67 (m, 1H), 4.15 (t, J = 8.9 Hz, 1H), 3.89 (dd, J = 8.9, 6.1 Hz, 1H), 3.75–3.65 (m, 1H), 3.62–3.54 (m, 1H). ^{13}C NMR (101 MHz, DMSO-d_6) δ 159.9 (d, J = 246.9 Hz), 154.4, 152.0 (d, J = 2.9 Hz), 149.8, 140.6 (d, J = 11.4 Hz), 137.0, 131.1 (d, J = 4.5 Hz), 123.8 (d, J = 9.5 Hz), 122.7, 121.3 (d, J = 11.8 Hz), 113.6 (d, J = 2.9 Hz), 105.2 (d, J = 29.2 Hz), 73.5, 61.6, 46.0. MSESI *m/z*: 289.0980 ($C_{15}H_{13}FN_2O_3$ + H^+ requires 289.0983).

(R)-3-(4-(2-Aminopyrimidin-5-yl)-3-fluorophenyl)-5-(hydroxymethyl)oxazolidin-2-one (8g).—

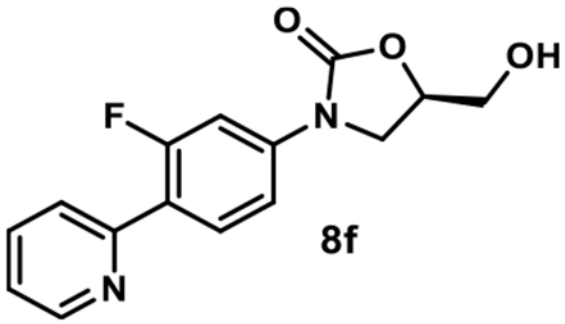

8f

A mixture of compound **7** (34 mg, 0.1 mmol), 2-amino-5-iodopyrimidine (33 mg, 0.15 mmol), sodium carbonate (23 mg, 0.2 mmol), and [1,1′-bis(diphenylphosphino)ferrocene]-dichloropalladium(II) complex with dichloromethane (8 mg, 0.01 mmol) in dioxane/H_2O (v/v = 9:1, 0.5 mL) was stirred at 130 °C under a nitrogen atmosphere. After the reaction was judged to be completed by TLC (2.5 h), it was cooled to room temperature and concentrated under reduced pressure by rotary evaporation. The resulting residue was purified by flash column chromatography (SiO_2, eluent gradient 0–10% MeOH in DCM) to afford compound **8g** as a gray amorphous solid (6 mg, 20%). ^{1}H NMR (400 MHz, DMSO-d_6) δ 8.47–8.33 (m, 2H), 7.62 (dd, J = 13.6, 2.3 Hz, 1H), 7.57 (t, J = 8.6 Hz, 1H), 7.41 (dd, J = 8.6, 2.3 Hz, 1H), 6.87 (s, 2H), 5.26 (s, 1H), 4.81–4.64 (m, 1H), 4.12 (t, J = 8.9 Hz, 1H), 3.86 (dd, J = 8.9, 6.1 Hz, 1H), 3.73–3.65 (m, 1H), 3.61–3.51 (m, 1H). ^{13}C NMR (101 MHz, DMSO-d_6) δ 162.7, 158.9 (d, J = 243.5 Hz), 157.3 (d, J = 3.9 Hz, 2C), 154.4, 139.1 (d, J = 11.1 Hz), 129.7 (d, J = 4.9 Hz), 117.7 (d, J = 14.2 Hz), 117.0 (d, J = 2.2 Hz), 113.9 (d, J = 3.1 Hz), 105.4 (d, J = 28.5 Hz), 73.4, 61.6, 46.0. MSESI *m/z*: 305.1038 ($C_{14}H_{13}FN_4O_3$ + H^+ requires 305.1044).

(R)-3-(tert-Butoxy)-5-(2-fluoro-4-(5-(hydroxymethyl)-2-oxooxazolidin-3-yl)phenyl)picolinonitrile (8h).—

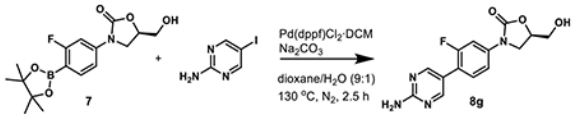

A mixture of compound 7 (121 mg, 0.36 mmol), compound **15** (77 mg, 0.3 mmol), potassium carbonate (166 mg, 1.2 mmol), and [1,1′-bis(diphenylphosphino)ferrocene]dichloropalladium(II) complex with dichloromethane (24 mg, 0.03 mmol) in dioxane/H_2O (v/v = 9:1, 1.5 mL) was stirred at 90 °C under a nitrogen atmosphere. After the reaction was judged to be completed by TLC (3 h), it was cooled to room temperature, diluted with EtOAc, washed with water, and concentrated under reduced pressure by rotary evaporation. The crude residue was purified by flash column chromatography (SiO_2, eluent gradient 0–100% EtOAc in hexanes) to afford compound **8h** as a yellow amorphous solid (46 mg, 61%). ^{1}H NMR (400 MHz, acetone-d_6) δ 8.59 (d, J = 1.6 Hz, 1H), 7.94 (d, J = 1.6 Hz, 1H), 7.78 (dd, J = 13.9, 2.2 Hz, 1H), 7.71 (t, J = 8.8 Hz, 1H), 7.54 (dd, J = 8.8, 2.2 Hz, 1H), 4.95–4.76 (m, 1H), 4.42 (t, J = 5.8 Hz, 1H), 4.26 (t, J = 8.8 Hz, 1H), 4.8 (dd, J = 8.8, 6.1 Hz, 1H), 3.92 (ddd, J = 12.3, 5.8, 3.3 Hz, 1H), 3.78 (ddd, J = 12.3, 5.8, 3.7 Hz, 1H), 1.55 (s, 9H). ^{13}C NMR (101 MHz, acetone-d_6) δ 160.8 (d,

J = 246.4 Hz), 156.4, 155.2, 145.3 (d, J = 3.9 Hz), 142.7 (d, J = 11.4 Hz), 136.2 (d, J = 2.2 Hz), 131.9 (d, J = 4.2 Hz), 130.4 (d, J = 4.0 Hz), 128.3, 118.8 (d, J = 13.4 Hz), 116.9, 114.6 (d, J = 3.1 Hz), 106.2 (d, J = 28.8 Hz), 84.4, 74.4, 63.1, 46.9, 29.0. MSESI *m/z*: 386.1517 ($C_{20}H_{20}FN_3O_4$ + H^+ requires 386.1511).

(R)-3-(3-Fluoro-4-(isoquinolin-6-yl)phenyl)-5-(hydroxymethyl)-oxazolidin-2-one (8i).—

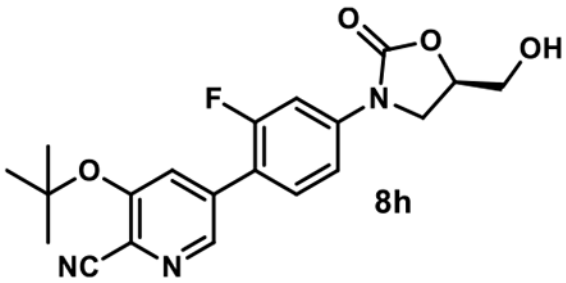

8h

Using general procedure 3, employing 6-bromoisoquinoline (42 mg, 0.2 mmol), compound **8i** was obtained as a yellow amorphous solid (20 mg, 59%). ^{1}H NMR (500 MHz, DMSO-d_6) δ 9.35 (s, 1H), 8.54 (d, J = 5.7 Hz, 1H), 8.21 (d, J = 8.6 Hz, 1H), 8.15 (s, 1H), 7.96–7.85 (m, 2H), 7.80–7.64 (m, 2H), 7.60–7.47 (m, 1H), 5.27 (s, 1H), 4.83–4.70 (m, 1H), 4.17 (t, J = 8.9 Hz, 1H), 3.91 (dd, J = 8.9, 6.1 Hz, 1H), 3.75–3.67 (m, 1H), 3.64–3.57 (m, 1H). ^{13}C NMR (101 MHz, DMSO-d_6) δ 159.3 (d, J = 245.6 Hz), 154.4, 152.1, 143.3, 140.2 (d, J = 11.3 Hz), 136.7, 135.3, 131.3 (d, J = 4.5 Hz), 128.2 (d, J = 3.2 Hz), 127.9, 127.2, 126.0 (d, J = 3.4 Hz), 121.8 (d, J = 13.2 Hz), 120.5, 113.9 (d, J = 3.3 Hz), 105.4 (d, J = 28.7 Hz), 73.5, 61.6, 46.0. MSESI *m/z*: 339.1135 ($C_{19}H_{15}FN_2O_3$ + H^+ requires 339.1139).

(R)-3-(3-Fluoro-4-(isoquinolin-7-yl)phenyl)-5-(hydroxymethyl)-oxazolidin-2-one (8j).—

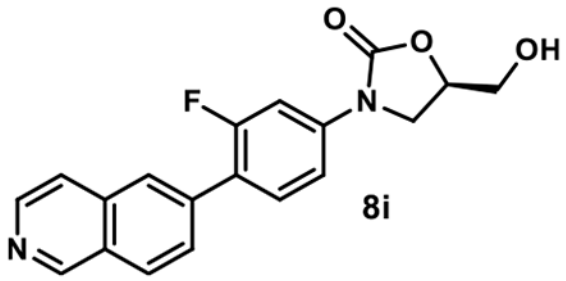

8i

Using general procedure 3, employing 7-bromoisoquinoline (42 mg, 0.2 mmol), compound **8j** was obtained as a yellow amorphous solid (16 mg, 47%). ^{1}H NMR (500 MHz, DMSO-d_6) δ 9.39 (s, 1H), 8.54 (d, J = 5.7 Hz, 1H), 8.31 (s, 1H), 8.07 (d, J = 8.6 Hz, 1H), 7.98 (d, J = 8.6 Hz, 1H), 7.87 (d, J = 5.7 Hz, 1H), 7.81–7.67 (m, 2H), 7.52 (dd, J = 8.5, 2.2 Hz, 1H), 5.27 (s, 1H), 4.96–4.71 (m, 1H), 4.17 (t, J = 9.0 Hz, 1H), 3.91 (dd, J = 9.0, 6.1 Hz, 1H), 3.77–3.68 (m, 1H), 3.64–3.55 (m, 1H). ^{13}C NMR (101 MHz, DMSO-d_6) δ 159.2 (d, J = 245.2 Hz), 154.4, 152.7, 143.2, 139.9 (d, J = 11.2 Hz), 134.3, 133.6, 131.2 (d, J = 2.4 Hz), 131.2, 128.3, 127.1 (d, J = 3.3 Hz), 126.8, 121.8 (d, J = 13.2 Hz), 120.1, 113.9 (d, J =

3.1 Hz), 105.4 (d, J = 28.8 Hz), 73.4, 61.6, 46.0. MSESI m/z: 339.1130 ($C_{19}H_{15}FN_2O_3$ + H^+ requires 339.1139).

(R)-3-(2-Fluoro-4′-(pyridin-4-yl)-[1,1′-biphenyl]-4-yl)-5-(hydroxymethyl)oxazolidin-2-one (8k).—

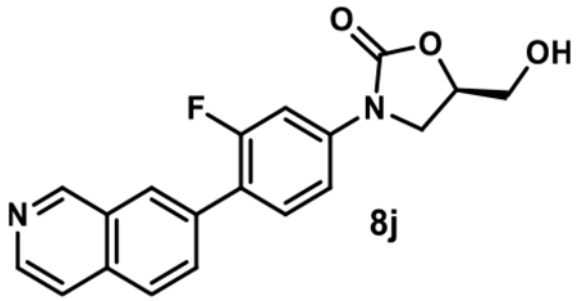

8j

Using general procedure 3, employing 4-(4-bromophenyl)pyridine (47 mg, 0.2 mmol), compound **8k** was obtained as a gray amorphous solid (14 mg, 38%). ^{1}H NMR (500 MHz, DMSO-d_6) δ 8.66 (d, J = 5.1 Hz, 2H), 7.92 (d, J = 8.0 Hz, 2H), 7.77 (d, J = 5.1 Hz, 2H), 7.71 (d, J = 8.0 Hz, 2H), 7.68–7.58 (m, 2H), 7.54–7.43 (m, 1H), 5.25 (t, J = 5.7 Hz, 1H), 4.86–4.68 (m, 1H), 4.15 (t, J = 9.0 Hz, 1H), 3.90 (dd, J = 9.0, 6.1 Hz, 1H), 3.78–3.67 (m, 1H), 3.63–3.52 (m, 1H). ^{13}C NMR (101 MHz, DMSO-d_6) δ 159.1 (d, J = 245.2 Hz), 154.4, 150.3 (2C), 146.4, 139.8 (d, J = 11.4 Hz), 136.2, 135.5, 130.8 (d, J = 4.7 Hz), 129.3 (d, J = 3.2 Hz, 2C), 127.1 (2C), 121.8 (d, J = 13.1 Hz), 121.1 (2C), 113.9 (d, J = 2.9 Hz), 105.4 (d, J = 28.7 Hz), 73.4, 61.6, 46.0. MSESI m/z: 365.1316 ($C_{21}H_{17}FN_2O_3$ + H^+ requires 365.1296).

(R)-3-(2-Fluoro-4′-(pyridin-3-yl)-[1,1′-biphenyl]-4-yl)-5-(hydroxymethyl)oxazolidin-2-one (8l).—

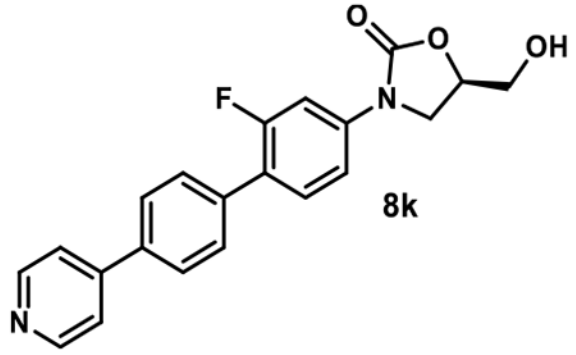

8k

Using general procedure 3, employing 3-(4-bromophenyl)pyridine (47 mg, 0.2 mmol), compound **8l** was obtained by flash column chromatography (SiO_2, eluent gradient 0–6% MeOH in DCM) as a yellow amorphous solid (17 mg, 47%). ^{1}H NMR (500 MHz, DMSO-d_6) δ 8.96 (d, J = 1.9 Hz, 1H), 8.60 (dd, J = 4.7, 1.9 Hz, 1H), 8.14 (dt, J = 8.1, 1.9 Hz, 1H), 7.93–7.82 (m, 2H), 7.75–7.59 (m, 4H), 7.55–7.45 (m, 2H), 5.37–5.18 (m, 1H), 4.84–4.71 (m, 1H), 4.15 (t, J = 8.9 Hz, 1H), 3.90 (dd, J = 8.9, 6.1 Hz, 1H), 3.77–3.66 (m, 1H), 3.63–3.54 (m, 1H). ^{13}C NMR (101 MHz, DMSO-d_6) δ 159.1 (d, J = 244.7 Hz), 154.4, 148.6, 147.6, 139.6 (d, J = 11.2 Hz), 136.2, 135.0, 134.4, 134.1, 130.8 (d, J = 4.7 Hz), 129.3 (d, J

= 3.3 Hz, 2C), 127.1 (2C), 123.9, 122.0 (d, J = 13.1 Hz), 113.9 (d, J = 3.0 Hz), 105.4 (d, J = 28.8 Hz), 73.4, 61.6, 46.0. MSESI m/z: 365.1279 ($C_{21}H_{17}FN_2O_3$ + H^+ requires 365.1296).

(R)-3-(2-Fluoro-4′-(pyridin-2-yl)-[1,1′-biphenyl]-4-yl)-5-(hydroxymethyl)oxazolidin-2-one (8m).—

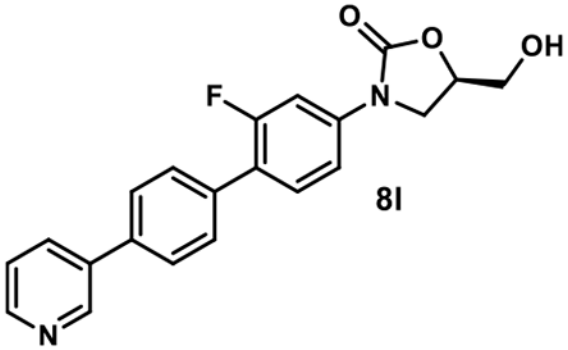

8l

Using general procedure 3, employing 2-(4-bromophenyl)pyridine (47 mg, 0.2 mmol), compound **8m** was obtained by flash column chromatography (SiO_2, eluent gradient 0–100% EtOAc in hexanes) as a yellow amorphous solid (24 mg, 66%). ^{1}H NMR (500 MHz, DMSO-d_6) δ 8.75–8.63 (m, 1H), 8.20 (d, J = 8.4 Hz, 2H), 8.02 (d, J = 8.0 Hz, 1H), 7.91 (td, J = 8.0, 1.8 Hz, 1H), 7.74–7.59 (m, 4H), 7.48 (dd, J = 8.6, 2.2 Hz, 1H), 7.38 (ddd, J = 8.6, 4.8, 1.0 Hz, 1H), 5.25 (t, J = 5.6 Hz, 1H), 4.83–4.71 (m, 1H), 4.15 (t, J = 8.9 Hz, 1H), 3.90 (dd, J = 8.9, 6.1 Hz, 1H), 3.71 (ddd, J = 12.4, 5.6, 3.3 Hz, 1H), 3.59 (ddd, J = 12.4, 5.6, 4.0 Hz, 1H). ^{13}C NMR (101 MHz, DMSO-d_6) δ 159.1 (d, J = 245.3 Hz), 155.4, 154.4, 149.6, 139.6 (d, J = 11.3 Hz), 137.8, 137.3, 135.2 (d, J = 1.7 Hz), 130.8 (d, J = 4.8 Hz), 128.9 (d, J = 3.2 Hz, 2C), 126.7 (2C), 122.7, 122.1 (d, J = 13.3 Hz), 120.3, 113.8 (d, J = 3.0 Hz), 105.4 (d, J = 28.9 Hz), 73.4, 61.6, 46.0. MSESI m/z: 365.1307 ($C_{21}H_{17}FN_2O_3$ + H^+ requires 365.1296).

(R)-3-(3-Fluoro-4-(isoxazol-4-yl)phenyl)-5-(hydroxymethyl)-oxazolidin-2-one (8n).[51]—

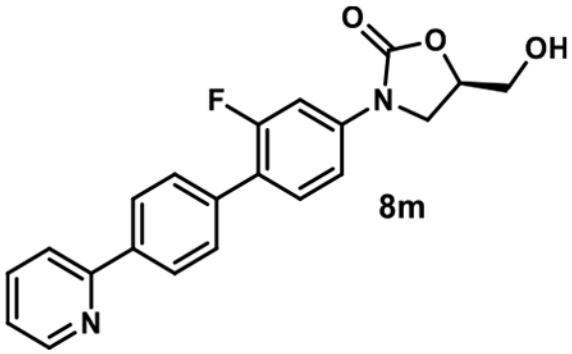

8m

A mixture of compound **6** (34 mg, 0.1 mmol), isoxazole-4-boronic acid (17 mg, 0.15 mmol), potassium phosphate monohydrate (46 mg, 0.2 mmol), and [1,1′-bis(diphenylphosphino)ferrocene]-dichloropalladium(II), complex with dichloromethane (8.2 mg, 0.01 mmol) in THF/H_2O (v/v = 4:1, 2 mL) was stirred at 80 °C. After the reaction

was judged to be completed by TLC (16 h), it was cooled to room temperature, diluted with EtOAc, washed with water, and concentrated under reduced pressure by rotary evaporation. The resulting residue was purified by flash column chromatography (SiO_2, eluent gradient 0–100% EtOAc in hexanes) to afford compound **8n** as a yellow amorphous solid (14 mg, 50%). ^{1}H NMR (300 MHz, acetone-d_6) δ 9.13 (d, J = 2.2 Hz, 1H), 8.94 (d, J = 2.2 Hz, 1H), 7.85–7.66 (m, 2H), 7.51–7.41 (m, 1H), 4.82 (ddt, J = 9.0, 6.2, 3.7 Hz, 1H), 4.44 (s, 1H), 4.22 (t, J = 9.0 Hz, 1H), 4.04 (dd, J = 9.0, 6.2 Hz, 1H), 3.95–3.85 (m, 1H), 3.83–3.71 (m, 1H). ^{13}C NMR (101 MHz, acetone-d_6) δ 160.3 (d, J = 245.4 Hz), 156.3 (d, J = 8.7 Hz), 155.2, 148.9 (d, J = 2.7 Hz), 141.0 (d, J = 11.3 Hz), 129.5 (d, J = 5.3 Hz), 115.3 (d, J = 2.3 Hz), 114.4 (d, J = 3.0 Hz), 112.0 (d, J = 14.8 Hz), 106.1 (d, J = 28.2 Hz), 74.3, 63.1, 46.9. MSESI m/z: 279.0787 ($C_{13}H_{11}FN_2O_4$ + H^+ requires 279.0776).

(R)-3-(3-Fluoro-4-(4,4,5,5-tetramethyl-1,3,2-dioxaborolan-2-yl)-phenyl)-5-((methoxymethoxy)methyl)oxazolidin-2-one (9).—

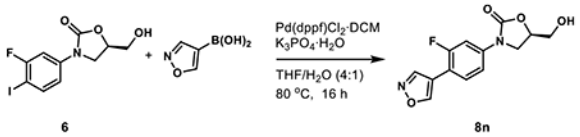

To a solution of compound **7** (1.44 g, 4.27 mmol) in DCM (30 mL), *N,N*-diisopropylethylamine (2.23 mL, 12.81 mmol) and methyl chloromethyl ether (0.97 mL, 12.81 mmol) were added. The reaction mixture was stirred at 25 °C. After the reaction was judged to be completed by TLC (1 h), it was diluted with EtOAc, washed with water, and concentrated under reduced pressure by rotary evaporation. The crude residue was purified by flash column chromatography (SiO_2, eluent gradient 0–66% EtOAc in hexanes) to afford compound **9** as a white amorphous solid (940 mg, 58%). ^{1}H NMR (400 MHz, chloroform-d) δ 7.72 (dd, J = 8.3, 6.9 Hz, 1H), 7.39 (dd, J = 11.7, 2.1 Hz, 1H), 7.28 (dd, J = 8.3, 2.1 Hz, 1H), 4.88–4.75 (m, 1H), 4.67 (s, 2H), 4.07 (t, J = 8.8 Hz, 1H), 3.93 (dd, J = 8.8, 6.3 Hz, 1H), 3.83 (dd, J = 11.2, 4.2 Hz, 1H), 3.76 (dd, J = 11.2, 4.1 Hz, 1H), 3.37 (s, 3H), 1.35 (s, 12H).

(R)-3-(tert-Butoxy)-5-(2-fluoro-4-(5-((methoxymethoxy)methyl)-2-oxooxazolidin-3-yl)phenyl)picolinonitrile (10).—

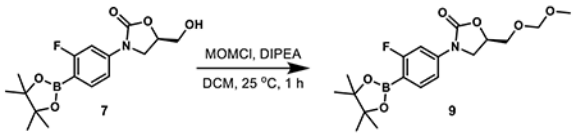

A mixture of compound **9** (152 mg, 0.4 mmol), compound **15** (122 mg, 0.48 mmol), potassium carbonate (221 mg, 1.6 mmol), and [1,1′-bis(diphenylphosphino)ferrocene]dichloropalladium(II), complex with dichloromethane (33 mg, 0.04 mmol) in dioxane/H_2O (v/v = 9:1, 2 mL) was stirred at 90 °C under a nitrogen atmosphere. After the reaction was judged to be completed by TLC (3 h), it was cooled to room temperature, diluted with EtOAc, washed with water, and concentrated under reduced pressure by rotary evaporation. The crude residue was purified by flash column chromatography (SiO_2, eluent gradient 0–100% EtOAc in hexanes) to afford compound **10** as a yellow amorphous solid (154 mg, 90%). ^{1}H NMR (400 MHz, acetone) δ 8.59 (t, J = 1.6

Hz, 1H), 7.94 (t, *J* = 1.6 Hz, 1H), 7.78 (dd, *J* = 13.8, 2.3 Hz, 1H), 7.71 (t, *J* = 8.6 Hz, 1H), 7.56 (dd, *J* = 8.6, 2.3 Hz, 1H), 5.05–4.90 (m, 1H), 4.67 (s, 2H), 4.33 (t, *J* = 9.0 Hz, 1H), 4.07 (dd, *J* = 9.0, 6.1 Hz, 1H), 3.94–3.75 (m, 2H), 3.33 (s, 3H), 1.56 (s, 9H).

(R)-3-(4-(6-(Aminomethyl)-5-hydroxypyridin-3-yl)-3-fluorophenyl)-5-(hydroxymethyl)oxazolidin-2-one Hydrochloride (8o).—

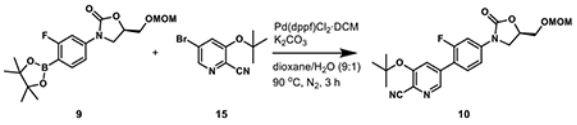

To a solution of compound **10** (86 mg, 0.2 mmol) in methanol (3 mL) in an ice bath were added nickel(II) chloride hexahydrate (24 mg, 0.1 mmol) and di-*tert*-butyl dicarbonate (30% in dioxane, 0.73 mL, 1 mmol). The resulting solution was charged with the addition of sodium borohydride (76 mg, 2 mmol) portionwise and stirred at 25 °C. After the reaction was judged to be completed by TLC (16 h), it was evaporated under reduced pressure by rotary evaporation. The resulting residue was purified by flash column chromatography (SiO_2, eluent gradient 0–100% EtOAc) to afford compound **10a** as a colorless oil (56 mg, 52%). ^{1}H NMR (500 MHz, acetone) δ 8.37 (t, *J* = 1.6 Hz, 1H), 7.73 (dd, *J* = 13.6, 2.3 Hz, 1H), 7.66 (t, *J* = 1.6 Hz, 1H), 7.61 (t, *J* = 8.6 Hz, 1H), 7.50 (dd, *J* = 8.6, 2.3 Hz, 1H), 6.20 (s, 1H), 4.97 (dddd, *J* = 9.0, 6.1, 4.5, 3.5 Hz, 1H), 4.67 (s, 2H), 4.44 (d, *J* = 5.0 Hz, 2H), 4.31 (t, *J* = 9.0 Hz, 1H), 4.05 (dd, *J* = 9.0, 6.1 Hz, 1H), 3.87 (dd, *J* = 11.3, 3.5 Hz, 1H), 3.82 (dd, *J* = 11.3, 4.5 Hz, 1H), 1.51 (s, 9H), 1.45 (s, 9H). A solution of compound **10a** (28 mg, 0.05 mmol) in DCM (1 mL) and TFA (0.5 mL) was stirred at 40 °C. After the reaction was judged to be completed by TLC (1 h), its solvent was evaporated under reduced pressure by rotary evaporation. The resulting residue was dissolved in MeOH (1 mL), charged with the addition of HCl/dioxane (4 M, 0.1 mL), and concentrated under reduced pressure by rotary evaporation. The resulting solid was washed with acetone (2 × 1 mL) and dried under high vacuum to give **8o** as a yellow amorphous solid (12 mg, 66%). ^{1}H NMR (400 MHz, CD_3OD) δ 8.42 (t, *J* = 1.5 Hz, 1H), 7.75 (dd, *J* = 13.6, 2.2 Hz, 1H), 7.69 (t, *J* = 1.5 Hz, 1h), 7.61 (t, *J* = 8.6 Hz, 1H), 7.49 (dd, *J* = 8.6, 2.2 Hz, 1H), 4.84–4.76 (m, 1H), 4.37 (s, 2H), 4.19 (t, *J* = 8.9 Hz, 1H), 4.00 (dd, *J* = 8.9, 6.3 Hz, 1H), 3.89 (dd, *J* = 12.6, 3.1 Hz, 1H), 3.72 (dd, *J* = 12.6, 3.8 Hz, 1H). ^{13}C NMR (101 MHz, CD_3OD) δ 161.2 (d, *J* = 246.6 Hz), 156.8, 153.9, 142.4 (d, *J* = 11.3 Hz), 138.5, 138.3 (d, *J* = 3.7 Hz), 135.2, 131.8 (d, *J* = 4.2 Hz), 125.9, 119.8 (d, *J* = 13.7 Hz), 115.3 (d, *J* = 3.1 Hz), 107.1 (d, *J* = 28.9 Hz), 75.3, 63.2, 47.5, 39.3. MSESI *m/z*: 334.1196 ($C_{16}H_{16}FN_3O_4$ + H^+ requires 334.1198).

General Procedure 4: Synthesis of Heterocyclic MOM-Protected Oxazolidinone Analogues 11a–h.—

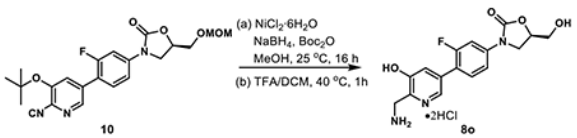

A mixture of compound **9** (76 mg, 0.2 mmol), heterocyclic bromide (0.26 mmol), potassium carbonate (110 mg, 0.8 mmol), and [1,1′-

bis(diphenylphosphino)ferrocene]dichloropalladium(II), complex with dichloromethane (16 mg, 0.02 mmol) in dioxane/H_2O (v/v = 9:1, 1 mL) was stirred at 90 °C under a nitrogen atmosphere. After the reaction was judged to be completed by TLC (3 h), it was cooled to room temperature, diluted with EtOAc, washed with water, and concentrated under reduced pressure by rotary evaporation. The crude residue was purified by flash column chromatography (SiO_2, eluent gradient 0–8% MeOH in DCM) to afford compounds **11a–h.**

(R)-3-(3-Fluoro-4-(pyridin-4-yl)phenyl)-5-((methoxymethoxy)-methyl)oxazolidin-2-one (11a).—

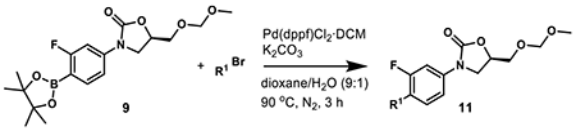

A mixture of compound **9** (125 mg, 0.33 mmol), 4-bromopyridine hydrochloride (83 mg, 0.43 mmol), potassium carbonate (182 mg, 1.32 mmol), and [1,1′-bis(diphenylphosphino)ferrocene]-dichloropalladium(II) complex with dichloromethane (27 mg, 0.033 mmol) in dioxane/H_2O (v/v = 9:1, 2 mL) was stirred at 90 °C under a nitrogen atmosphere. After the reaction was judged to be completed by TLC (3 h), it was cooled to room temperature, diluted with EtOAc, washed with water, and concentrated under reduced pressure by rotary evaporation. The crude residue was purified by flash column chromatography (SiO_2, eluent gradient 0–10% MeOH in DCM) followed by preparative TLC (SiO_2, eluent gradient 100% EtOAc) to afford compound **11a** as a brown amorphous solid (80 mg, 73%). ^{1}H NMR (300 MHz, acetone-d_6) δ 8.65 (d, J = 6.2 Hz, 2H), 7.75 (dd, J = 13.9, 2.3 Hz, 1H), 7.67 (t, J = 8.7 Hz, 1H), 7.61–7.47 (m, 3H), 5.02–4.90 (m, 1H), 4.67 (s, 2H), 4.32 (t, J = 9.0 Hz, 1H), 4.06 (dd, J = 9.0, 6.1 Hz, 1H), 3.93–3.70 (m, 2H), 3.33 (s, 3H).

(R)-3-(3-Fluoro-4-(pyridin-3-yl)phenyl)-5-((methoxymethoxy)-methyl)oxazolidin-2-one (11b).—

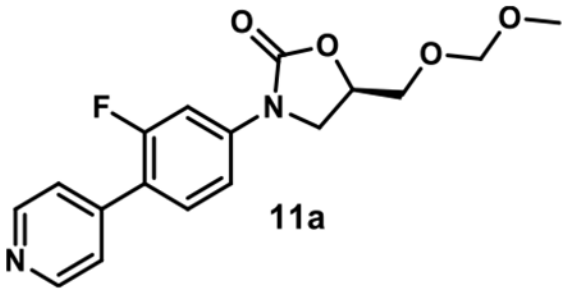

A mixture of compound **9** (67.5 mg, 0.177 mmol), 3-bromopyridine (25 μL, 0.26 mmol), potassium carbonate (110 mg, 0.8 mmol), and [1,1′-bis(diphenylphosphino)ferrocene]dichloropalladium(II) complex with dichloromethane (16 mg, 0.02 mmol) in dioxane/H_2O (v/ v = 9:1, 1 mL) was stirred at 90 °C under a nitrogen atmosphere. After the reaction was judged to be completed by TLC (2 h), it was cooled to room temperature, diluted with EtOAc, washed with water, and concentrated under reduced pressure by rotary evaporation. The crude residue was purified by flash column chromatography (SiO_2, eluent gradient 0–100% EtOAc in hexanes) to afford compound **11b**

as a colorless oil (42 mg, 71%). ^{1}H NMR (300 MHz, acetone-d_6) δ δ 8.78 (s, 1H), 8.58 (dd, J = 4.8, 1.7 Hz, 1H), 8.03–7.89 (m, 1H), 7.75 (dd, J = 13.6, 2.3 Hz, 1H), 7.61 (t, J = 8.6 Hz, 1H), 7.57–7.41 (m, 2H), 5.03–4.90 (m, 1H), 4.68 (s, 2H), 4.32 (t, J = 9.0 Hz, 1H), 4.06 (dd, J = 9.0, 6.1 Hz, 1H), 3.94–3.70 (m, 2H), 3.34 (s, 3H).

(R)-3-(3-Fluoro-4-(pyridin-2-yl)phenyl)-5-((methoxymethoxy)-methyl)oxazolidin-2-one (11c).—

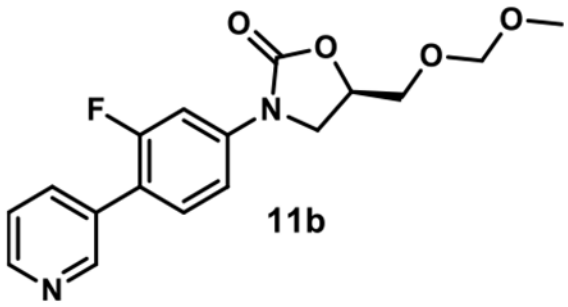

11b

A mixture of compound **9** (67.5 mg, 0.177 mmol), 2-bromopyridine (26.1 μL, 0.26 mmol), potassium carbonate (110 mg, 0.8 mmol), and [1,1′-bis(diphenylphosphino)ferrocene]dichloropalladium(II) complex with dichloromethane (16 mg, 0.02 mmol) in dioxane/H_2O (v/ v = 9:1, 1 mL) was stirred at 90 °C under a nitrogen atmosphere. After the reaction was judged to be completed by TLC (2 h), it was cooled to room temperature, diluted with EtOAc, washed with water, and concentrated under reduced pressure by rotary evaporation. The crude residue was purified by flash column chromatography (SiO_2, eluent gradient 0–100% EtOAc in hexanes) to afford compound **11c** as a white amorphous solid (41 mg, 70%). ^{1}H NMR (300 MHz, acetone-d_6) δ 8.70 (dd, J = 4.8, 1.5 Hz, 1H), 8.13 (t, J = 8.9 Hz, 1H), 7.92–7.80 (m, 2H), 7.74 (dd, J = 14.4, 2.3 Hz, 1H), 7.49 (dd, J = 8.8, 2.3 Hz, 1H), 7.38–7.29 (m, 1H), 5.07–4.93 (m, 1H), 4.68 (s, 2H), 4.32 (t, J = 9.0 Hz, 1H), 4.06 (dd, J = 9.0, 6.1 Hz, 1H), 3.96–3.74 (m, 2H), 3.33 (s, 3H).

(R)-3-(3-Fluoro-4-(isoquinolin-6-yl)phenyl)-5-((methoxymethoxy)methyl)oxazolidin-2-one (11d).—

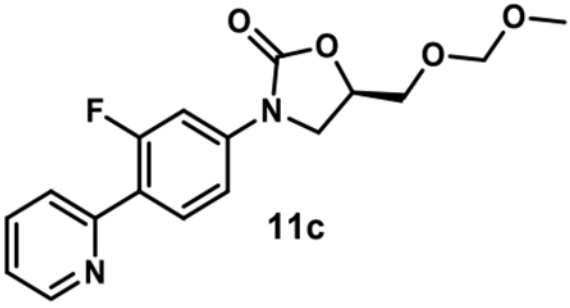

11c

Using general procedure 4, employing 6-bromoisoquinoline (54 mg), compound **11d** was obtained as a yellow amorphous solid (69 mg, 90%). ^{1}H NMR (400 MHz, acetone-d_6) δ 9.33 (s, 1H), 8.54 (d, J = 5.7 Hz, 1H), 8.19 (d, J = 8.5 Hz, 1H), 8.13 (s, 1H), 7.89 (dt, J = 8.5, 1.8 Hz, 1H), 7.84 (d, J = 5.7 Hz, 1H), 7.77 (dd, J = 13.8, 2.3 Hz, 1H), 7.71 (t, J = 8.6 Hz,

1H), 7.55 (dd, J = 8.6, 2.3 Hz, 1H), 5.04–4.94 (m, 1H),4.68 (s, 2H), 4.33 (t, J = 8.9 Hz, 1H), 4.07 (dd, J = 8.9, 6.1 Hz, 1H), 3.89 (dd, J = 11.3, 3.4 Hz, 1H), 3.83 (dd, J = 11.3, 4.5 Hz, 1H), 3.34 (s, 3H). ^{13}C NMR (101 MHz, acetone-d_6) δ 160.8 (d, J = 245.5 Hz), 155.1, 153.1, 144.5, 141.6 (d, J = 11.3 Hz), 138.1 (d, J = 1.6 Hz), 136.7, 132.1 (d, J = 4.6, Hz), 129.2 (d, J = 3.2 Hz), 128.6, 127.0 (d, J = 3.3 Hz), 123.3 (d, J = 13.5 Hz), 121.3, 114.6 (d, J = 3.1 Hz), 106.4 (d, J = 29.0 Hz), 97.3, 72.7, 68.7, 55.5, 47.4.

(R)-3-(3-Fluoro-4-(isoquinolin-7-yl)phenyl)-5-((methoxymethoxy)methyl)oxazolidin-2-one (11e).—

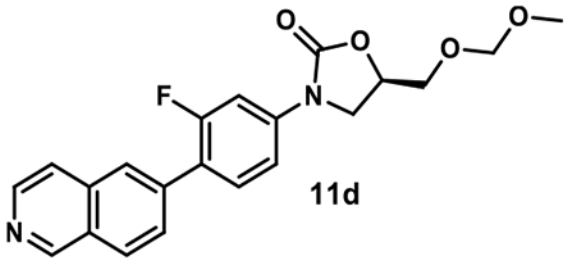

11d

Using general procedure 4, employing 7-bromoisoquinoline (54 mg), compound **11e** was obtained as a yellow amorphous solid (68 mg, 89%). ^{1}H NMR (400 MHz, acetone-d_6) δ 9.37 (s, 1H), 8.54 (d, J = 5.7 Hz, 1H), 8.29 (s, 1H), 8.05 (d, J = 8.6 Hz, 1H), 8.01–7.96 (m, 1H), 7.82 (d, J = 5.7 Hz, 1H), 7.77 (dd, J = 13.9, 2.2 Hz, 1H), 7.72 (t, J = 8.6 Hz, 1H), 7.55 (dd, J = 8.6, 2.2 Hz, 1H), 5.04–4.93 (m, 1H), 4.68 (s, 2H), 4.33 (t, J = 8.9 Hz, 1H), 4.07 (dd, J = 8.9, 6.2 Hz, 1H), 3.89 (dd, J = 11.3, 3.4 Hz, 1H), 3.83 (dd, J = 11.3, 4.4 Hz, 1H), 3.34 (s, 3H). ^{13}C NMR (101 MHz, acetone-d_6) δ 160.7 (d, J = 245.0 Hz), 155.1, 153.6, 144.3, 141.3 (d, J = 11.4 Hz), 135.6, 135.2 (d, J = 1.7 Hz), 132.1 (d, J = 3.3 Hz), 132.0 (d, J = 4.8 Hz), 129.7, 128.1 (d, J = 3.3 Hz), 127.6, 123.3 (d, J = 13.4 Hz), 120.9, 114.6 (d, J = 3.1 Hz), 106.3 (d, J = 29.1 Hz), 97.3, 72.7, 68.7, 55.4, 47.4.

(R)-3-(2-Fluoro-4′-(pyridin-4-yl)-[1,1′-biphenyl]-4-yl)-5-((methoxymethoxy)methyl)oxazolidin-2-one (11f).—

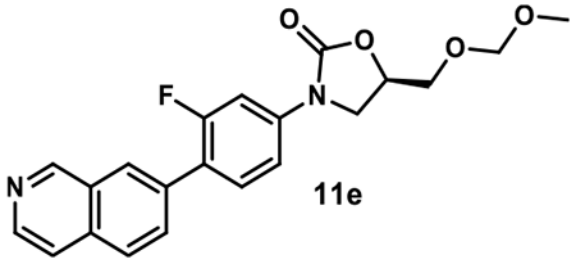

11e

Using general procedure 4, employing 4-(4-bromophenyl)pyridine (61 mg), compound **11f** was obtained as a yellow amorphous solid (75 mg, 90%). ^{1}H NMR (400 MHz, acetone-d_6) δ 8.75–8.61 (m, 2H), 7.90 (d, J = 8.1 Hz, 2H), 7.81–7.65 (m, 5H), 7.63 (t, J = 8.7 Hz, 1H), 7.51 (dd, J = 8.7, 2.2 Hz, 1H), 5.04–4.93 (m, 1H), 4.68 (s, 2H), 4.32 (t, J = 8.9 Hz, 1H), 4.06 (dd, J = 8.9, 6.1 Hz, 1H), 3.88 (dd, J = 11.3, 3.4 Hz, 1H), 3.82 (dd, J = 11.3, 4.4 Hz, 1H), 3.34 (s, 3H). ^{13}C NMR (101 MHz, acetone-d_6) δ 160.6 (d, J = 245.0 Hz), 155.1, 151.3 (2C), 148.0, 141.1 (d, J = 11.4 Hz), 137.9, 137.0, 131.6 (d, J = 4.8 Hz), 130.3 (d, J = 3.4 Hz, 2C),

127.9 (2C), 123.3 (d, J = 13.2 Hz), 122.1 (2C), 114.5 (d, J = 3.3 Hz), 106.3, (d, J = 29.1 Hz), 97.3, 72.6, 68.7, 55.4, 47.4.

(R)-3-(2-Fluoro-4′-(pyridin-3-yl)-[1,1′-biphenyl]-4-yl)-5-((methoxymethoxy)methyl)oxazolidin-2-one (11g).—

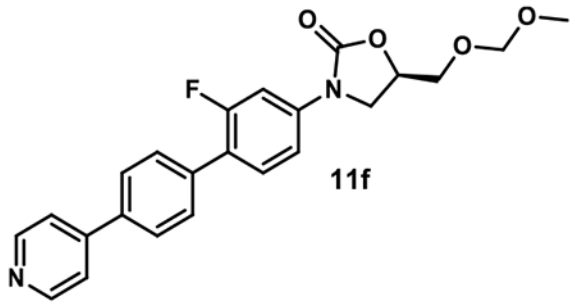

11f

Using general procedure 4, employing 3-(4-bromophenyl)pyridine (61 mg), compound **11g** was obtained as a yellow amorphous solid (68 mg, 83%). ^{1}H NMR (400 MHz, acetone-d_6) δ 8.94 (d, J = 2.4 Hz, 1H), 8.73–8.55 (m, 1H), 8.18–8.03 (m, 1H), 7.82 (d, J = 8.3 Hz, 2H), 7.78–7.68 (m, 3H), 7.63 (t, J = 8.8 Hz, 1H), 7.57–7.44 (m, 2H), 5.03–4.93 (m, 1H), 4.68 (s, 2H), 4.32 (t, J = 8.9 Hz, 1H), 4.06 (dd, J = 8.9, 6.2 Hz, 1H), 3.88 (dd, J = 11.3, 3.4 Hz, 1H), 3.83 (dd, J = 11.3, 4.4 Hz, 1H), 3.35 (s, 3H). ^{13}C NMR (101 MHz, acetone-d_6) δ 160.6 (d, J = 245.2 Hz), 155.1, 149.6, 148.8, 141.0 (d, J = 11.3 Hz), 137.8, 136.6, 136.0, 134.8, 131.6 (d, J = 4.9 Hz), 130.3 (d, J = 3.3 Hz, 2C), 128.0 (2C), 124.6, 123.5 (d, J = 13.0 Hz), 114.5 (d, J = 3.2 Hz), 106.3 (d, J = 29.1 Hz), 97.3, 72.6, 68.7, 55.4, 47.4.

(R)-3-(2-Fluoro-4′-(pyridin-2-yl)-[1,1′-biphenyl]-4-yl)-5-((methoxymethoxy)methyl)oxazolidin-2-one (11h).—

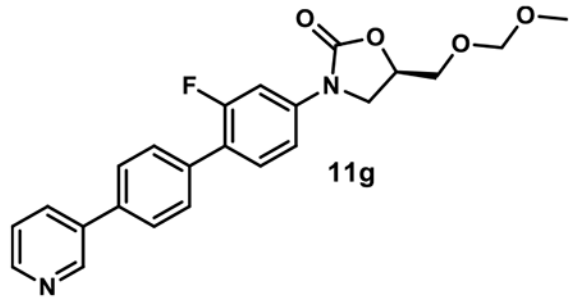

11g

Using general procedure 4, employing 2-(4-bromophenyl)pyridine (61 mg), compound **11h** was obtained after flash column chromatography (SiO_2, eluent gradient 0–100% EtOAc in hexanes) as a yellow amorphous solid (64 mg, 78%). ^{1}H NMR (400 MHz, acetone-d_6) δ 8.69 (ddd, J = 4.7, 1.8, 0.9 Hz, 1H), 8.23 (d, J = 8.5 Hz, 2H), 8.03–7.97 (m, 1H), 7.89 (td, J = 7.7, 1.8 Hz, 1H), 7.77–7.67 (m, 3H), 7.63 (t, J = 8.8 Hz, 1H), 7.50 (dd, J = 8.8, 2.3 Hz, 1H), 7.34 (ddd, J = 7.5, 4.8, 1.1 Hz, 1H), 5.04–4.92 (m, 1H), 4.68 (s, 2H), 4.31 (t, J = 8.9 Hz, 1H), 4.05 (dd, J = 8.9, 6.2 Hz, 1H), 3.88 (dd, J = 11.3, 3.5 Hz, 1H), 3.82 (dd, J = 11.3, 4.5 Hz, 1H), 3.34 (s, 3H). ^{13}C NMR (101 MHz, acetone-d_6) δ 159.7 (d, J = 245.2 Hz), 156.2, 154.21, 149.7, 140.1 (d, J = 11.2 Hz), 138.4, 136.9, 135.8 (d, J = 1.9 Hz), 130.7 (d, J

= 4.8 Hz), 129.0 (d, *J* = 3.4 Hz, 2C), 126.8, 122.8 (d, *J* = 13.6 Hz), 122.4 (2C), 120.0, 113.6 (d, *J* = 3.2 Hz), 105.4 (d, *J* = 29.3 Hz), 96.4, 71.7, 67.8, 54.5, 46.5.

General Procedure 5: Synthesis of Positively Charged Oxazolidinone Analogues 12a–l.

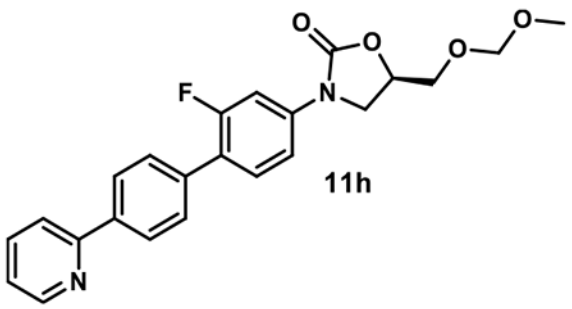

A mixture of compound **11** (0.1 mmol) and haloalkane (0.5 mmol) in CH_3CN (1 mL) was stirred in a sealed tube at 80 °C for 24 h. The reaction mixture was cooled to room temperature, purged with a nitrogen flow for 5 min to remove most of the haloalkane, and concentrated under reduced pressure by rotary evaporation. The resulting residue was charged with the addition of HCl/dioxane (4 M, 1 mL) [if necessary, MeOH (1 mL) was employed as a cosolvent]. The reaction mixture was stirred at 25 °C for 1 h, purged with a nitrogen flow for 5 min to remove most of the hydrogen chloride, and concentrated under reduced pressure by rotary evaporation. The residue was further purified to give compounds **12** (their purification protocols are reported individually).

(R)-4-(2-Fluoro-4-(5-(hydroxymethyl)-2-oxooxazolidin-3-yl)-phenyl)-1-methylpyridin-1-ium Chloride (12a).—

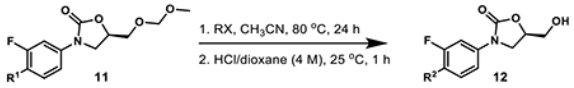

A mixture of compound **11a** (72 mg, 0.22 mmol) and methyl iodide (30 μL, 0.54 mmol) in CH_3CN (2 mL) was stirred in a sealed tube at 80 °C for 24 h. The reaction mixture was cooled to room temperature, purged with a nitrogen flow for 5 min to remove most of methyl iodide, and concentrated under reduced pressure by rotary evaporation. The resulting residue was charged with the addition of HCl/dioxane (4 M, 2 mL). The reaction mixture was stirred at 25 °C for 1 h, purged with a nitrogen flow for 5 min to remove most of the hydrogen chloride, and concentrated under reduced pressure by rotary evaporation. The crude residue was dissolved in methanol (2 mL). The solution was precipitated with the addition of acetone (4 mL) and kept still overnight. The supernatant was removed carefully, and the solid was resuspended in acetone (4 mL). The acetone supernatant was removed carefully, and the solid was dried under high vacuum to afford **12a** as a yellow amorphous solid (30 mg, 40%). ^{1}H NMR (500 MHz, DMSO-d_6) δ 9.05 (d, *J* = 6.6 Hz, 2H), 8.35 (d, *J* = 6.6 Hz, 2H), 7.97 (t, *J* = 8.8 Hz, 1H), 7.77 (dd, *J* = 14.4, 2.2 Hz, 1H), 7.62 (dd, *J* = 8.8, 2.2 Hz, 1H), 5.44–5.32 (m, 1H), 4.88–4.74 (m, 1H), 4.36 (s, 3H), 4.17 (t, *J* = 9.0 Hz, 1H), 3.97 (dd, *J* = 9.0, 5.9 Hz, 1H), 3.76–3.66 (m, 1H), 3.66–3.55 (m, 1H). ^{13}C NMR (151 MHz, DMSO-d_6) δ 160.2 (d, *J* = 250.4 Hz), 154.3, 149.7, 145.5 (2C), 143.2 (d, *J* = 11.9 Hz),

131.7 (d, J = 3.5 Hz), 125.9 (d, J = 5.3 Hz, 2C), 116.3 (d, J = 11.5 Hz), 114.1 (d, J = 2.9 Hz), 105.4 (d, J = 28.4 Hz), 73.7, 61.4, 47.2, 46.0. MSESI *m/z*: 303.1145 ($C_{16}H_{16}FN_2O_3^+$ requires 303.1139).

(R)-3-(2-Fluoro-4-(5-(hydroxymethyl)-2-oxooxazolidin-3-yl)-phenyl)-1-methylpyridin-1-ium Chloride (12b).—

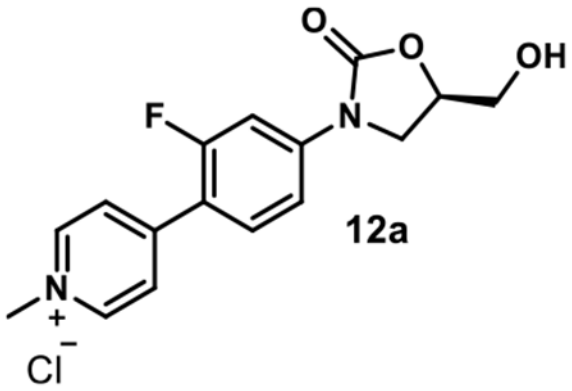

Using general procedure 5, employing **11b** (33 mg, 0.1 mmol) and methyl iodide (31.1 μL, 0.5 mmol), compound **12b** was obtained as a yellow amorphous solid (10 mg, 30%). Pyridinium **12b** purification protocol: the crude residue was dissolved in methanol (1 mL). The solution was precipitated with the addition of acetone (5 mL) and kept still overnight. The supernatant was removed carefully, and the solid was resuspended in acetone (2 mL). The acetone supernatant was removed carefully, and the solid was dried under high vacuum to afford **12b**. ^{1}H NMR (400 MHz, DMSO-d_6) δ 9.34 (s, 1H), 9.02 (d, J = 6.0 Hz, 1H), 8.78 (d, J = 8.2 Hz, 1H), 8.22 (dd, J = 8.2, 6.0 Hz, 1H), 7.89–7.71 (m, 2H), 7.59 (dd, J = 8.7, 2.3 Hz, 1H), 5.36 (t, J = 5.5 Hz, 1H), 4.85–4.72 (m, 1H), 4.43 (s, 3H), 4.17 (t, J = 9.0 Hz, 1H), 3.95 (dd, J = 9.0, 6.0 Hz, 1H), 3.70 (ddd, J = 12.3, 5.5, 3.1 Hz, 1H), 3.58 (ddd, J = 12.3, 5.5, 3.7 Hz, 1H). ^{13}C NMR (101 MHz, DMSO-d_6) δ 159.3 (d, J = 247.2 Hz), 154.4, 144.8 (d, J = 3.3 Hz), 144.1, 144.0, 141.9 (d, J = 11.6 Hz), 134.1 (d, J = 1.3 Hz), 131.3 (d, J = 3.6 Hz), 127.5, 115.5 (d, J = 12.8 Hz), 114.1 (d, J = 2.9 Hz), 105.3 (d, J = 27.9 Hz), 73.6, 61.5, 48.2, 46.0. MSESI *m/z*: 303.1122 ($C_{16}H_{16}FN_2O_3^+$ requires 303.1139).

(R)-2-(2-Fluoro-4-(5-(hydroxymethyl)-2-oxooxazolidin-3-yl)-phenyl)-1-methylpyridin-1-ium Chloride (12c).—

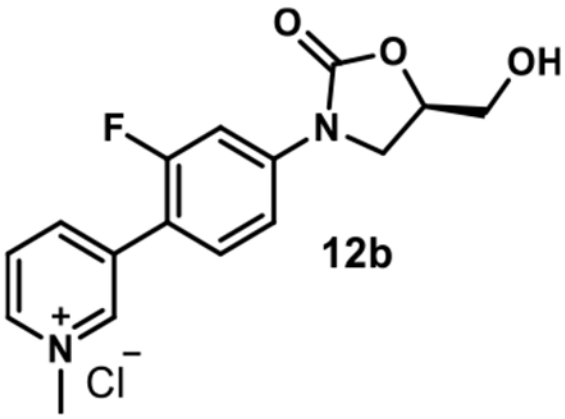

Using general procedure 5, employing **11c** (33 mg, 0.1 mmol) and methyl iodide (31.1 μL, 0.5 mmol), compound **12c** was obtained as a yellow amorphous solid (5 mg, 15%). Pyridinium **12c** purification protocol: the crude residue was dissolved in methanol (1 mL). The solution was precipitated with the addition of acetone (5 mL) and kept still overnight. The supernatant was removed carefully, and the solid was resuspended in acetone (2 mL). The acetone supernatant was removed carefully, and the solid was dried under high vacuum to afford **12c**. ^{1}H NMR (400 MHz, methanol-d_4) δ 9.10 (d, J = 6.1 Hz, 1H), 8.70–8.59 (m, 1H), 8.20–8.05 (m, 2H), 7.90 (dd, J = 13.0, 2.1 Hz, 1H), 7.71–7.53 (m, 2H), 4.84–4.75 (m, 1H), 4.27–4.19 (m, 4H), 4.02 (dd, J = 9.0, 6.2 Hz, 1H), 3.88 (dd, J = 12.6, 3.0 Hz, 1H), 3.71 (dd, J = 12.6, 3.7 Hz, 1H). ^{13}C NMR (101 MHz, DMSO-d_6) δ 158.8 (d, J = 246.7 Hz), 154.3, 149.2, 147.5, 145.6, 143.2 (d, J = 11.4Hz), 131.9 (d, J = 2.9 Hz), 130.8, 127.3, 113.8 (d, J = 3.0 Hz), 113.3 (d, J = 15.0 Hz), 104.9 (d, J = 26.8 Hz), 73.6, 61.5, 46.6 (d, J = 2.6 Hz), 46.0. MSESI m/z: 303.1156 ($C_{16}H_{16}FN_2O_3^+$ requires 303.1139).

(R)-6-(2-Fluoro-4-(5-(hydroxymethyl)-2-oxooxazolidin-3-yl)-phenyl)-2-methylisoquinolin-2-ium Chloride (12d).—

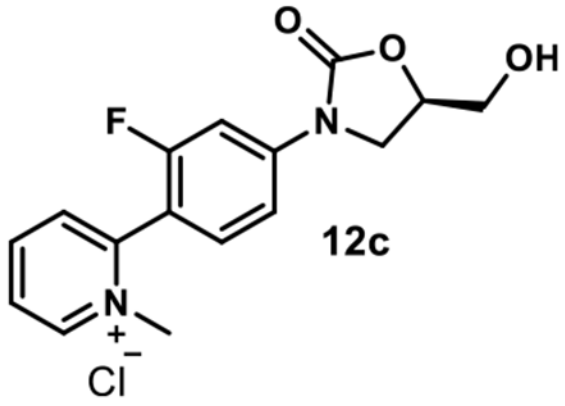

Using general procedure 5, employing **11d** (38 mg, 0.1 mmol) and methyl iodide (31.1 μL, 0.5 mmol), employing MeOH (1 mL) as the cosolvent in the deprotection step, compound **12d** was obtained as a yellow amorphous solid (25 mg, 64%). Pyridinium **12d** purification protocol: the crude residue was dissolved in methanol (2 mL), and the solution was added to EtOAc (20 mL). The suspension was kept still overnight. The supernatant was removed

carefully. The solid was washed with EtOAc (5 mL) and dried under high vacuum to afford **12d**. ^{1}H NMR (400 MHz, methanol-d_4) δ 9.82 (s, 1H), 8.58 (d, J = 6.7 Hz, 1H), 8.53–8.42 (m, 3H), 8.25 (dd, J = 8.7, 2.0 Hz, 1H), 7.85–7.70 (m, 2H), 7.51 (dd, J = 8.7, 2.2 Hz, 1H), 4.82–4.77 (m, 1H), 4.55 (s, 3H), 4.20 (t, J = 8.9 Hz, 1H),4.01 (dd, J = 8.9, 6.3 Hz, 1H), 3.90 (dd, J = 12.6, 3.1 Hz, 1H), 3.73 (dd, J = 12.6, 3.8 Hz, 1H). ^{13}C NMR (101 MHz, methanol-d_4) δ 161.5 (d, J = 248.2 Hz), 156.7, 151.3, 145.4 (d, J = 2.0 Hz), 142.9 (d, J = 11.5 Hz), 138.9, 137.0, 133.3 (d, J = 3.9 Hz), 132.6 (d, J = 4.0 Hz), 131.5, 128.0, 127.6 (d, J = 4.1 Hz), 127.1, 122.3 (d, J = 12.7 Hz), 115.4 (d, J = 3.1 Hz), 107.1 (d, J = 29.1 Hz), 75.3, 63.1, 48.7, 47.5. MSESI m/z: 353.1300 ($C_{20}H_{18}FN_2O_3^+$ requires 353.1296).

(R)-7-(2-Fluoro-4-(5-(hydroxymethyl)-2-oxooxazolidin-3-yl)-phenyl)-2-methylisoquinolin-2-ium Chloride (12e).—

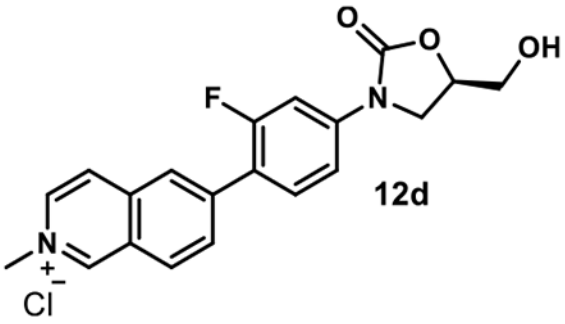

Using general procedure 5, employing **11e** (38 mg, 0.1 mmol) and methyl iodide (31.1 μL, 0.5 mmol), employing MeOH (1 mL) as the cosolvent in the deprotection step, compound **12e** was obtained as a yellow amorphous solid (25 mg, 64%). Pyridinium **12e** purification protocol: the crude residue was dissolved in a mixture of methanol (2 mL) and acetone (4 mL). The solution was precipitated with the addition of EtOAc (10 mL) and kept still overnight. The suspension was centrifuged, and the supernatant was removed carefully. The solid was resuspended in EtOAc (5 mL), and the suspension was centrifuged. The EtOAc supernatant was removed carefully, and the solid was dried under high vacuum to afford **12e**. ^{1}H NMR (400 MHz, DMSO-d_6) δ 10.05 (s, 1H), 8.73 (d, J = 6.8 Hz, 1H), 8.65 (s, 1H), 8.60 (d, J = 6.8 Hz, 1H), 8.44 (s, 2H), 7.91–7.71 (m, 2H), 7.59 (d, J = 8.8 Hz, 1H), 5.32 (t, J = 5.6 Hz, 1H), 4.87–4.69 (m, 1H), 4.49 (s, 3H), 4.17 (t, J = 9.0 Hz, 1H), 3.98–3.88 (m, 1H), 3.78–3.67 (m, 1H), 3.65–3.55 (m, 1H). ^{13}C NMR (101 MHz, DMSO-d_6) δ 159.4 (d, J = 246.4 Hz), 154.4, 150.9, 140.9 (d, J = 11.6 Hz), 137.1 (d, J = 2.3 Hz), 137.0, 136.2, 135.7, 131.4 (d, J = 4.1 Hz), 129.1 (d, J = 4.2 Hz), 127.8, 127.4, 125.3, 120.2 (d, J = 12.8 Hz), 114.1 (d, J = 3.0 Hz), 105.4 (d, J = 28.4 Hz), 73.5, 61.6, 48.1, 46.0 MSESI m/z: 353.1306 ($C_{20}H_{18}FN_2O_3^+$ requires 353.1296).

(R)-4-(2′-Fluoro-4′-(5-(hydroxymethyl)-2-oxooxazolidin-3-yl)- [1,1′-biphenyl]-4-yl)-1-methylpyridin-1-ium Chloride (12f).—

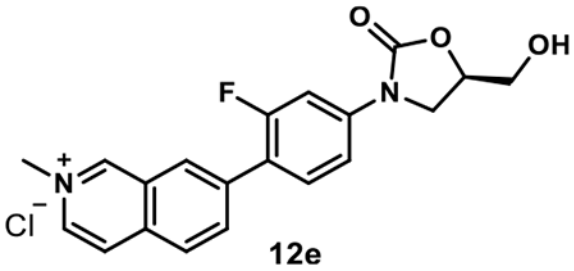

12e

Using general procedure 5, employing **11f** (41 mg, 0.1 mmol) and methyl iodide (31.1 μL, 0.5 mmol), compound **12f** was obtained as a brown amorphous solid (20 mg, 48%). Pyridinium **12f** purification protocol: the crude residue was suspended in acetone (3 mL), and the suspension was kept still for 30 min. The supernatant was removed carefully, and the solid was resuspended in acetone (3 mL). The acetone supernatant was removed carefully, and the solid was dried under high vacuum to afford **12f**. ^{1}H NMR (400 MHz, DMSO-d_6) δ 9.05 (d, J = 6.6 Hz, 2H), 8.57 (d, J = 6.6 Hz, 2H), 8.39–8.15 (m, 2H), 7.86–7.81 (m, 2H), 7.74–7.64 (m, 2H), 7.52 (dd, J = 8.6, 2.3 Hz, 1H), 5.31 (s, 1H), 4.86–4.69 (m, 1H), 4.34 (s, 3H), 4.15 (t, J = 9.0 Hz, 1H), 3.91 (dd, J = 9.0, 6.1 Hz, 1H), 3.76–3.66 (m, 1H), 3.64–3.55 (m, 1H). ^{13}C NMR (101 MHz, DMSO-d_6) δ 159.3 (d, J = 245.4 Hz), 154.4, 153.6, 145.7 (2C), 140.3 (d, J = 11.1 Hz), 138.3 (d, J = 1.9 Hz), 132.5, 131.0 (d, J = 4.4 Hz), 129.7 (d, J = 3.5 Hz, 2C), 128.4 (2C), 124.0 (2C), 121.2 (d, J = 13.0 Hz), 114.0 (d, J = 3.0 Hz), 105.4 (d, J = 28.6 Hz), 73.5, 61.6, 47.1, 46.0. MSESI m/z: 379.1418 ($C_{22}H_{20}FN_2O_3^+$ requires 379.1452).

(R)-3-(2′-Fluoro-4′-(5-(hydroxymethyl)-2-oxooxazolidin-3-yl)-[1,1′-biphenyl]-4-yl)-1-methylpyridin-1-ium Chloride (12g).—

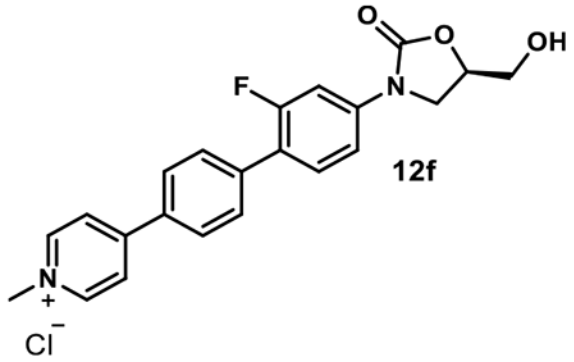

12f

Using general procedure 5, employing **11g** (41 mg, 0.1 mmol) and methyl iodide (31.1 μL, 0.5 mmol), compound **12g** was obtained as a gray amorphous solid (20 mg, 48%). Pyridinium **12g** purification protocol: the crude residue was suspended in acetone (3 mL), and the suspension was kept still for 30 min. The supernatant was removed carefully, and the solid was resuspended in acetone (3 mL). The acetone supernatant was removed carefully. The solid was suspended in MeOH (2 mL), and the suspension was added to EtOAc (10 mL). The resulting suspension was kept still overnight. The supernatant was removed carefully, and the solid was further washed with EtOAc (5 mL) and then dried under high vacuum to afford **12g**. ^{1}H NMR (400 MHz, DMSO-d_6) δ 9.53 (s, 1H), 9.00 (d, J = 6.0 Hz,

1H), 8.96 (d, J = 8.1 Hz, 1H), 8.23 (dd, J = 8.1, 6.0 Hz, 1H), 8.03 (d, J = 8.0 Hz, 2H), 7.81 (d, J = 8.0 Hz, 2H), 7.73–7.60 (m, 2H), 7.50 (dd, J = 8.6, 2.2 Hz, 1H), 5.33 (t, J = 5.6 Hz, 1H), 4.85–4.71 (m, 1H), 4.44 (s, 3H), 4.15 (t, J = 9.0 Hz, 1H), 3.92 (dd, J = 9.0, 6.1 Hz, 1H), 3.78–3.66 (m, 1H), 3.63–3.52 (m, 1H). ^{13}C NMR (101 MHz, DMSO-d_6) δ 159.2 (d, J = 245.1 Hz), 154.4, 143.9, 143.8, 142.0, 140.0 (d, J = 11.4 Hz), 138.6, 136.4, 132.3, 131.0 (d, J = 4.8 Hz), 129.6 (d, J = 3.4 Hz,2C), 127.73, 127.71 (2C), 121.5 (d, J = 13.0 Hz), 113.9 (d, J = 3.0 Hz), 105.4 (d, J = 28.6 Hz), 73.5, 61.6, 48.1, 46.0. MSESI m/z: 379.1468 ($C_{22}H_{20}FN_2O_3^+$ requires 379.1452).

(R)-2-(2′-Fluoro-4′-(5-(hydroxymethyl)-2-oxooxazolidin-3-yl)-[1,1′-biphenyl]-4-yl)-1-methylpyridin-1-ium Chloride (12h).—

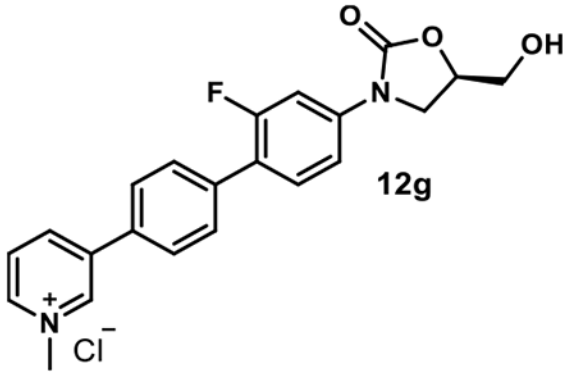

Using general procedure 5, employing **11h** (41 mg, 0.1 mmol) and methyl iodide (31.1 μL, 0.5 mmol), compound **12h** was obtained as a gray amorphous solid (10 mg, 24%). Pyridinium **12h** purification protocol: the crude residue was suspended in MeOH (2 mL), and the suspension was added to acetone (10 mL). The resulting suspension was kept still overnight. The supernatant was removed carefully, and the solid was further washed with acetone (2 × 10 mL) and then dried under high vacuum to afford **12h**. ^{1}H NMR (400 MHz, DMSO-d_6) δ 9.19 (d, J = 6.1 Hz, 1H), 8.66 (dd, J = 8.6, 7.2 Hz, 1H), 8.33–8.10 (m, 2H), 7.93–7.76 (m, 4H), 7.74–7.63 (m, 2H), 7.53 (dd, J = 8.7, 2.3 Hz, 1H), 5.30 (s, 1H), 4.82–4.70 (m, 1H), 4.39–4.08 (m, 4H), 3.91 (dd, J = 8.9, 6.0 Hz, 1H), 3.71 (dd, J = 12.4, 3.3 Hz, 1H), 3.58 (dd, J = 12.4, 3.8 Hz, 1H). ^{13}C NMR (101 MHz, DMSO-d_6) δ 159.2 (d, J = 245.5 Hz), 154.7, 154.4, 146.8, 145.5, 140.2 (d, J = 11.5 Hz), 137.3, 131.1 (d, J = 4.5 Hz), 130.9, 129.9, 129.7 (2C), 129.1 (d, J = 3.3 Hz, 2C), 126.8, 121.3 (d, J = 13.0 Hz), 114.0 (d, J = 3.1 Hz), 105.4 (d, J = 28.6 Hz), 73.5, 61.6, 47.2, 46.0. MSESI m/z: 379.1451 ($C_{22}H_{20}FN_2O_3^+$ requires 379.1452).

(R)-1-Ethyl-4-(2-fluoro-4-(5-(hydroxymethyl)-2-oxooxazolidin-3-yl)phenyl)pyridin-1-ium Chloride (12i).—

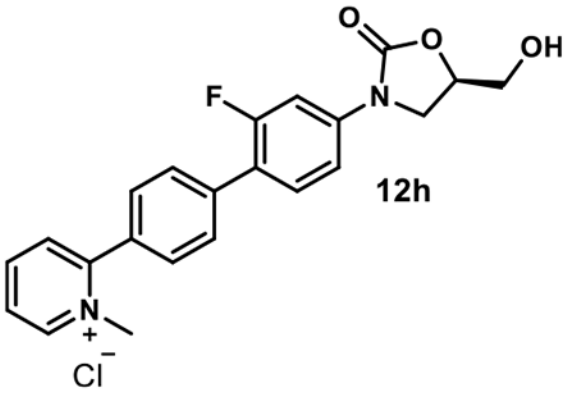

Using general procedure 5, employing **11a** (33 mg, 0.1 mmol) and ethyl iodide (40 μL, 0.5 mmol), compound **12i** was obtained as a yellow amorphous solid (15 mg, 42%). Pyridinium **12i** purification protocol: the crude residue was dissolved in MeOH (2 mL), and the solution was added to EtOAc (80 mL). The resulting suspension was kept still overnight. The supernatant was removed carefully, and the solid was further washed with EtOAc (10 mL) and then dried under high vacuum to afford **12i**. ^{1}H NMR (500 MHz, DMSO-d_6) δ 9.14 (d, J = 6.3 Hz, 2H), 8.37 (d, J = 6.3 Hz, 2H), 7.97 (t, J = 8.8 Hz, 1H), 7.85–7.73 (m, 1H), 7.66–7.55 (m, 1H), 5.31 (t, J = 5.6 Hz, 1H), 4.88–4.74 (m, 1H), 4.64 (q, J = 7.2 Hz, 2H), 4.18 (t, J = 9.1 Hz, 1H), 3.95 (dd, J = 9.1, 5.8 Hz, 1H), 3.78–3.66 (m, 1H), 3.62–3.54 (m, 1H), 1.57 (t, J = 7.2 Hz, 3H). ^{13}C NMR (101 MHz, DMSO-d_6) δ 160.2 (d, J = 250.6 Hz), 154.3, 150.1 (d, J = 1.9 Hz), 144.4 (2C), 143.3 (d, J = 11.9 Hz), 131.7 (d, J = 3.3 Hz), 126.3 (d, J = 5.3 Hz, 2C), 116.3 (d, J = 11.3 Hz), 114.1 (d, J = 2.8 Hz), 105.4 (d, J = 28.5 Hz), 73.7, 61.5, 55.7, 46.0, 16.3. MSESI *m/z*: 317.1291 ($C_{17}H_{18}FN_2O_3^+$ requires 317.1296).

(R)-4-(2-Fluoro-4-(5-(hydroxymethyl)-2-oxooxazolidin-3-yl)-phenyl)-1-propylpyridin-1-ium Chloride (12j).—

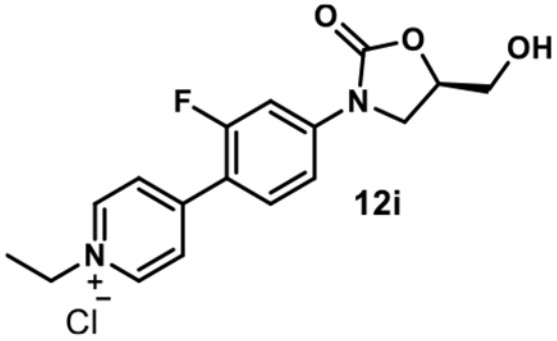

Using general procedure 5, employing **11a** (33 mg, 0.1 mmol) and propyl iodide (48.7 μL, 0.5 mmol), compound **12j** was obtained as a gray amorphous solid (15 mg, 41%). Pyridinium **12j** purification protocol: the crude residue was dissolved in MeOH (2 mL), and the solution was added to EtOAc (60 mL). The resulting suspension was kept still overnight. The supernatant was removed carefully, and the solid was further washed with EtOAc (2 × 20 mL) and then dried under high vacuum to afford **12j**. ^{1}H NMR (500 MHz, DMSO-d_6) δ 9.13 (d, J = 6.4 Hz, 2H), 8.38 (d, J = 6.4 Hz, 2H), 7.99 (t, J = 8.8 Hz, 1H), 7.78 (dd, J = 14.4,

2.2 Hz, 1H), 7.62 (dd, J = 8.8, 2.2 Hz, 1H), 5.31 (s, 1H), 4.89–4.75 (m, 1H), 4.58 (t, J = 7.3 Hz, 2H), 4.18 (t, J = 9.0 Hz, 1H), 3.95 (dd, J = 9.0, 5.9 Hz, 1H), 3.71 (dd, J = 12.5, 3.2 Hz, 1H), 3.59 (dd, J = 12.5, 3.8 Hz, 1H), 2.10–1.89 (m, 2H), 0.92 (t, J = 7.3 Hz, 3H). ^{13}C NMR (101 MHz, DMSO-d_6) δ 160.2 (d, J = 250.6 Hz), 154.3, 150.1 (d, J = 2.0 Hz), 144.6 (2C), 143.3 (d, J = 11.9 Hz), 131.7 (d, J = 3.4 Hz), 126.2 (d, J = 5.3 Hz, 2C), 116.2 (d, J = 11.4 Hz), 114.1 (d, J = 2.9 Hz), 105.4 (d, J = 28.4 Hz), 73.7, 61.5, 61.4, 46.0, 24.1, 10.3. MSESI m/z: 331.1463 ($C_{18}H_{20}FN_2O_3^+$ requires 331.1452).

(R)-4-(2-Fluoro-4-(5-(hydroxymethyl)-2-oxooxazolidin-3-yl)-phenyl)-1-isopropylpyridin-1-ium Chloride (12k).—

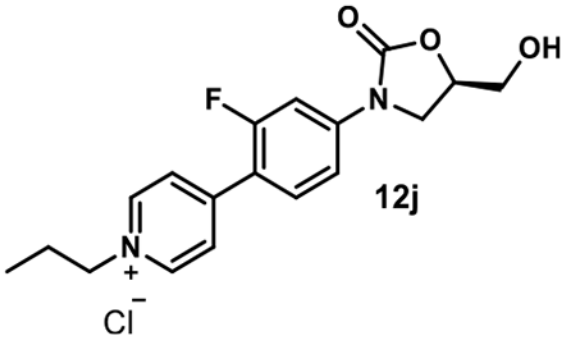

Using general procedure 5, employing **11a** (33 mg, 0.1 mmol) and isopropyl iodide (50 μL, 0.5 mmol), compound **12k** was obtained as a yellow amorphous solid (5 mg, 14%). Pyridinium **12k** purification protocol: the crude residue was dissolved in MeOH (1 mL), and the solution was added to EtOAc (80 mL). The resulting suspension was kept still overnight. The supernatant was removed carefully, and the solid was further washed with EtOAc (2 × 20 mL) and then dried under high vacuum to afford **12k**. ^{1}H NMR (400 MHz, methanol-d_4) δ 9.05 (d, J = 6.4 Hz, 2H), 8.31 (d, J = 6.4 Hz, 2H), 7.99–7.86 (m, 1H), 7.83–7.75 (m, 1H), 7.55 (dd, J = 9.5, 2.1 Hz, 1H), 5.02 (p, J = 6.7 Hz, 1H), 4.84–4.72 (m, 1H), 4.30–4.06 (m, 1H), 4.04–3.92 (m, 1H), 3.92–3.83 (m, 1H), 3.74–3.66 (m, 1H), 1.72 (d, J = 6.7 Hz, 6H). ^{13}C NMR (101 MHz, methanol-d_4) δ 162.3 (d, J = 251.4 Hz), 156.4, 153.1 (d, J = 2.1 Hz), 145.1 (d, J = 12.1 Hz), 143.8 (2C), 132.6 (d, J = 3.3 Hz), 127.9 (d, J = 5.9 Hz, 2C), 117.9 (d, J = 11.4 Hz), 115.5 (d, J = 3.0 Hz), 107.1 (d, J = 29.0 Hz), 75.4, 65.7, 63.1, 47.4, 23.1. MSESI m/z: 331.1446 ($C_{18}H_{20}FN_2O_3^+$ requires 331.1452).

(R)-1-Benzyl-4-(2-fluoro-4-(5-(hydroxymethyl)-2-oxooxazolidin-3-yl)phenyl)pyridin-1-ium Chloride (12l).—

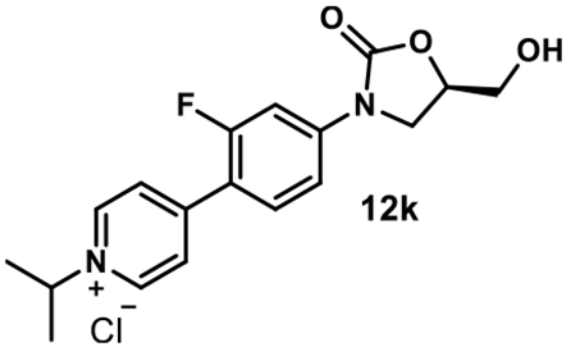

Using general procedure 5, employing **11a** (33 mg, 0.1 mmol) and benzyl bromide (59.4 μL, 0.5 mmol), compound **12l** was obtained as a gray amorphous solid (27 mg, 65%). Pyridinium **12l** purification protocol: the crude residue was dissolved in MeOH (2 mL), and the solution was added to EtOAc (15 mL). The resulting suspension was kept still overnight. The supernatant was removed carefully, and the solid was further washed with EtOAc (5 mL) and then dried under high vacuum to afford **12l**. ^{1}H NMR (500 MHz, DMSO-d_6) δ 9.23 (d, J = 6.5 Hz, 2H), 8.40 (d, J = 6.3 Hz, 2H), 7.97 (t, J = 8.8 Hz, 1H), 7.77 (dd, J = 14.4, 2.2 Hz, 1H), 7.62 (dd, J = 8.8, 2.2 Hz, 1H), 7.60–7.56 (m, 2H), 7.50–7.42 (m, 3H), 5.87 (s, 2H), 5.27 (t, J = 5.6 Hz, 1H), 4.84–4.69 (m, 1H), 4.17 (t, J = 9.1 Hz, 1H), 3.93 (dd, J = 9.1, 6.0 Hz, 1H), 3.71 (ddd, J = 12.4, 5.6, 3.2 Hz, 1H), 3.58 (ddd, J = 12.4, 5.6, 3.8 Hz, 1H). ^{13}C NMR (101 MHz, DMSO-d_6) δ 160.3 (d, J = 250.8 Hz), 154.2, 150.6 (d, J = 2.1 Hz), 144.6 (2C), 143.4 (d, J = 12.3 Hz), 134.4, 131.8 (d, J = 3.3 Hz), 129.4, 129.3 (2C), 128.8 (2C), 126.6 (d, J = 5.5 Hz, 2C), 116.2 (d, J = 11.1 Hz), 114.1 (d, J = 2.7 Hz), 105.4 (d, J = 28.3 Hz), 73.7, 62.6, 61.5, 46.0. MSESI m/z: 379.1469 ($C_{22}H_{20}FN_2O_3^+$ requires 379.1452).

General Procedure 6: Synthesis of Alkynyl Oxazolidinone Analogues 13a–ab.

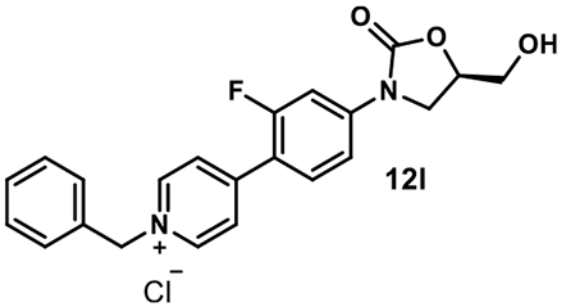

A solution of compound **6** (34 mg, 0.1 mmol), alkyne (0.15 mmol), tetrakis(triphenylphosphine)palladium(0) (12 mg, 0.01 mmol), and copper(I) iodide (2 mg, 0.01 mmol) in DMF (1 mL) was evacuated and purged with nitrogen three times. *N,N*-Diisopropylethylamine (0.5 mL) was added under the protection of a nitrogen atmosphere. The mixture was stirred at 25 °C. After the reaction was judged to be completed by TLC (16 h), it was diluted with EtOAc, washed with water three times, and concentrated under reduced pressure by rotary evaporation. The crude residue was purified by flash column chromatography (SiO_2) to afford compound **13**.

(R)-3-(4-((3,5-Dichlorophenyl)ethynyl)-3-fluorophenyl)-5-(hydroxymethyl)oxazolidin-2-one (13a).—

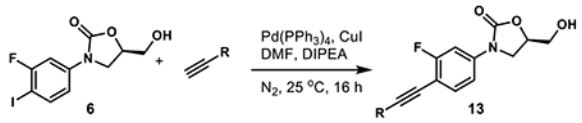

Using general procedure 6, employing 1,3-dichloro-5-ethynylbenzene (26 mg, 0.15 mmol), compound **13a** was obtained after flash column chromatography (SiO_2, 0–100% EtOAc in hexanes) as a yellow amorphous solid (34 mg, 89%). ^{1}H NMR (400 MHz, acetone-d_6) δ 7.72 (dd, J = 12.5, 2.2 Hz, 1H), 7.62 (t, J = 8.4 Hz, 1H), 7.54 (s, 3H), 7.45 (dd, J = 8.4, 2.2 Hz, 1H), 4.93–4.75 (m, 1H), 4.43 (s, 1H), 4.23 (t, J = 8.9 Hz, 1H), 4.05 (dd, J = 8.9, 6.3 Hz, 1H), 3.95–3.87 (m, 1H), 3.78 (dd, J = 12.5, 3.6 Hz, 1H). ^{13}C NMR (101 MHz, Acetone-d_6) δ 163.7 (d, J = 248.8 Hz), 155.2, 142.7 (d, J = 11.0 Hz), 135.9 (2C), 134.9 (d, J = 2.4 Hz), 130.5 (2C), 129.6, 127.0, 114.2 (d, J = 3.1 Hz), 105.7 (d, J = 27.1 Hz), 105.4 (d, J = 16.2 Hz), 91.4 (d, J = 3.0 Hz), 86.0, 74.5, 63.2, 47.0.

(R)-1-(3-((2-Fluoro-4-(5-(hydroxymethyl)-2-oxooxazolidin-3-yl)-phenyl)ethynyl)phenyl)thiourea (13b).—

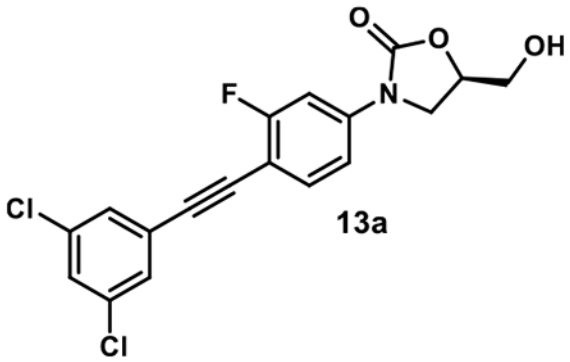

Using general procedure 6, employing (3-ethynylphenyl)thiourea (26 mg, 0.15 mmol), compound **13b** was obtained after flash column chromatography (SiO_2, 0–15% MeOH in DCM) followed by high-performance liquid chromatography purification as a yellow amorphous solid (17 mg, 44%). ^{1}H NMR (400 MHz, DMSO) δ 9.77 (s, 1H), 7.76–7.60 (m, 3H), 7.43 (d, J = 8.8 Hz, 2H), 7.37 (t, J = 7.8 Hz, 1H), 7.31–7.26 (m, 1H), 5.21 (t, J = 5.6 Hz, 1H), 4.79–4.65 (m, 1H), 4.13 (t, J = 9.0 Hz, 1H), 3.87 (dd, J = 9.0, 6.0 Hz, 2H), 3.75–3.63 (m, 1H), 3.64–3.51 (m, 1H). ^{13}C NMR (101 MHz, DMSO-d_6) δ 181.1, 162.0 (d, J = 247.4 Hz), 154.3, 140.7 (d, J = 11.1 Hz), 139.7, 133.8 (d, J = 2.5 Hz), 129.3, 127.1, 125.2, 123.5, 122.1, 113.5 (d, J = 3.0 Hz), 104.7 (d, J = 26.8 Hz), 104.6 (d, J = 15.7 Hz), 93.5 (d, J = 2.02 Hz), 82.5, 73.5, 61.6, 46.0.

(R)-3-(3-Fluoro-4-((1,3,5-trimethyl-1H-pyrazol-4-yl)ethynyl)-phenyl)-5-(hydroxymethyl)oxazolidin-2-one (13c).—

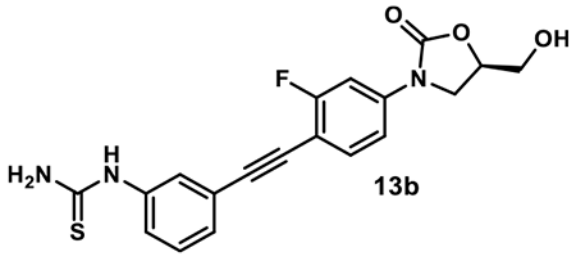

13b

Using general procedure 6, employing 4-ethynyl-1,3,5-trimethyl-1*H*-pyrazole (20 mg, 0.15 mmol), compound **13c** was obtained after flash column chromatography (SiO_2, 0–10% MeOH in DCM) as a white amorphous solid (20 mg, 59%). ^{1}H NMR (300 MHz, DMSO-d_6) δ 7.75–7.49 (m, 2H), 7.38 (dd, J = 8.6, 2.2 Hz, 1H), 5.25 (t, J = 5.6 Hz, 1H), 4.84–4.53 (m, 1H), 4.11 (t, J = 9.0 Hz, 1H), 3.85 (dd, J = 9.0, 6.1 Hz, 1H), 3.76–3.62 (m, 4H), 3.56 (ddd, J = 12.4, 5.6, 3.9 Hz, 1H), 2.30 (s, 3H), 2.18 (s, 3H). ^{13}C NMR (151 MHz, DMSO-d_6) δ 161.4 (d, J = 246.4 Hz), 154.2, 147.7, 142.0, 139.6 (d, J = 10.6 Hz), 133.0, 113.4 (d, J = 2.8 Hz), 105.9 (d, J = 15.9 Hz), 104.7 (d, J = 26.9 Hz), 100.1, 86.7 (d, J = 1.5 Hz), 85.2, 73.4, 61.5, 45.9, 36.0, 12.1, 10.0.

Methyl (R)-2-(4-((2-Fluoro-4-(5-(hydroxymethyl)-2-oxooxazolidin-3-yl)phenyl)ethynyl)-1H-pyrazol-1-yl)acetate (13d).—

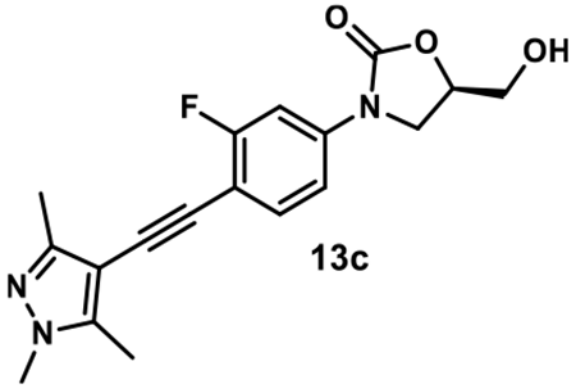

13c

Using general procedure 6, employing methyl (4-ethynyl-1H-pyrazol- 1-yl)acetate (25 mg, 0.15 mmol), compound **13d** was obtained after flash column chromatography (SiO_2, 0–10% MeOH in DCM) as a white amorphous solid (17 mg, 46%). ^{1}H NMR (400 MHz, acetone-d_6) δ 8.03 (s, 1H), 7.73–7.63 (m, 2H), 7.52 (t, J = 8.6 Hz, 1H), 7.40 (dd, J = 8.6, 2.3 Hz, 1H), 5.09 (s, 2H), 4.89–4.72 (m, 1H), 4.44 (s, 1H), 4.22 (t, J = 8.9 Hz, 1H), 4.03 (dd, J = 8.9, 6.2 Hz, 1H), 3.90 (d, J = 12.7 Hz, 1H), 3.81–3.64 (m, 4H). ^{13}C NMR (101 MHz, acetone-d_6) δ 168.9, 163.2 (d, J = 247.2 Hz), 155.1, 142.5, 141.5 (d, J = 10.9 Hz), 135.0, 134.2 (d, J = 2.9 Hz), 114.0 (d, J = 3.1 Hz), 106.8 (d, J = 16.3 Hz), 105.6 (d, J = 27.2 Hz), 104.0, 86.0 (d, J = 2.9 Hz), 83.5, 74.4, 63.1, 53.5, 52.7, 46.9.

(R)-4-((2-Fluoro-4-(5-(hydroxymethyl)-2-oxooxazolidin-3-yl)-phenyl)ethynyl)-1-methyl-1H-pyrazole-5-carboxylic Acid (13e).—

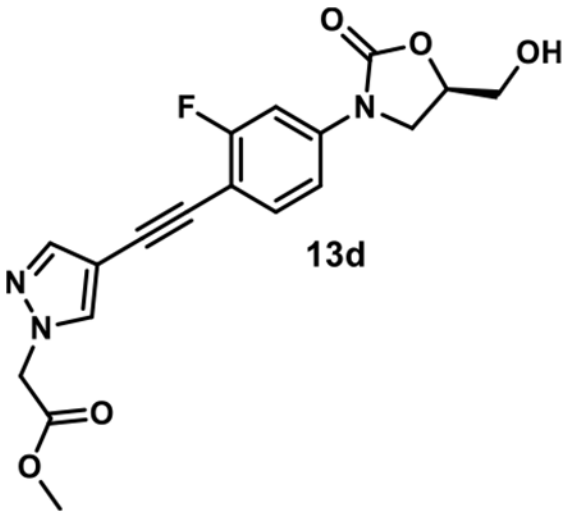

13d

Using general procedure 6, employing 4-ethynyl-1-methyl-1*H*-pyrazole-5-carboxylic acid (23 mg, 0.15 mmol), compound **13e** was obtained after flash column chromatography (SiO_2, 0–15% MeOH in DCM) followed by high-performance liquid chromatography purification as a gray amorphous solid (11 mg, 42%). ^{1}H NMR (400 MHz, DMSO-d_6) δ 7.97 (s, 1H), 7.82 (t, J = 8.9 Hz, 1H), 7.70 (dd, J = 14.6, 2.3 Hz, 1H), 7.49 (dd, J = 8.9, 2.3 Hz, 1H), 7.25 (s, 1H), 5.27 (t, J = 5.6 Hz, 1H), 4.82–4.70 (m, 1H), 4.21 (s, 3H), 4.13 (t, J = 8.9 Hz, 1H), 3.88 (dd, J = 8.9, 6.0 Hz, 1H), 3.70 (ddd, J = 12.3, 5.6, 3.2 Hz, 1H), 3.57 (ddd, J = 12.3, 5.6, 3.9 Hz, 1H). ^{13}C NMR (101 MHz, DMSO-d_6) δ 159.0 (d, J = 248.9 Hz), 154.3, 153.5, 146.6 (d, J = 4.8 Hz), 140.7 (d, J = 11.8 Hz), 133.9, 128.7 (d, J = 3.4 Hz), 125.9, 124.9, 114.3 (d, J = 10.8 Hz), 113.6 (d, J = 2.8 Hz), 105.4 (d, J = 28.7 Hz), 100.7 (d, J = 13.0 Hz), 73.6, 61.6, 46.0, 38.4.

(R)-3-(4-((6-Aminopyridin-2-yl)ethynyl)-3-fluorophenyl)-5-(hydroxymethyl)oxazolidin-2-one (13f).—

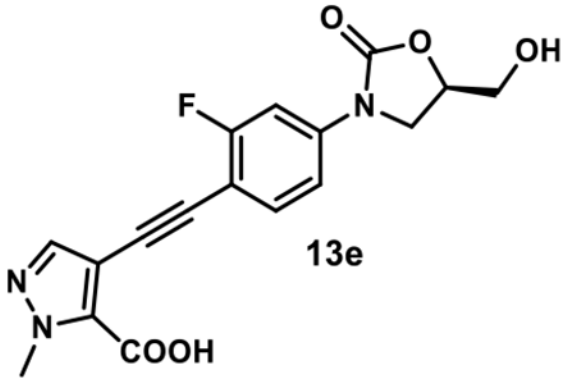

13e

Using general procedure 6, employing 6-ethynylpyridin-2-amine (18 mg, 0.15 mmol), compound **13f** was obtained after flash column chromatography (SiO_2, 0–8% MeOH in DCM) followed by high-performance liquid chromatography purification as a yellow amorphous solid (14 mg, 42%). ^{1}H NMR (400 MHz, DMSO-d_6) δ 7.73–7.56 (m, 2H), 7.48–7.33 (m, 2H), 6.74 (d, J = 7.2 Hz, 1H), 6.46 (d, J = 8.4 Hz, 1H), 6.19 (s, 2H), 5.33–5.16 (m,

1H), 4.82–4.67 (m, 1H), 4.12 (t, J = 9.0 Hz, 1H), 3.86 (dd, J = 9.0, 6.0 Hz, 1H), 3.72–3.64 (m, 1H), 3.61–3.52 (m, 1H). ^{13}C NMR (101 MHz, DMSO-d_6) δ 162.2 (d, J = 247.7 Hz), 159.8, 154.2, 140.8 (d, J = 11.1 Hz), 139.8, 137.4, 133.9 (d, J = 2.5 Hz), 115.6, 113.5 (d, J = 3.0 Hz), 108.8, 104.8 (d, J = 26.8 Hz), 104.3 (d, J = 15.8 Hz), 94.1 (d, J = 2.9 Hz), 79.7, 73.5, 61.6, 46.0.

(R)-3-(3-Fluoro-4-(3-methoxyprop-1-yn-1-yl)phenyl)-5-(hydroxymethyl)oxazolidin-2-one (13g).—

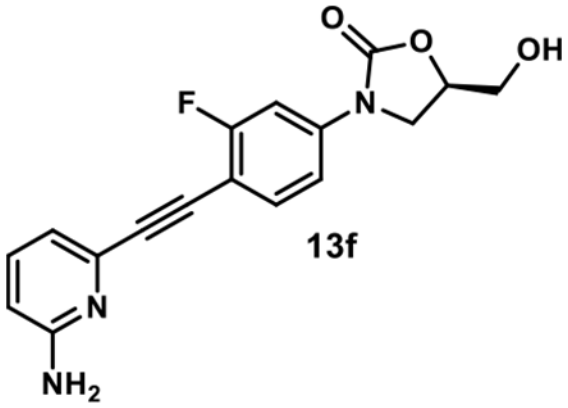

13f

Using general procedure 6, employing methyl propargyl ether (12.7 μL, 0.15 mmol), compound **13g** was obtained after flash column chromatography (SiO_2, 0–100% EtOAc in hexanes) as a white amorphous solid (22 mg, 79%). ^{1}H NMR (600 MHz, acetone-d_6) δ 7.67 (dd, J = 12.4, 2.1 Hz, 1H), 7.50 (t, J = 8.5 Hz, 1H), 7.38 (dd, J = 8.5, 2.1 Hz, 1H), 4.85–4.75 (m, 1H), 4.38 (t, J = 6.0 Hz, 1H), 4.33 (s, 2H), 4.21 (t, J = 8.9 Hz, 1H), 4.02 (dd, J = 8.9, 6.2 Hz, 1H), 3.92–3.86 (m, 1H), 3.79–3.72 (m, 1H), 3.38 (s, 3H). ^{13}C NMR (101 MHz, acetone-d$_6$) δ 163.7 (d, J = 247.8 Hz), 155.1, 142.0 (d, J = 10.9 Hz), 134.6 (d, J = 2.8 Hz), 113.9 (d, J = 3.2 Hz), 105.9 (d, J = 16.3 Hz), 105.6 (d, J = 27.3 Hz), 90.9 (d, J = 3.1 Hz), 79.7, 74.4, 63.1, 60.5, 57.5, 46.9.

(R)-3-(3-Fluoro-4-(3-(methylthio)prop-1-yn-1-yl)phenyl)-5-(hydroxymethyl)oxazolidin-2-one (13h).—

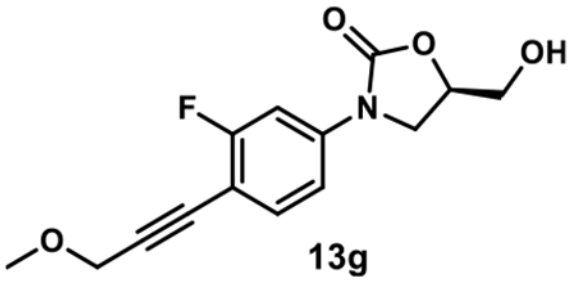

13g

A solution of compound **6** (34 mg, 0.1 mmol), 3-(methylsulfanyl)-1-propyne (39 mg, 0.3 mmol), tetrakis(triphenylphosphine)- palladium(0) (23 mg, 0.02 mmol), and copper(I) iodide (3.8 mg, 0.02 mmol) in DMF (1 mL) was evacuated and purged with nitrogen three times. *N,N*-Diisopropylethylamine (0.5 mL) was added under the protection of a nitrogen atmosphere. The mixture was stirred at 25 °C. After the reaction was judged to be completed

by TLC (16 h), it was diluted with EtOAc, washed with water three times, and concentrated under reduced pressure by rotary evaporation. The crude residue was purified by flash column chromatography (SiO_2, 0–100% EtOAc in hexanes) to afford compound 13h as a yellow amorphous solid (20 mg, 68%). ^{1}H NMR (400 MHz, acetone-d_6) δ 7.65 (dd, J = 12.4, 2.3 Hz, 1H), 7.47 (t, J = 8.5 Hz, 1H), 7.36 (dd, J = 8.5, 2.3 Hz, 1H), 4.89–4.73 (m, 1H), 4.41 (t, J = 5.9 Hz, 1H), 4.20 (t, J = 8.9 Hz, 1H), 4.01 (dd, J = 8.9, 6.2 Hz, 1H), 3.90 (ddd, J = 12.3, 5.9, 3.3 Hz, 1H), 3.76 (ddd, J = 12.3, 5.9, 3.9 Hz, 1H), 3.57 (s, 2H), 2.26 (s, 3H). ^{13}C NMR (101 MHz, acetone-d_6) δ 163.6 (d, J = 247.3 Hz), 155.1, 141.6 (d, J = 10.9 Hz), 134.5 (d, J = 2.9 Hz), 113.9 (d, J = 3.1 Hz), 106.4 (d, J = 16.2 Hz), 105.5 (d, J = 27.3 Hz), 91.2 (d, J = 3.1 Hz), 76.3, 74.3, 63.1, 46.9, 22.3, 15.1.

Ethyl (R)-5-(2-Fluoro-4-(5-(hydroxymethyl)-2-oxooxazolidin-3-yl)phenyl)-2,2-dimethylpent-4-ynoate (13i).—

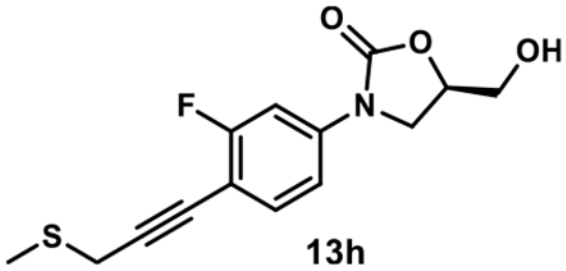

13h

Using general procedure 6, employing ethyl 2,2-dimethyl-4-pentynoate (23 mg, 0.15 mmol), compound **13i** was obtained after flash column chromatography (SiO_2, 0–100% EtOAc in hexanes) as a yellow oil (21 mg, 58%). ^{1}H NMR (400 MHz, acetone-d_6) δ 7.63 (dd, J = 12.4, 2.3 Hz, 1H), 7.42 (t, J = 8.6 Hz, 1H), 7.34 (dd, J = 8.6, 2.3 Hz, 1H), 4.85–4.68 (m, 1H), 4.39 (t, J = 5.7 Hz, 1H), 4.24–4.07 (m, 3H), 4.00 (dd, J = 8.9, 6.2 Hz, 1H), 3.93–3.81 (m, 1H), 3.82–3.69 (m, 1H), 2.70 (s, 2H), 1.31 (s, 6H), 1.23 (t, J = 7.1 Hz, 3H). ^{13}C NMR (101 MHz, acetone-d_6) δ 176.5, 163.6 (d, J = 247.0 Hz), 155.1, 141.3 (d, J = 10.8 Hz), 134.4 (d, J = 2.9 Hz), 113.8 (d, J = 3.1 Hz), 106.9 (d, J = 16.3 Hz), 105.6 (d, J = 27.3 Hz), 92.5 (d, J = 3.0 Hz), 76.2, 74.3, 63.1, 61.1, 46.9, 43.0, 31.1, 24.9, 14.5.

(R)-1-(3-(2-Fluoro-4-(5-(hydroxymethyl)-2-oxooxazolidin-3-yl)-phenyl)prop-2-yn-1-yl)-3-methylurea (13j).—

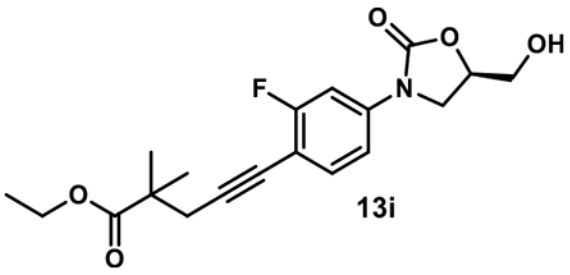

13i

Using general procedure 6, employing *N*-methyl-*N*′-(2-propynyl)urea (17 mg, 0.15 mmol), compound **13j** was obtained after flash column chromatography (SiO_2, 0–10% MeOH in DCM) as a yellow amorphous solid (7 mg, 22%). ^{1}H NMR (400 MHz, DMSO-d_6) δ 7.58

(dd, J = 12.3, 2.3 Hz, 1H), 7.49 (t, J = 8.6 Hz, 1H), 7.37 (dd, J = 8.6, 2.3 Hz, 1H), 6.39 (t, J = 5.8 Hz, 1H), 5.92 (q, J = 4.6 Hz, 1H), 5.25 (t, J = 5.5 Hz, 1H), 4.78–4.67 (m, 1H), 4.15–3.98 (m, 3H), 3.83 (dd, J = 8.9, 6.0 Hz, 1H), 3.73–3.62 (m, 1H), 3.60–3.51 (m, 1H), 2.56 (d, J = 4.6 Hz, 3H). ^{13}C NMR (101 MHz, DMSO-d_6) δ 162.2 (d, J = 246.9 Hz), 158.1, 154.2, 140.2 (d, J = 10.9 Hz), 133.8 (d, J = 2.7 Hz), 113.4 (d, J = 3.0 Hz), 104.9 (d, J = 15.6 Hz), 104.7 (d, J = 26.8 Hz), 93.3 (d, J = 3.0 Hz), 74.2, 73.5, 61.6, 45.9, 29.7, 26.5.

(R)-3-(3-Fluoro-4-(3-(2-oxoimidazolidin-1-yl)prop-1-yn-1-yl)-phenyl)-5-(hydroxymethyl)oxazolidin-2-one (13k).—

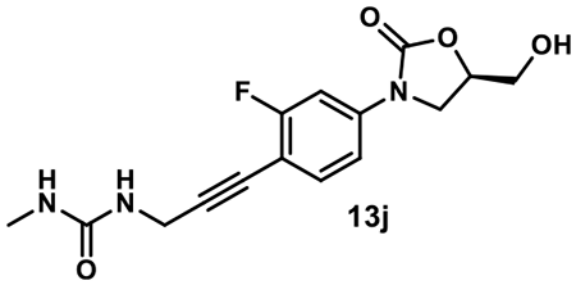

13j

Using general procedure 6, employing 1-(2-propynyl)-2-imidazolidinone (19 mg, 0.15 mmol), compound **13k** was obtained after flash column chromatography (SiO_2, 0–10% MeOH in DCM) as a yellow amorphous solid (10 mg, 30%). ^{1}H NMR (400 MHz, DMSO-d_6) δ 7.59 (dd, J = 12.4, 2.2 Hz, 1H), 7.53 (t, J = 8.5 Hz, 1H), 7.37 (dd, J = 8.5, 2.2 Hz, 1H), 6.61 (s, 1H), 5.22 (t, J = 5.6 Hz, 1H), 4.83–4.57 (m, 1H), 4.16 (s, 2H), 4.09 (t, J = 9.0 Hz, 1H), 3.84 (dd, J = 9.0, 6.0 Hz, 1H), 3.67 (ddd, J = 12.5, 5.6, 3.2 Hz, 1H), 3.56 (ddd, J = 12.5, 7.9, 5.6 Hz, 1H), 3.50–3.37 (m, 2H), 3.30–3.15 (m, 2H). ^{13}C NMR (101 MHz, DMSO-d_6) δ 162.2 (d, J = 247.2 Hz), 161.6, 154.2, 140.4 (d, J = 10.9 Hz), 133.8 (d, J = 2.6 Hz), 113.4 (d, J = 3.0 Hz), 104.6 (d, J = 42.8 Hz), 104.5, 89.7 (d, J = 2.9 Hz), 76.4, 73.4, 61.5, 45.9, 44.0, 37.2, 33.7.

(5R)-3-(3-Fluoro-4-(3-(4-(1-hydroxyethyl)phenoxy)prop-1-yn-1-yl)phenyl)-5-(hydroxymethyl)oxazolidin-2-one (13l).—

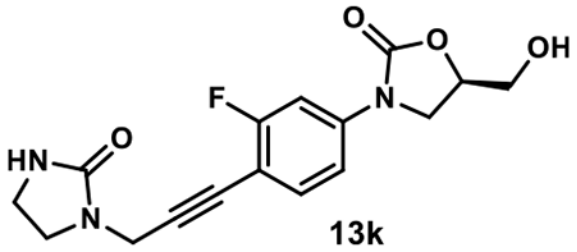

13k

Using general procedure 6, employing 1-[4-(2-propynyloxy)phenyl]-ethanol (26 mg, 0.15 mmol), compound **13l** was obtained after flash column chromatography (SiO_2, 0–10% MeOH in DCM) as a yellow oil (30 mg, 79%). ^{1}H NMR (300 MHz, acetone-d_6) δ 7.66 (dd, J = 12.4, 2.2 Hz, 1H), 7.49 (t, J = 8.3 Hz, 1H), 7.40–7.28 (m, 3H), 7.01 (d, J = 8.2 Hz, 2H), 5.02 (s, 2H), 4.88–4.71 (m, 2H), 4.42 (t, J = 5.8 Hz, 1H), 4.19 (t, J = 8.9 Hz, 1H), 4.09 (d, J = 4.0 Hz, 1H),4.01 (dd, J = 8.9, 6.2 Hz, 1H), 3.93–3.84 (m, 1H), 3.81–3.68 (m, 1H), 1.37 (d, J = 6.4 Hz, 3H). ^{13}C NMR (101 MHz, acetone-d_6) δ 163.7 (d, J = 248.3 Hz), 157.6, 155.1,

142.2 (d, J = 11.0 Hz), 141.1, 134.7 (d, J = 2.8 Hz), 127.3 (2C), 115.3 (2C), 113.9 (d, J = 3.1 Hz), 105.5 (d, J = 27.2 Hz), 105.5 (d, J = 16.2 Hz), 90.1 (d, J = 3.0 Hz), 80.4, 74.4, 69.5, 63.1, 57.0, 46.9, 26.2.

(R)-3-(2-Fluoro-4-(5-(hydroxymethyl)-2-oxooxazolidin-3-yl)-phenyl)prop-2-yn-1-yl Acetate (13m).—

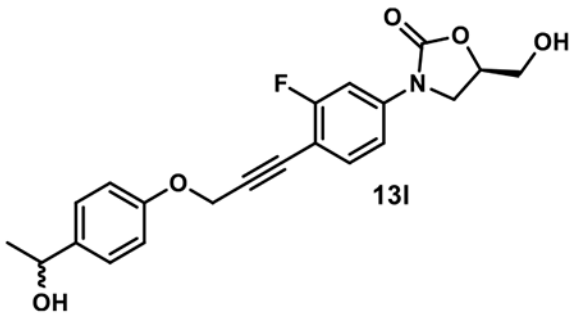

Using general procedure 6, employing propargyl acetate (15 mg, 0.15 mmol), compound **13m** was obtained after flash column chromatography (SiO_2, 0–100% EtOAc in hexanes) as a yellow amorphous solid (20 mg, 65%). ^{1}H NMR (400 MHz, acetone-d_6) δ 7.67 (dd, J = 12.5, 2.3 Hz, 1H), 7.50 (t, J = 8.3 Hz, 1H), 7.39 (dd, J = 8.3, 2.3 Hz, 1H), 4.94 (s, 2H), 4.86–4.72 (m, 1H), 4.39 (t, J = 5.8 Hz, 1H), 4.21 (t, J = 8.9 Hz, 1H), 4.02 (dd, J = 8.9, 6.1 Hz, 1H), 3.90 (ddd, J = 12.4, 5.8, 3.3 Hz, 1H), 3.77 (ddd, J = 12.4, 5.8, 3.8 Hz, 1H), 2.09 (s, 3H). ^{13}C NMR (101 MHz, acetone-d_6) δ 170.4, 163.8 (d, J = 248.2 Hz), 155.1, 142.3 (d, J = 10.9 Hz), 134.8 (d, J = 2.7 Hz), 114.0 (d, J = 3.1 Hz), 105.6 (d, J = 27.2 Hz), 105.4 (d, J = 16.1 Hz), 89.1 (d, J = 3.2 Hz), 79.7, 74.4, 63.1, 52.9, 46.9, 20.6.

(R)-3-(3-Fluoro-4-(3-hydroxyprop-1-yn-1-yl)phenyl)-5-(hydroxymethyl)oxazolidin-2-one (13n).—

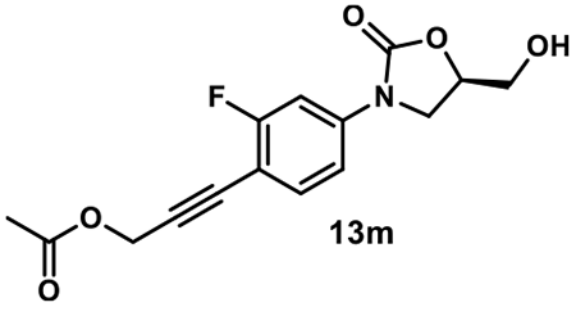

To a solution of compound **13m** (39 mg, 0.127 mmol) in THF (1.5 mL), MeOH (0.5 mL), and H_2O (0.5 mL) was added lithium hydroxide monohydrate (53 mg, 1.27 mmol). The reaction mixture was stirred at 25 °C for 1 h, quenched with the addition of water, and extracted with EtOAc four times. The combined organic layers were concentrated under reduced pressure by rotary evaporation. The residue was purified by flash column chromatography (SiO_2, 0–10% MeOH in DCM) followed by preparative TLC (SiO_2, 10% MeOH in DCM) to give compound **13n** as a yellow amorphous solid (16 mg, 47%). ^{1}H NMR (400 MHz, methanol-d_4) δ 7.56 (d, J = 12.1 Hz, 1H), 7.42 (t, J = 8.6 Hz, 1H), 7.26

(d, J = 8.6 Hz, 1H), 4.77–4.66 (m, 1H), 4.39 (s, 2H), 4.20–4.03 (m, 1H), 3.95–3.86 (m, 1H), 3.85–3.78 (m, 1H), 3.70–3.63 (m, 1H). ^{13}C NMR (101 MHz, methanol-d_4) δ 164.2 (d, J = 248.6 Hz), 156.6, 141.6 (d, J = 10.8 Hz), 134.9 (d, J = 2.8 Hz), 114.4 (d, J = 3.2 Hz), 107.4 (d, J = 16.1 Hz), 106.4 (d, J = 27.3 Hz), 93.7 (d, J = 3.0 Hz), 78.4, 75.2, 63.2, 51.2, 47.5.

(R)-6-(2-Fluoro-4-(5-(hydroxymethyl)-2-oxooxazolidin-3-yl)-phenyl)hex-5-ynoic Acid (13o).—

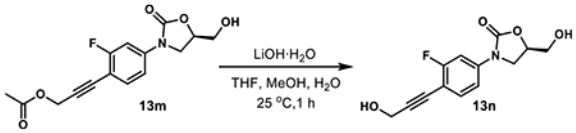

A solution of compound **6** (34 mg, 0.1 mmol), 5-hexynoic acid (17 mg, 0.15 mmol), tetrakis(triphenylphosphine)palladium(0) (12 mg, 0.01 mmol), and copper(I) iodide (2 mg, 0.01 mmol) in CH_3CN (1 mL) was evacuated and purged with nitrogen three times. *N,N*-Diisopropylethylamine (0.5 mL) was added under the protection of a nitrogen atmosphere. The mixture was stirred at 25 °C. After the reaction was judged to be complete by TLC (16 h), its solvent was concentrated under reduced pressure by rotary evaporation. The residue was diluted with MeOH (10 mL), acidified with formic acid (2 mL), and concentrated under reduced pressure by a rotary evaporator. The residue was purified by flash column chromatography (SiO_2, 10–20% MeOH in DCM with 0.1% formic acid) to give compound **13o** as a yellow amorphous solid (10 mg, 31%). ^{1}H NMR (400 MHz, methanol-d_4) δ 7.51 (dd, J = 12.1, 2.3 Hz, 1H), 7.34 (t, J = 8.6 Hz, 1H), 7.20 (dd, J = 8.6, 2.3 Hz, 1H), 4.75–4.63 (m, 1H), 4.06 (t, J = 8.9 Hz, 1H), 3.87 (dd, J = 8.9, 6.3 Hz, 1H), 3.80 (dd, J = 12.5, 3.2 Hz, 1H), 3.64 (dd, J = 3.9 Hz, 1H), 2.53–2.36 (m, 4H), 1.91–1.76 (m, 2H). ^{13}C NMR (101 MHz, methanol-d_4) δ 177.4, 164.1 (d, J = 247.8 Hz), 156.7, 140.9 (d, J = 10.6 Hz), 134.7 (d, J = 2.9 Hz), 114.4 (d, J = 3.4 Hz), 108.4 (d, J = 16.5 Hz), 106.4 (d, J = 27.4 Hz), 95.0 (d, J = 3.0 Hz), 75.2, 75.0, 63.2, 47.5, 34.2, 25.3, 19.6.

(R)-3-(4-(3-(4-Acetylpiperazin-1-yl)prop-1-yn-1-yl)-3-fluorophenyl)-5-(hydroxymethyl)oxazolidin-2-one (13p).—

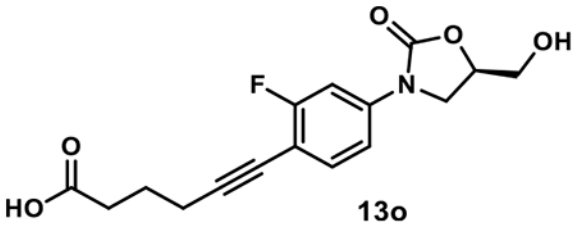

Using general procedure 6, employing 1-(4-(prop-2-yn-1-yl)piperazin-1-yl)ethan-1-one (25 mg, 0.15 mmol), compound **13p** was obtained after flash column chromatography (SiO_2, 0–15% MeOH in DCM) as a white amorphous solid (27 mg, 71%). ^{1}H NMR (400 MHz, DMSO-d_6) δ 7.64 (dd, J = 12.3, 2.2 Hz, 1H), 7.56 (t, J = 8.4 Hz, 1H), 7.41 (dd, J = 8.4, 2.1 Hz, 1H), 5.29 (t, J = 5.5 Hz, 1H), 4.89–4.63 (m, 1H), 4.13 (t, J = 9.0 Hz, 1H), 3.88 (dd, J = 9.0, 6.1 Hz, 1H), 3.72 (ddd, J = 12.4, 5.5, 3.2 Hz, 1H), 3.69–3.55 (m, 3H), 3.55–3.45 (m, 4H), 2.73–2.52 (m, 4H), 2.03 (s, 3H). ^{13}C NMR (151 MHz, DMSO-d_6) δ 168.1, 162.1 (d, J = 246.9 Hz), 154.2, 140.2 (d, J = 10.8 Hz), 133.7 (d, J = 2.7 Hz), 113.3 (d, J = 3.0 Hz), 104.7

(d, J = 16.1 Hz), 104.7 (d, J = 26.9 Hz), 89.8 (d, J = 3.0 Hz), 78.0, 73.4, 61.5, 51.5, 51.0, 46.7, 45.9, 45.5, 40.6, 21.2.

Ethyl (R)-1-(3-(2-Fluoro-4-(5-(hydroxymethyl)-2-oxooxazolidin-3-yl)phenyl)prop-2-yn-1-yl)piperidine-4-carboxylate (13q).—

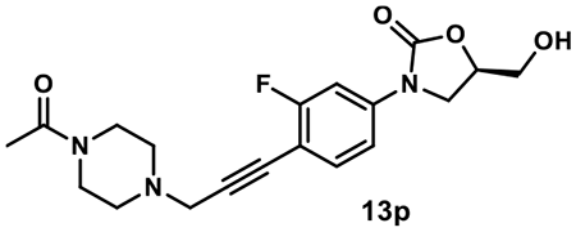

13p

Using general procedure 6, employing ethyl 1-(prop-2-yn-1-yl)- piperidine-4-carboxylate (29 mg, 0.15 mmol), compound **13q** was obtained after flash column chromatography (SiO_2, 0–15% MeOH in DCM) as a yellow amorphous solid (23 mg, 57%). ^{1}H NMR (400 MHz, DMSO-d_6) δ 7.59 (d, J = 12.4 Hz, 1H), 7.51 (t, J = 8.6 Hz, 1H), 7.36 (d, J = 8.6 Hz, 1H), 5.24 (t, J = 5.6 Hz, 1H), 4.87–4.61 (m, 1H), 4.17–4.00 (m, 3H), 3.84 (t, J = 7.6 Hz, 1H), 3.67 (dt, J = 8.5, 4.1 Hz, 1H), 3.60–3.45 (m, 3H), 2.90–2.70 (m, 2H), 2.44–2.10 (m, 3H), 1.90–1.70 (m, 2H), 1.70–1.46 (m, 2H), 1.17 (t, J = 7.1 Hz, 3H). ^{13}C NMR (101 MHz, DMSO-d_6) δ 174.3, 162.1 (d, J = 246.9 Hz), 154.2, 140.1 (d, J = 10.9 Hz), 133.7 (d, J = 2.6 Hz), 113.3 (d, J = 3.0 Hz), 104.9 (d, J = 16.1 Hz), 104.7 (d, J = 27.0 Hz), 90.3 (d, J = 3.1 Hz), 77.8, 73.4, 61.6, 59.8, 51.0 (2C), 47.2, 45.9, 39.8, 27.9 (2C), 14.1.

tert-Butyl 2-(2-((tert-Butoxycarbonyl)amino)-5-(2-fluoro-4-((R)-5-(hydroxymethyl)-2-oxooxazolidin-3-yl)phenyl)pent-4-ynoyl)- hydrazine-1-carboxylate (13r).—

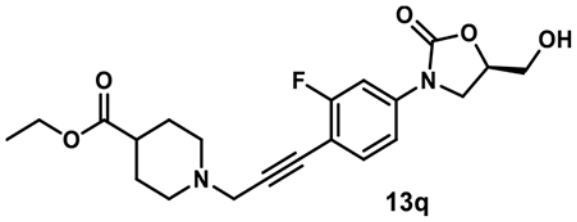

13q

A solution of compound **6** (34 mg, 0.1 mmol), compound **17** (49 mg, 0.15 mmol), tetrakis(triphenylphosphine)palladium(0) (30 mg, 0.025 mmol), and copper(I) iodide (4 mg, 0.02 mmol) in DMF (1 mL) was evacuated and purged with nitrogen three times. *N,N*-Diisopropylethylamine (0.5 mL) was added under the protection of a nitrogen atmosphere. The mixture was stirred at 50 °C. After the reaction was judged to be completed by TLC (12 h), it was diluted with EtOAc, washed with water three times, and concentrated under reduced pressure by rotary evaporation. The crude residue was purified by flash column chromatography (SiO_2 eluent gradient 0–100% EtOAc in hexanes) followed by preparative TLC purification (SiO_2, eluent 100% EtOAc) to afford compound **13r** as a white amorphous solid (32 mg, 59%). ^{1}H NMR (400 MHz, acetone-d_6) δ 9.17 (s, 1H), 7.97 (s, 1H), 7.63 (dd, J = 12.3, 2.3 Hz, 1H), 7.47 (t, J = 8.5 Hz, 1H), 7.33 (dd, J = 8.5, 2.3 Hz, 1H), 6.29 (d, J = 8.8 Hz, 1H), 4.87–4.74 (m, 1H), 4.55–4.29 (m, 2H), 4.19 (t, J = 8.9 Hz, 1H), 4.00 (dd, J =

8.9, 6.2 Hz, 1H), 3.89 (dd, J = 12.3, 3.3 Hz, 1H), 3.76 (dd, J = 12.3, 3.8 Hz, 1H), 2.98 (dd, J = 5.4 Hz, 1H), 2.86 (dd, J = 17.0, 8.0 Hz, 1H), 1.51–1.34 (m, 18H). ^{13}C NMR (101 MHz, acetone-d_6) δ 170.9, 163.5 (d, J = 247.4 Hz), 156.2, 156.1, 155.1, 141.3 (d, J = 10.9 Hz), 134.8, 113.7 (d, J = 3.2 Hz), 106.8 (d, J = 16.0 Hz), 105.4 (d, J = 27.4 Hz), 91.3, 80.5, 79.7, 74.3, 63.1, 55.4, 52.9, 46.9, 28.5, 28.4, 24.2.

tert-Butyl (R)-(3-(2-Fluoro-4-(5-(hydroxymethyl)-2-oxooxazolidin-3-yl)phenyl)prop-2-yn-1-yl)carbamate (13s).—

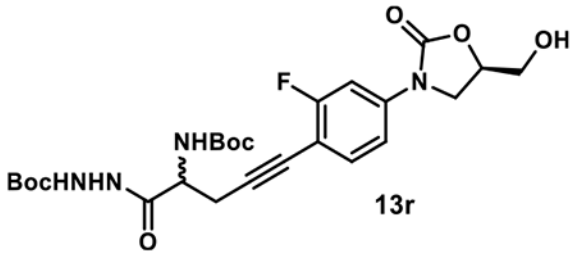

13r

A solution of compound **6** (67 mg, 0.2 mmol), **18** (37 mg, 0.24 mmol), tetrakis(triphenylphosphine)palladium(0) (23 mg, 0.02 mmol), and copper(I) iodide (4 mg, 0.02 mmol) in DMF (2 mL) was evacuated and purged with nitrogen three times. *N,N*-Diisopropylethylamine (1 mL) was added under the protection of a nitrogen atmosphere. The mixture was stirred at 50 °C for 3 h, diluted with EtOAc, washed with water three times, and concentrated under reduced pressure by rotary evaporation. The crude residue was purified by flash column chromatography (SiO_2, eluent gradient 0–10% MeOH in DCM) followed by preparative TLC purification (SiO_2, eluent 100% EtOAc) to give **13s** as a yellow amorphous solid (64 mg, 88%). ^{1}H NMR (400 MHz, acetone-d_6) δ 7.64 (dd, J = 12.4, 2.3 Hz, 1H), 7.45 (t, J = 8.5 Hz, 1H), 7.36 (dd, J = 8.5, 2.3 Hz, 1H), 6.48 (s, 1H), 4.88–4.72 (m, 1H), 4.40 (t, J = 5.8 Hz, 1H), 4.20 (t, J = 8.9 Hz, 1H), 4.13 (d, J = 5.8 Hz, 2H), 4.01 (dd, J = 8.9, 6.2 Hz, 1H), 3.89 (ddd, J = 12.3, 5.8, 3.2 Hz, 1H), 3.76 (ddd, J = 12.3, 5.8, 3.8 Hz, 1H), 1.42 (s, 9H). ^{13}C NMR (101 MHz, acetone-d_6) δ 163.6 (d, J = 247.7 Hz), 156.3, 155.1, 141.7 (d, J = 10.8 Hz), 134.6 (d, J = 2.9 Hz), 113.9 (d, J = 3.1 Hz), 106.3 (d, J = 16.2 Hz), 105.5 (d, J = 27.5 Hz), 92.3, 79.3, 75.6, 74.3, 63.1, 46.9, 31.3, 28.6.

(R)-3-(4-(3-Aminoprop-1-yn-1-yl)-3-fluorophenyl)-5-(hydroxymethyl)oxazolidin-2-one Hydrochloride (13t).—

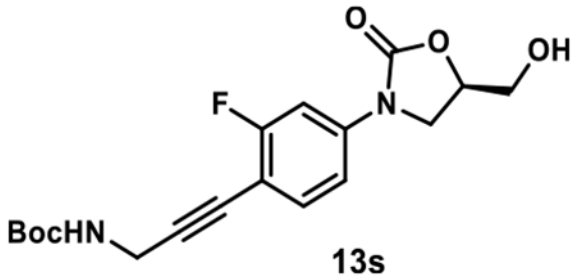

13s

A solution of **13s** (8 mg, 0.022 mmol) in TFA (0.2 mL) and DCM (0.6 mL) was stirred at 25 °C. After the reaction was judged to be completed by TLC (30 min), its solvent was removed under reduced pressure by rotary evaporation. The residue was dissolved in MeOH

(1 mL), charged with the addition of HCl/dioxane (4 M, 20 μL), and concentrated under reduced pressure by rotary evaporation. The resulting residue was washed with acetone (1 mL) and dried under high vacuum to give compound **13t** as a yellow amorphous solid (6 mg, 91%). ^{1}H NMR (400 MHz, methanol-d_4) δ 7.65 (dd, J = 12.2, 2.3 Hz, 1H), 7.52 (t, J = 8.3 Hz, 1H),7.35 (dd, J = 8.3, 2.3 Hz, 1H), 4.84–4.68 (m, 1H), 4.14 (t, J = 9.0 Hz, 1H), 4.08 (s, 2H), 3.94 (dd, J = 9.0, 6.2 Hz, 1H), 3.87 (dd, J = 12.6, 3.1 Hz, 1H), 3.69 (dd, J = 12.6, 3.8 Hz, 1H). ^{13}C NMR (101 MHz, methanol-d_4) δ 164.5 (d, J = 249.4 Hz), 156.6, 142.6 (d, J = 10.9 Hz), 135.1 (d, J = 2.6 Hz), 114.6 (d, J = 3.1 Hz), 106.4 (d, J = 27.1 Hz), 105.7 (d, J = 16.0 Hz), 86.1 (d, J = 2.9 Hz), 81.0, 75.2, 63.1, 47.4, 30.8.

tert-Butyl (R)-(3-((3-(2-Fluoro-4-(5-(hydroxymethyl)-2-oxooxazolidin-3-yl)phenyl)prop-2-yn-1-yl)oxy)-4-methoxybenzyl)carbamate (13u).—

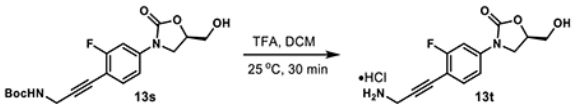

A solution of compound **6** (34 mg, 0.1 mmol), **19** (44 mg, 0.15 mmol), tetrakis(triphenylphosphine)palladium(0) (12 mg, 0.01 mmol), and copper(I) iodide (2 mg, 0.01 mmol) in DMF (1 mL) was evacuated and purged with nitrogen three times. *N,N*-Diisopropylethylamine (0.5 mL) was added under the protection of a nitrogen atmosphere. The mixture was stirred at 50 °C. After the reaction was judged to be completed by TLC (3 h), it was diluted with EtOAc, washed with water three times, and concentrated under reduced pressure by rotary evaporation. The crude residue was purified by flash column chromatography (SiO_2, eluent gradient 0–100% EtOAc in hexanes) followed by preparative TLC purification (SiO_2, eluent 100% EtOAc) to give **13u** as a yellow amorphous solid (35 mg, 70%). ^{1}H NMR (300 MHz, acetone) δ 7.65 (dd, J = 12.4, 2.2 Hz, 1H), 7.51 (t, J = 8.7 Hz, 1H), 7.37 (dd, J = 8.7, 2.2 Hz, 1H), 7.15–7.10 (m, 1H), 6.99–6.85 (m, 2H), 6.38 (s, 1H), 5.00 (s, 2H), 4.89–4.69 (m, 1H), 4.41 (t, J = 5.9 Hz, 1H), 4.27–4.12 (m, 3H), 4.01 (dd, J = 8.9, 6.2 Hz, 1H), 3.89 (ddd, J = 5.5, 3.3 Hz, 1H), 3.84–3.67 (m, 4H), 1.41 (s, 9H). ^{13}C NMR (75 MHz, acetone-d_6) δ 163.7 (d, J = 248.4 Hz), 156.8, 155.1, 150.0, 148.0, 142.1 (d, J = 10.9 Hz), 134.9 (d, J = 2.2 Hz), 133.6, 122.0, 115.6 (d, J = 1.5 Hz), 113.9 (d, J = 2.2 Hz), 112.9, 105.6 (d, J = 15.9 Hz), 105. 3 (d, J = 2.2 Hz), 90.1 (d, J = 2.9 Hz), 80.6, 78.7, 74.4, 63.0, 58.1, 56.13, 56.08, 46.9, 44.4.

(R)-3-(4-(3-(5-(Aminomethyl)-2-methoxyphenoxy)prop-1-yn-1-yl)-3-fluorophenyl)-5-(hydroxymethyl)oxazolidin-2-one Hydrochloride (13v).—

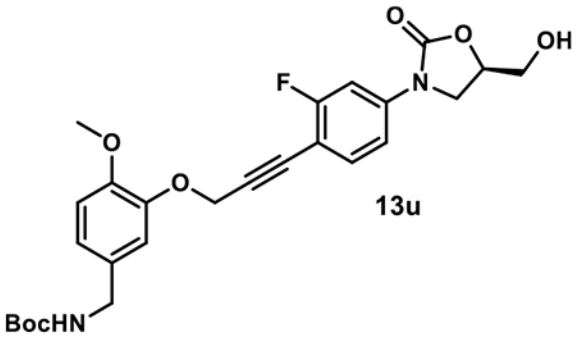

A solution of **13u** (30 mg, 0.06 mmol) in TFA (0.3 mL) and DCM (0.9 mL) was stirred at 25 °C. After the reaction was judged to be completed by TLC (30 min), its solvent was removed under reduced pressure by rotary evaporation. The residue was dissolved in MeOH (2 mL), charged with the addition of HCl/dioxane (4 M, 80 μL), and concentrated under reduced pressure by rotary evaporation. The resulting residue was washed with acetone (2 mL) and dried under high vacuum to give compound **13v** as a yellow amorphous solid (10 mg, 40%). ^{1}H NMR (400 MHz, methanol-d_4) δ 7.62 (dd, J = 12.2, 2.2 Hz, 1H), 7.45 (t, J = 8.6 Hz, 1H), 7.30 (dd, J = 8.6, 2.2 Hz, 1H), 7.24 (d, J = 2.0 Hz, 1H), 7.13–7.01 (m, 2H), 5.04 (s, 2H), 4.80–4.71 (m, 1H), 4.12 (t, J = 9.1 Hz, 1H), 4.06 (s, 2H), 3.97–3.77 (m, 5H), 3.68 (dd, J = 12.5, 3.8 Hz, 1H). ^{13}C NMR (101 MHz, methanol-d_4) δ 164.4 (d, J = 248.8 Hz), 156.6, 152.3, 148.6, 142.1 (d, J = 10.9 Hz), 135.0 (d, J = 2.8 Hz), 126.7, 124.4, 117.4, 114.5 (d, J = 3.2 Hz), 113.6, 106.6 (d, J = 16.1 Hz), 106.3 (d, J = 27.3 Hz), 89.8 (d, J = 2.9 Hz), 81.2, 75.2, 63.1, 58.8, 56.5, 47.4, 44.1.

tert-Butyl (5-(2-Fluoro-4-((R)-5-(hydroxymethyl)-2-oxooxazolidin-3-yl)phenyl)-1-hydroxypent-4-yn-2-yl)carbamate (13w).—

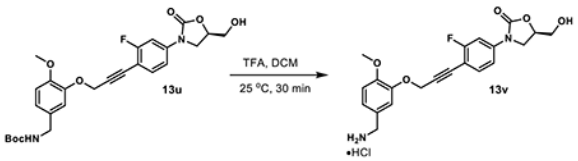

A solution of compound **6** (52 mg, 0.155 mmol), **20** (37 mg, 0.186 mmol), tetrakis(triphenylphosphine)palladium(0) (18 mg, 0.0155 mmol), and copper(I) iodide (3 mg, 0.0155 mmol) in DMF (2 mL) was evacuated and purged with nitrogen three times. *N,N*-Diisopropylethylamine (1 mL) was added under the protection of a nitrogen atmosphere. The mixture was stirred at 50 °C. After the reaction was judged to be completed by TLC (5 h), it was diluted with EtOAc, washed with water three times, and concentrated under reduced pressure by rotary evaporation. The crude residue was purified by flash column chromatography (SiO_2, eluent gradient 0–10% MeOH in DCM) followed by preparative TLC purification (SiO_2, eluent 100% EtOAc) to give **13w** as a white amorphous solid (34 mg, 54%). ^{1}H NMR (400 MHz, acetone-d_6) δ 7.63 (dd, J = 12.4, 2.3 Hz, 1H), 7.44 (t, J = 8.6 Hz, 1H), 7.34 (dd, J = 8.6, 2.3 Hz, 1H), 5.90 (d, J = 8.3 Hz, 1H), 4.89–4.75 (m, 1H), 4.40 (t, J = 5.8 Hz, 1H), 4.19 (t, J = 9.0 Hz, 1H), 4.11–3.95 (m, 2H), 3.94–3.58 (m, 5H), 2.86–2.65 (m, 2H), 1.40 (s, 9H). ^{13}C NMR (101 MHz, acetone-d_6) δ 163.6 (d, J = 246.9 Hz), 156.3, 155.1, 141.2 (d, J = 10.7 Hz), 134.6 (d, J = 2.9 Hz), 113.8 (d, J = 3.2 Hz),

107.1 (d, J = 16.3 Hz), 105.5 (d, J = 27.4 Hz), 92.6 (d, J = 3.0 Hz), 78.9, 75.5, 74.3, 63.5, 63.1, 52.7, 46.9, 28.6, 22.7.

(5R)-3-(4-(4-Amino-5-hydroxypent-1-yn-1-yl)-3-fluorophenyl)-5-(hydroxymethyl)oxazolidin-2-one Hydrochloride (13x).—

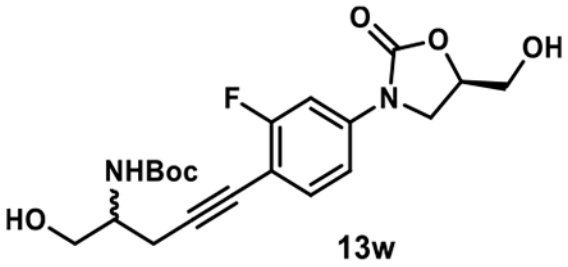

A solution of **13w** (16 mg, 0.039 mmol) in TFA (0.2 mL) and DCM (0.6 mL) was stirred at 25 °C. After the reaction was judged to be completed by TLC (30 min), its solvent was removed under reduced pressure by rotary evaporation. The residue was dissolved in MeOH (1 mL), charged with the addition of HCl/dioxane (4 M, 40 μL), and concentrated under reduced pressure by rotary evaporation. The resulting residue was washed with acetone (1 mL) and dried under high vacuum to give compound **13x** as a yellow amorphous solid (7 mg, 52%). ^{1}H NMR (400 MHz, methanol-d_4) δ 7.61 (dd, J = 12.1, 2.3 Hz, 1H), 7.48 (t, J = 8.3 Hz, 1H), 7.31 (dd, J = 8.3, 2.3 Hz, 1H), 4.83–4.71 (m, 1H), 4.13 (t, J = 9.0 Hz, 1H), 3.97–3.83 (m, 3H), 3.78 (dd, J = 11.6, 6.0 Hz, 1H), 3.69 (dd, J = 11.6, 3.8 Hz, 1H), 3.56–3.42 (m, 1H), 2.89 (dd, J = 6.7, 4.1 Hz, 2H). ^{13}C NMR (101 MHz, methanol-d_4) δ 164.4 (d, J = 248.4 Hz), 156.6, 141.7 (d, J = 10.8 Hz), 134.9 (d, J = 2.6 Hz), 114.4 (d, J = 3.3 Hz), 107.1 (d, J = 16.2 Hz), 106.3 (d, J = 27.3 Hz), 88.9 (d, J = 3.0 Hz), 77.9, 75.2, 63.1, 61.6, 53.2, 47.5, 21.1.

(R)-N-(tert-Butoxycarbonyl)-N-(3-(2-fluoro-4-(5-(hydroxymethyl)-2-oxooxazolidin-3-yl)phenyl)prop-2-yn-1-yl)glycine (13y).—

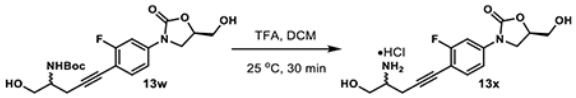

A solution of compound **6** (82 mg, 0.24 mmol), **21** (62 mg, 0.29 mmol), tetrakis(triphenylphosphine)palladium(0) (28 mg, 0.024 mmol), and copper(I) iodide (5 mg, 0.024 mmol) in CH_3CN (2 mL) was evacuated and purged with nitrogen three times. *N,N*-Diisopropylethylamine (1 mL) was added under the protection of a nitrogen atmosphere. The mixture was stirred at 50 °C. After the reaction was judged to be completed by TLC (4 h), its solvent was concentrated under reduced pressure by rotary evaporation. The residue was dissolved in acetone, acidified with the addition of formic acid (1 mL), and concentrated under reduced pressure by rotary evaporation. The crude residue was purified by flash column chromatography (SiO_2, eluent gradient 0–10% MeOH in DCM with 1% formic acid) followed by preparative TLC purification (SiO_2, eluent 10% MeOH in DCM) to give **13y** as a white amorphous solid (84 mg, 83%). ^{1}H NMR (600 MHz, acetonitrile-$d_{3>}$) δ 7.54 (dd, J = 12.4, 2.3 Hz, 1H), 7.44 (t, J = 8.3 Hz, 1H), 7.29 (dd, J = 8.3 Hz, 2.3 Hz, 1H),

4.76–4.64 (m, 1H), 4.41–4.30 (m, 2H), 4.09–3.97 (m, 3H), 3.83 (dd, J = 8.9, 6.1 Hz, 1H), 3.78 (dd, J = 12.5, 3.3 Hz, 1H), 3.64 (dd, J = 12.5, 4.2 Hz, 1H), 1.57–1.19 (m, 9H). ^{13}C NMR (101 MHz, acetonitril-d_3) δ 172.5, 163.7 (d, J = 247.3 Hz), 155.8, 155.5, 141.6 (d, J = 11.0 Hz), 134.8 (d, J = 2.0 Hz), 114.2 (d, J = 3.2 Hz), 105.8 (d, J = 27.2 Hz), 90.4 (d, J = 3.3 Hz), 81.3, 81.2, 77.5, 77.3, 74.4, 63.0, 48.6, 48.5, 48.4, 47.1, 39.0, 38.1, 28.4, 28.3.

(R)-(3-(2-Fluoro-4-(5-(hydroxymethyl)-2-oxooxazolidin-3-yl)-phenyl)prop-2-yn-1-yl)glycine Hydrochloride (13z).—

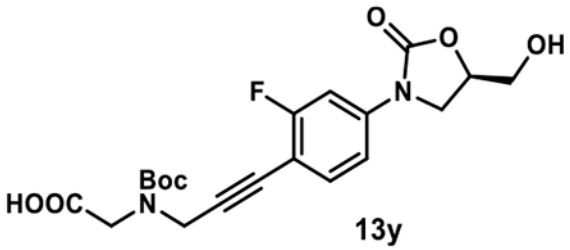

13y

A solution of **13y** (10 mg, 0.024 mmol) in TFA (0.2 mL) and DCM (0.6 mL) was stirred at 25 °C. After the reaction was judged to be completed by TLC (30 min), its solvent was removed under reduced pressure by rotary evaporation. The residue was dissolved in MeOH (1 mL), charged with the addition of HCl/dioxane (4 M, 20 μL), and concentrated under reduced pressure by rotary evaporation. The resulting residue was washed with acetone (1 mL) and dried under high vacuum to give compound **13z** as a yellow amorphous solid (6 mg, 70%). ^{1}H NMR (400 MHz, methanol-d_4) δ 7.67 (dd, J = 12.2, 2.2 Hz, 1H), 7.55 (t, J = 8.3 Hz, 1H), 7.36 (dd, J = 8.3, 2.2 Hz, 1H), 4.84–4.69 (m, 1H), 4.28 (s, 2H), 4.14 (t, J = 9.0 Hz, 1H), 4.06 (s, 2H), 3.95 (dd, J = 9.0, 6.2 Hz, 1H), 3.87 (dd, J = 12.6, 3.1 Hz, 1H), 3.70 (dd, J = 12.6, 3.8 Hz, 1H). ^{13}C NMR (101 MHz, methanol-d_4) δ 168.7, 164.6 (d, J = 249.6 Hz), 156.5, 142.8 (d, J = 11.0 Hz), 135.2 (d, J = 2.4 Hz), 114.6 (d, J = 3.1 Hz), 106.3 (d, J = 27.1 Hz), 105.3 (d, J = 16.1 Hz), 83.9 (d, J = 3.0 Hz), 83.0, 75.2, 63.1, 47.4, 47.3, 38.0.

tert-Butyl 4-(1-((3-(2-Fluoro-4-((R)-5-(hydroxymethyl)-2-oxooxazolidin-3-yl)phenyl)prop-2-yn-1-yl)amino)-1-oxopropan-2-yl)-piperazine-1-carboxylate (13aa).—

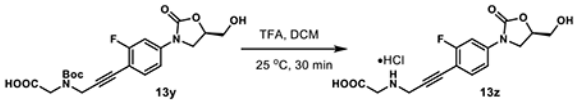

13y 13z

A solution of compound **6** (34 mg, 0.1 mmol), **22** (35 mg, 0.12 mmol), tetrakis(triphenylphosphine)palladium(0) (12 mg, 0.01 mmol), and copper(I) iodide (2 mg, 0.01 mmol) in DMF (2 mL) was evacuated and purged with nitrogen three times. *N,N*-Diisopropylethylamine (1 mL) was added under the protection of a nitrogen atmosphere. The mixture was stirred at 50 °C. After the reaction was judged to be completed by TLC (2 h), it was diluted with EtOAc, washed with water three times, and concentrated under reduced pressure by rotary evaporation. The crude residue was purified by flash column chromatography (SiO_2, eluent gradient 0–10% MeOH in DCM) followed by preparative TLC purification (SiO_2, eluent 100% EtOAc) to give **13aa** as a white amorphous solid (45 mg, 89%). ^{1}H NMR (400 MHz, acetone-d_6) δ 7.93 (t, J = 5.7 Hz, 1H), 7.64 (dd, J = 12.4,

2.2 Hz, 1H), 7.43 (t, J = 8.7 Hz, 1H), 7.35 (dd, J = 8.7, 2.2 Hz, 1H), 4.90–4.74 (m, 1H), 4.43 (s, 1H), 4.25 (d, J = 5.7 Hz, 2H), 4.19 (t, J = 8.9 Hz, 1H), 4.00 (dd, J = 8.9, 6.2 Hz, 1H), 3.94–3.85 (m, 1H), 3.79–3.71 (m, 1H), 3.47–3.34 (m, 4H), 3.17 (q, J = 6.9 Hz, 1H), 2.57–2.35 (m, 4H), 1.42 (s, 9H), 1.17 (d, J = 6.9 Hz, 3H). ^{13}C NMR (101 MHz, acetone-d_6) δ 173.2, 163.6 (d, J = 247.4 Hz), 155.1, 154.9, 141.7 (d, J = 10.9 Hz), 134.5 (d, J = 2.7 Hz), 113.9 (d, J = 3.1 Hz), 106.2 (d, J = 16.3 Hz), 105.5 (d, J = 27.3 Hz), 92.1 (d, J = 3.1 Hz), 79.5, 75.4, 74.3, 64.4, 63.1, 50.2, 46.9, 29.6, 28.5, 11.7.

N-(3-(2-Fluoro-4-((R)-5-(hydroxymethyl)-2-oxooxazolidin-3-yl)-phenyl)prop-2-yn-l-yl-(piperazin-1-yl)propenamide Dihydrochloride (13ab).—

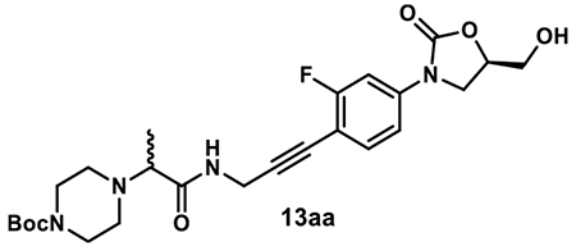

13aa

A solution of **13aa** (40 mg, 0.079 mmol) in TFA (0.8 mL) and DCM (2.4 mL) was stirred at 25 °C. After the reaction was judged to be completed by TLC (1 h), its solvent was removed under reduced pressure by rotary evaporation. The residue was dissolved in MeOH (4 mL), charged with the addition of HCl/dioxane (4 M, 80 μL), and concentrated under reduced pressure by rotary evaporation. The resulting residue was washed with acetone (4 mL) and dried under high vacuum to give compound **13ab** as a yellow amorphous solid (22 mg, 58%). ^{1}H NMR (400 MHz, methanol-d_4) δ 7.61 (dd, J = 12.2, 2.2 Hz, 1H), 7.44 (t, J = 8.3 Hz, 1H), 7.29 (dd, J = 8.3, 2.2 Hz, 1H), 4.83–4.70 (m, 1H), 4.31 (d, J = 2.0 Hz, 2H), 4.12 (t, J = 8.9 Hz, 1H), 4.02 (q, J = Hz, 1H), 3.93 (dd, J = 8.9, 6.3 Hz, 1H), 3.86 (dd, J = 12.6, 3.0 Hz, 1H), 3.77–3.45 (m, 9H), 1.59 (d, J = 6.9 Hz, 3H). ^{13}C NMR (101 MHz, methanol-d_4) δ 169.8, 164.3 (d, J = 247.9 Hz), 156.6, 141.8 (d, J = Hz), 134.9 (d, J = 2.0 Hz), 114.5 (d, J = 3.0 Hz), 106.9 (d, J = 16.7 Hz), 106.3 (d, J = 27.4 Hz), 90.2 (d, J = 3.0 Hz), 77.0, 75.2, 65.1, 63.1, 47.9 (2C), 47.4, 42.7 (2C), 30.5, 14.3.

4-Bromo-N'-hydroxybenzimidamide (14).—

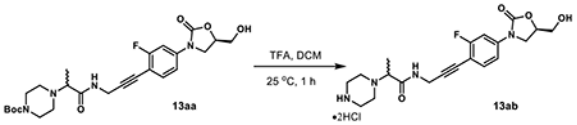

13aa 13ab

A mixture of 4-bromobenzonitrile (182 mg, 1 mmol), hydroxylammonium chloride (70 mg, 1 mmol), and sodium hydroxide (40 mg, 1 mmol) in ethanol (2 mL) and water (70 μL) was stirred under a nitrogen atmosphere at 80 °C. After the reaction was judged to be completed by TLC (4 h), it was concentrated under reduced pressure by rotary evaporation. The residue was purified by flash column chromatography (SiO_2, eluent gradient 0–10% MeOH in DCM) to afford compound **14** as a yellow amorphous solid (181 mg, 84%). ^{1}H NMR (400 MHz, DMSO) δ 9.73 (s, 1H), 8.20–7.05 (m, 4H), 5.86 (s, 2H).

5-Bromo-3-(tert-butoxy)picolinonitrile (15).—

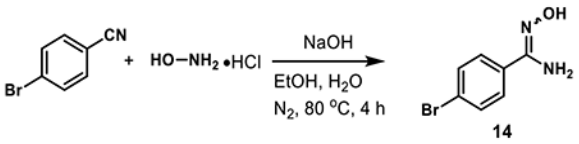

To a solution of 5-bromo-3-fluoropicolinonitrile (1 g, 5 mmol) in anhydrous DMF (25 mL), sodium *tert*-butoxide (625 mg, 6.5 mmol) was added. The reaction mixture was stirred at 25 °C for 4 h, quenched with the addition of water, and extracted with a mixture of hexanes/EtOAc (v/v = 1:2). The organic layer was washed with water three times and evaporated under reduced pressure by rotary evaporation. The crude residue was purified by flash column chromatography (SiO_2, eluent gradient 0–20% EtOAc in hexanes) to afford compound **15** as a yellow oil (419 mg, 33%). ^{1}H NMR (400 MHz, chloroform-*d*) δ 8.41 (d, J = 1.9 Hz, 1H), 7.67 (d, J = 1.9 Hz, 1H), 1.52 (s, 9H).

tert-Butyl 2-(2-((tert-Butoxycarbonyl)amino)pent-4-ynoyl)-hydrazine-1-carboxylate (17).[52]—

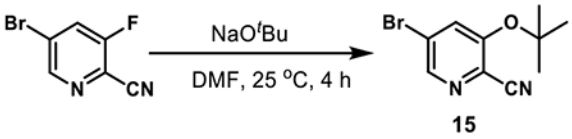

Sodium bicarbonate (336 mg, 4 mmol) and di-*tert*-butyl dicarbonate (327 mg, 1.5 mmol) were added to a solution of 2-amino-4-pentynoic acid hydrochloride (150 mg, 1 mmol) in THF/H_2O (v/v = 1:1, 5 mL) at 0 °C. The reaction mixture was stirred at 25 °C for 16 h. The mixture was diluted with Et_2O and extracted with water three times. The combined aqueous layers were acidified to pH = 4–5 by carefully adding saturated aqueous citric acid in an ice bath and extracted with dichloromethane three times. The combined organic layers were dried over magnesium sulfate and concentrated under reduced pressure by rotary evaporation. Residue **16** was used in the next step without further purification (94 mg, 44%). Toa solution of compound **16** (94 mg, 0.44 mmol) in DMF (1.0 mL) were added *tert*-butyl carbazate (87 mg, 0.66 mmol), HATU (335 mg, 0.88 mmol), and *N*,*N*-diisopropylethylamine (0.3 mL). The reaction mixture was stirred at 25 °C for 16 h, quenched with the addition of water, and extracted with EtOAc. The organic layer was washed with water two times as well as brine and evaporated under reduced pressure by rotary evaporation. The crude residue was purified by flash column chromatography (SiO_2, eluent gradient 0–50% EtOAc in hexanes) to afford compound **17** as a yellow amorphous solid (119 mg, 83%). ^{1}H NMR (400 MHz, $CDCl_3$) δ 8.48 (s, 1H), 6.70 (s, 1H), 5.44 (d, J = 8.5 Hz, 1H), 4.42 (s, 1H), 2.83–2.55 (m, 2H), 2.08 (d, J = Hz, 1H), 1.58–1.35 (m, 18H).

tert-Butyl Prop-2-yn-1-ylcarbamate (18).—

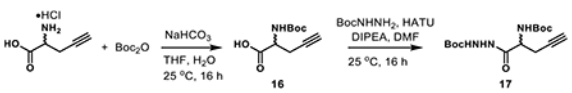

To a solution of propargylamine (110 mg, 2 mmol) in DCM (2 mL) was added a solution of di-*tert*-butyl dicarbonate (458 mg, 2.1 mmol) in DCM (3 mL) dropwise with a syringe at 0 °C. The reaction mixture was stirred at 25 °C for 30 min and concentrated under reduced pressure by rotary evaporation. The crude residue was purified by flash column chromatography (SiO_2, eluent gradient 0–10% MeOH in DCM) to afford compound **18** as a yellow amorphous solid (260 mg, 84%). ^{1}H NMR (400 MHz, $CDCl_3$) δ 4.69 (s, 1H), 3.92 (s, 2H), 2.22 (s, 1H), 1.45 (s, 9H).

tert-Butyl (4-Methoxy-3-(prop-2-yn-1-yloxy)benzyl)carbamate (19).—

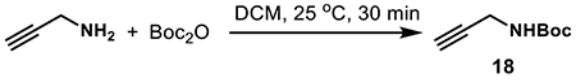

18

Di-*tert*-butyl dicarbonate (98 mg, 0.45 mmol) was added to a solution of [4-methoxy-3-(2-propynyloxy)phenyl]methanamine hydrochloride (67 mg, 0.3 mmol) and triethylamine (126 μL, 0.9 mmol) in DCM (2 mL). The reaction mixture was stirred at 25 °C for 2 h, quenched with water, and extracted with EtOAc three times. The combined organic layers were evaporated under reduced pressure by rotary evaporation. The crude residue was purified by flash column chromatography (SiO_2, eluent gradient 0–50% EtOAc in hexanes) to afford compound **19** as a white amorphous solid (64 mg, 73%). ^{1}H NMR (400 MHz, $CDCl_3$) δ 6.96 (s, 1H), 6.90–6.74 (m, 2H), 4.94–4.78 (m, 1H), 4.74 (d, J = 2.5 Hz, 2H), 4.24 (d, J = 5.8 Hz, 2H), 3.84 (s, 3H), 2.50 (t, J = 2.5 Hz, 1H), (s, 9H).

tert-Butyl (1-Hydroxypent-4-yn-2-yl)carbamate (20).—

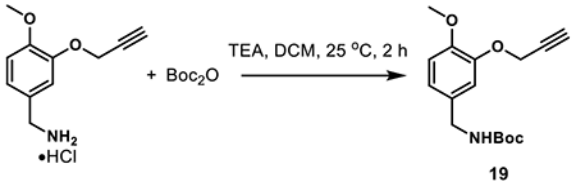

19

A mixture of 2-aminopent-4-yn-1-ol (20 mg, 0.2 mmol), di-*tert*-butyl dicarbonate (87 mg, 0.4 mmol), and triethylamine (56μL, 0.4 mmol) in CH_3CN (1 mL) was stirred at 50 °C for 5 h. The mixture was evaporated under reduced pressure by rotary evaporation, and the resulting residue was purified by flash column chromatography (SiO_2, eluent gradient 0–3% MeOH in DCM) to afford compound **20** as a yellow amorphous solid (39 mg, 99%). ^{1}HNMR (400 MHz, acetone) δ 3.95 (s, 1H), 3.77–3.50 (m, 2H), 2.60–2.30 (m, 3H), 1.77 (s, 1H), 1.40 (s, 9H).

N-(tert-Butoxycarbonyl)-N-(prop-2-yn-1-yl)glycine (21).[53]—

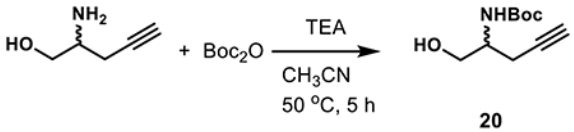

20

To a solution of 2-[(prop-2-yn-1-yl)amino]acetic acid hydrochloride (45 mg, 0.3 mmol) in H_2O (1 mL) were added di-*tert*-butyl dicarbonate (262 mg, 1.2 mmol) and triethylamine (293 μL, 2.1 mmol). The mixture was stirred at 25 °C for 16 h, diluted with water, and

washed withhexanes (20 mL) to remove di-*tert*-butyl dicarbonate. The aqueous layer was acidified with the addition of aqueous HCl (1 M) to pH = 3 and extracted with EtOAc three times. The combined organic layers were dried over magnesium sulfate and concentrated under reduced pressure by rotary evaporation to give compound **21** (63 mg, 99%), which was used in the next step without further purification. ^{1}H NMR (400 MHz, $CDCl_3$) δ 4.43–3.89 (m, 4H), 2.27 (s, 1H), 1.66–0.87 (m, 9H).

tert-Butyl 4-(1-Oxo-1-(prop-2-yn-1-ylamino)propan-2-yl)-piperazine-1-carboxylate (22).—

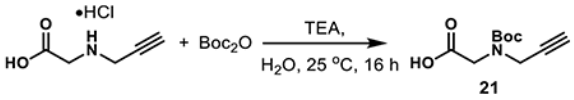

A mixture of 2-(1-piperazinyl)-*N*-(2-propynyl)propanamide dihydrochloride (53 mg, 0.2 mmol), di-*tert*-butyl dicarbonate (174 mg, 0.8 mmol), and triethylamine (111 μL, 0.8 mmol) in CH_3CN (2 mL) was stirred at 50 °C for 16 h. The mixture was evaporated under reduced pressure by rotary evaporation, and the resulting residue was purified by flash column chromatography (SiO_2, eluent gradient 0–15% MeOH in DCM) to afford compound **22** as a yellow amorphous solid (30 mg, 51%). Compound **22** was not pure but used in the next step without further purification.

Bacterial Strains and Growth Conditions.

The construction of strains and their properties were described previously. Bacterial strains (see the Supporting Information (SI))[42,48,54–57] were grown in either Luria-Bertani broth (10 g of Bacto tryptone, 5 g of yeast extract, and 5 g of NaCl per liter; pH 7.0), LB agar (LB broth with 15 g of agar per liter), or a minimal M9 medium (1×) supplemented with 50 mM MOPS buffer (pH 7.2), which were used for bacterial growth. The M9-MOPS medium was optimized to support the growth and expression of the OM pore in strains of all three species. We previously found that in *E. coli* and *A. baumannii* cells, the expression of the pore was the most consistent under an arabinose-inducible promoter, but in *P. aeruginosa* the most consistent expression was achieved under an IPTG-inducible promoter. Since glucose acts as a repressor for an arabinose-inducible promoter, this sugar could not be used as a carbon source in these experiments. Therefore, M9-MOPS medium was supplemented with 0.2% xylose (*E. coli, A. baumannii,* and *P. aeruginosa*) plus 0.5% sodium citrate (*P. aeruginosa* and *A. baumannii* only) as carbon sources.

Minimum Inhibitory Concentrations.

Compounds were dissolved in DMSO (10 mM). The twofold serial dilution method in 96-well plates was used to determine MICs. *E. coli*, *A. baumannii*, and *P. aeruginosa* cultures grown in indicated media were induced with 0.1%, 1% arabinose, or 0.1 mM IPTG, respectively. The MIC was noted visually after 24 h of incubation at 37 °C, and OD_{600} was measured for all 96-well plates followed by the determination of IC_{50} values, as described previously.[58]

Cell-Free Coupled Transcription–Translation Assay.

The Expressway Lumio Cell-Free Expression and Detection System (Invitrogen) was used for cell-free transcription–translation of the target protein CALML3 (GenBank accession number NM_005185; molecular mass of 19.5 kDa) from the pEXP5-NT/CALML3 plasmid. For this purpose, CALML3 was tagged with the N-terminal tetracysteine Lumio tag (Cys-Cys-Pro-Gly-Cys-Cys) using Q5^{R} Site-Directed Mutagenesis Kit (New England BioLabs). We followed the manufacturer's instructions for the cell-free transcription–translation. LZD was added to the reactions to the final concentrations 0.02, 0.2, 2, 20 μM, and **3h**, **8o**, **8d**, and **12f** were added at 1× and 0.1× MICs (Table S1). The amounts of the synthesized protein were detected using In-Gel Lumio Detection method. For this purpose, after 5 hours of incubation at 37 °C, the biarsenical Lumio Green Detection Reagent was added to the reactions. This reagent becomes fluorescent upon binding covalently to proteins containing the Lumio tag.[2] Samples were loaded on 16% SDS-PA gel and visualized immediately after electrophoresis (Figure 3B). The ImageJ software (ImageJ (nih.gov)) was used to calculate the area of the picks from the intensity of the fluorescent protein bands on gels. The amounts of the synthesized CALML3 in the absence of oxazolidinones were set as 100%. The nonlinear fit to sigmoidal curves was performed to calculate the drug concentration that yields a 50% inhibition of protein synthesis (K_I^{app}).

Supplementary Material

Refer to Web version on PubMed Central for supplementary material.

ACKNOWLEDGMENTS

This work was supported by the National Institute of Allergy and Infectious Disease of the National Institutes of Health (R01AI136795, H.I.Z., V.V.R., and A.S.D.) The content included in this manuscript does not necessarily reflect the position or the policy of the federal government, and no official endorsement should be inferred.
The authors thank Dr. Alexander S. Mankin for sharing *E. coli* strains. The authors gratefully acknowledge the collegiality, collaboration, and scientific discussion provided by the other SPEAR-GN team members.

ABBREVIATIONS USED

Δ	efflux knockout
AB	*Acinetobacter baumannii*
CLSI	Clinical & Laboratory Standards Institute
DIPEA	diisopropylethyl-amine
***E*/PE**	OM impact ratio
EC	*Escherichia coli*
GNB	Gram-negative bacteria
LB	Luria-Bertani broth
LZD	line-zolid

M9-MOPS	M9 medium supplemented with MOPS buffer
MDR	multidrug-resistant
MHI	Mueller-Hinton broth
OM	outer membrane
***P*/PE**	efflux impact ratio
PA	*Pseudomonas aeruginosa*
PC	principal component
PMBN	polymyxin B nonapeptide
Pore	hyperporinated strain
PTC	peptidyl transferase center
SAR	structure–activity relationship
SUR	structure–uptake relationship
WT	wild type

REFERENCES

(1). Fischbach MA; Walsh CT Antibiotics for emerging pathogens. Science 2009, 325, 1089–1093. [PubMed: 19713519]

(2). Boucher HW; Talbot GH; Bradley JS; Edwards JE; Gilbert D; Rice LB; Scheld M; Spellberg B; Bartlett J Bad bugs, no drugs: No ESKAPE! An update from the Infectious Diseases Society of America. Clin. Infect. Dis 2009, 48, 1–12. [PubMed: 19035777]

(3). Antibiotic resistance threats in the United States; US Centers for Disease Control and Prevention (CDC), 2019.

(4). Silver LL Challenges of antibacterial discovery. Clin. Microbiol. Rev 2011, 24, 71–109. [PubMed: 21233508]

(5). Spellberg B; Guidos R; Gilbert D; Bradley J; Boucher HW; Scheld WM; Bartlett JG; Edwards J Jr.; Infectious Diseases Society of America. The epidemic of antibiotic-resistant infections: A call to action for the medical community from the Infectious Diseases Society of America. Clin. Infect. Dis 2008, 46, 155–164. [PubMed: 18171244]

(6). Rice LB Federal funding for the study of antimicrobial resistance in nosocomial pathogens: No ESKAPE. J. Infect. Dis 2008,197, 1079–1081. [PubMed: 18419525]

(7). Zgurskaya HI; Lopez CA; Gnanakaran S Permeability barrier of Gram-negative cell envelopes and approaches to bypass it. ACS Infect. Dis 2015, 1, 512–522. [PubMed: 26925460]

(8). Rybenkov VV; Zgurskaya HI; Ganguly C; Leus IV; Zhang Z; Moniruzzaman M The whole is bigger than the sum of its parts: Drug transport in the context of two membranes with active efflux. Chem. Rev 2021, 121, 5597–5631. [PubMed: 33596653]

(9). Brown DG; May-Dracka TL; Gagnon MM; Tommasi R Trends and exceptions of physical properties on antibacterial activity for Gram-positive and Gram-negative pathogens. J. Med. Chem 2014, 57, 10144–10161. [PubMed: 25402200]

(10). Payne DJ; Gwynn MN; Holmes DJ; Pompliano DL Drugs for bad bugs: Confronting the challenges of antibacterial discovery. Nat. Rev. Drug Discovery 2007, 6, 29–40. [PubMed: 17159923]

(11). Tommasi R; Brown DG; Walkup GK; Manchester JI; Miller AA Eskapeing the labyrinth of antibacterial discovery. Nat. Rev. Drug Discovery 2015, 14, 529–542. [PubMed: 26139286]

(12). Vaara M Polymyxin derivatives that sensitize Gram-negative bacteria to other antibiotics. Molecules 2019, 24, 249. [PubMed: 30641878]

(13). Cochrane SA; Vederas JC Unacylated tridecaptin a(1) acts as an effective sensitiser of Gram-negative bacteria to other antibiotics. Int. J. Antimicrob. Agents 2014, 44, 493–499. [PubMed: 25315408]

(14). Chiorean S; Antwi I; Carney DW; Kotsogianni I; Giltrap AM; Alexander FM; Cochrane SA; Payne RJ; Martin NI; Henninot A; Vederas JC Dissecting the binding interactions of teixobactin with the bacterial cell-wall precursor lipid II. ChemBioChem 2020, 21, 789–792. [PubMed: 31552694]

(15). O'Shea R; Moser HE Physicochemical properties of antibacterial compounds: Implications for drug discovery. J. Med. Chem 2008, 51, 2871–2878. [PubMed: 18260614]

(16). Richter MF; Hergenrother PJ The challenge of converting Gram-positive-only compounds into broad-spectrum antibiotics. Ann. N.Y. Acad. Sci 2019, 1435, 18–38. [PubMed: 29446459]

(17). Richter MF; Drown BS; Riley AP; Garcia A; Shirai T; Svec RL; Hergenrother PJ Predictive compound accumulation rules yield a broad-spectrum antibiotic. Nature 2017, 545, 299–304. [PubMed: 28489819]

(18). Lukežič T; Fayad AA; Bader C; Harmrolfs K; Bartuli J; Gross S; Lesnik U; Hennessen F; Herrmann J; Pikl S; Petkovic H; Muller R Engineering atypical tetracycline formation in amycolatopsis sulphurea for the production of modified chelocardin antibiotics. ACS Chem. Biol 2019, 14, 468–477. [PubMed: 30747520]

(19). Perlmutter SJ; Geddes EJ; Drown BS; Motika SE; Lee MR; Hergenrother PJ Compound uptake into *E. coli* can be facilitated by N-alkyl guanidiniums and pyridiniums. ACS Infect. Dis 2021,7, 162–173. [PubMed: 33228356]

(20). Li Y; Gardner JJ; Fortney KR; Leus IV; Bonifay V; Zgurskaya HI; Pletnev AA; Zhang S; Zhang ZY; Gribble GW; Spinola SM; Duerfeldt AS First-generation structure-activity relationship studies of 2,3,4,9-tetrahydro-1h-carbazol-1-amines as CpxA phosphatase inhibitors. Bioorg. Med. Chem. Lett 2019, 29, 1836–1841. [PubMed: 31104993]

(21). Cohen F; Aggen JB; Andrews LD; Assar Z; Boggs J; Choi T; Dozzo P; Easterday AN; Haglund CM; Hildebrandt DJ; Holt MC; Joly K; Jubb A; Kamal Z; Kane TR; Konradi AW; Krause KM; Linsell MS; Machajewski TD; Miroshnikova O; Moser HE; Nieto V; Phan T; Plato C; Serio AW; Seroogy J; Shakhmin A; Stein AJ; Sun AD; Sviridov S; Wang Z; Wlasichuk K; Yang W; Zhou X; Zhu H; Cirz RT Optimization of LpxC inhibitors for antibacterial activity and cardiovascular safety. Chem-MedChem 2019, 14, 1560–1572.

(22). Masci D; Hind C; Islam MK; Toscani A; Clifford M; Coluccia A; Conforti I; Touitou M; Memdouh S; Wei X; La Regina G; Silvestri R; Sutton JM; Castagnolo D Switching on the activity of 1,5-diaryl-pyrrole derivatives against drug-resistant ESKAPE bacteria: Structure-activity relationships and mode of action studies. Eur. J. Med. Chem 2019, 178, 500–514. [PubMed: 31202995]

(23). Motika SE; Ulrich RJ; Geddes EJ; Lee HY; Lau GW; Hergenrother PJ Gram-negative antibiotic active through inhibition of an essential riboswitch. J. Am. Chem. Soc 2020, 142, 10856–10862. [PubMed: 32432858]

(24). Andrews LD; Kane TR; Dozzo P; Haglund CM; Hilderbrandt DJ; Linsell MS; Machajewski T; McEnroe G; Serio AW; Wlasichuk KB; Neau DB; Pakhomova S; Waldrop GL; Sharp M; Pogliano J; Cirz RT; Cohen F Optimization and mechanistic characterization of pyridopyrimidine inhibitors of bacterial biotin carboxylase. J. Med. Chem 2019, 62, 7489–7505. [PubMed: 31306011]

(25). Hu Y; Shi H; Zhou M; Ren Q; Zhu W; Zhang W; Zhang Z; Zhou C; Liu Y; Ding X; Shen HC; Yan SF; Dey F; Wu W; Zhai G; Zhou Z; Xu Z; Ji Y; Lv H; Jiang T; Wang W; Xu Y; Vercruysse M; Yao X; Mao Y; Yu X; Bradley K; Tan X Discovery of pyrido[2,3-b]indole derivatives with Gram-negative activity targeting both DNA gyrase and topoisomerase iv. J. Med. Chem 2020, 63, 9623–9649. [PubMed: 32787097]

(26). Parker EN; Drown BS; Geddes EJ; Lee HY; Ismail N; Lau GW; Hergenrother PJ Implementation of permeation rules leads to a FabI inhibitor with activity against Gram-negative pathogens. Nat. Microbiol 2020, 5, 67–75. [PubMed: 31740764]

(27). Sohlenkamp C; Geiger O Bacterial membrane lipids: Diversity in structures and pathways. FEMS Microbiol. Rev 2016, 40, 133–159. [PubMed: 25862689]

(28). Leach KL; Swaney SM; Colca JR; McDonald WG; Blinn JR; Thomasco LM; Gadwood RC; Shinabarger D; Xiong L; Mankin AS The site of action of oxazolidinone antibiotics in living bacteria and in human mitochondria. Mol. Cell 2007, 26, 393–402. [PubMed: 17499045]

(29). Michalska K; Karpiuk I; Krol M; Tyski S Recent development of potent analogues of oxazolidinone antibacterial agents. Bioorg. Med. Chem. Lett 2013, 21, 577–591.

(30). Poce G; Zappia G; Cesare Porretta G; Botta B; Biava M New oxazolidinone derivatives as antibacterial agents with improved activity. Exp. Opin. Ther. Patents 2008, 18, 97–121.

(31). Renslo AR; Luehr GW; Gordeev MF Recent developments in the identification of novel oxazolidinone antibacterial agents. Bioorg. Med. Chem 2006, 14, 4227–4240. [PubMed: 16527486]

(32). Deshmukh MS; Jain N Design, synthesis, and antibacterial evaluation of oxazolidinones with fused heterocyclic C-ring sub-structure. ACS Med. Chem. Lett 2017, 8, 1153–1158. [PubMed: 29152047]

(33). Wu Y; Ding X; Ding L; Zhang Y; Cui L; Sun L; Li W; Wang D; Zhao Y Synthesis and antibacterial activity evaluation of novel biaryloxazolidinone analogues containing a hydrazone moiety as promising antibacterial agents. Eur. J. Med. Chem 2018,158, 247–258. [PubMed: 30218910]

(34). Xin Q; Fan H; Guo B; He H; Gao S; Wang H; Huang Y; Yang Y Design, synthesis, and structure-activity relationship studies of highly potent novel benzoxazinyl-oxazolidinone antibacterial agents. J. Med. Chem 2011, 54, 7493–7502. [PubMed: 21955296]

(35). Seetharamsingh B; Ramesh R; Dange SS; Khairnar PV; Singhal S; Upadhyay D; Veeraraghavan S; Viswanadha S; Vakkalanka S; Reddy DS Design, synthesis, and identification of silicon incorporated oxazolidinone antibiotics with improved brain exposure. ACS Med. Chem. Lett 2015, 6, 1105–1110. [PubMed: 26617962]

(36). Yang T; Chen G; Sang Z; Liu Y; Yang X; Chang Y; Long H; Ang W; Tang J; Wang Z; Li G; Yang S; Zhang J; Wei Y; Luo Y Discovery of a teraryl oxazolidinone compound (s)-N-((3-(3-fluoro-4-(4-(pyridin-2-yl)-1h-pyrazol-1-yl)phenyl)-2-oxooxazolidin-5-yl)-methyl)acetamide phosphate as a novel antimicrobial agent with enhanced safety profile and efficacies. J. Med. Chem 2015, 58, 6389–6409. [PubMed: 26212502]

(37). Paulen A; Gasser V; Hoegy F; Perraud Q; Pesset B; Schalk IJ; Mislin GL Synthesis and antibiotic activity of oxazolidinone-catechol conjugates against Pseudomonas aeruginosa. Org. Biomol. Chem 2015, 13, 11567–11579.

(38). Spaulding A; Takrouri K; Mahalingam P; Cleary DC; Cooper HD; Zucchi P; Tear W; Koleva B; Beuning PJ; Hirsch EB; Aggen JB Compound design guidelines for evading the efflux and permeation barriers of *Escherichia coli* with the oxazolidinone class of antibacterials: Test case for a general approach to improving whole cell Gram-negative activity. Bioorg. Med. Chem. Lett 2017, 27, 5310–5321. [PubMed: 29102393]

(39). Suzuki H; Utsunomiya I; Shudo K; Fukuhara N; Iwaki T; Yasukata T Antibacterial oxazolidinone analogues having a N-hydroxyacetyl-substituted seven-membered [1,2,5]triazepane or [1,2,5]oxadiazepane C-ring unit. Eur. J. Med. Chem 2013, 63, 811–825. [PubMed: 23584544]

(40). Takrouri K; Cooper HD; Spaulding A; Zucchi P; Koleva B; Cleary DC; Tear W; Beuning PJ; Hirsch EB; Aggen JB Progress against *Escherichia coli* with the oxazolidinone class of antibacterials: Test case for a general approach to improving whole-cell Gram-negative activity. ACS Infect. Dis 2016, 2, 405–426. [PubMed: 27627629]

(41). Barbachyn MR; Ford CW Oxazolidinone structure-activity relationships leading to linezolid. Angew. Chem., Int. Ed 2003, 42, 2010–2023.

(42). Krishnamoorthy G; Leus IV; Weeks JW; Wolloscheck D; Rybenkov VV; Zgurskaya HI Synergy between active efflux and outer membrane diffusion defines rules of antibiotic permeation into Gram-negative bacteria. mBio 2017, 8, No. e01172–17. [PubMed: 29089426]

(43). Phenotypic screening. In Methods in Molecular Biology; Springer Nature, 2018.

(44). Jelsbak L; Hartman H; Schroll C; Rosenkrantz JT; Lemire S; Wallrodt I; Thomsen LE; Poolman M; Kilstrup M; Jensen PR; Olsen JE Identification of metabolic pathways essential for fitness of *Salmonella* typhimurium *in vivo*. PLoS One 2014, 9, No. e101869. [PubMed: 24992475]

(45). Palmer KL; Mashburn LM; Singh PK; Whiteley M Cystic fibrosis sputum supports growth and cues key aspects of *Pseudomonas aeruginosa* physiology. J. Bacteriol 2005, 187, 5267–5277. [PubMed: 16030221]

(46). Eyal Z; Matzov D; Krupkin M; Wekselman I; Paukner S; Zimmerman E; Rozenberg H; Bashan A; Yonath A Structural insights into species-specific features of the ribosome from the pathogen *Staphylococcus aureus*. Proc. Natl. Acad. Sci. U.S.A 2015, 112, E5805–E5814. [PubMed: 26464510]

(47). Shinabarger DL; Marotti KR; Murray RW; Lin AH; Melchior EP; Swaney SM; Dunyak DS; Demyan WF; Buysse JM Mechanism of action of oxazolidinones: Effects of linezolid and eperezolid on translation reactions. Antimicrob. Agents Chemother 1997, 41, 2132–2136. [PubMed: 9333037]

(48). Orelle C; Carlson S; Kaushal B; Almutairi MM; Liu H; Ochabowicz A; Quan S; Pham VC; Squires CL; Murphy BT; Mankin AS Tools for characterizing bacterial protein synthesis inhibitors. Antimicrob. Agents Chemother 2013, 57, 5994–6004. [PubMed: 24041905]

(49). Topliss JG Utilization of operational schemes for analog synthesis in drug design. J. Med. Chem 1972, 15, 1006–1011. [PubMed: 5069767]

(50). Meanwell NA Synopsis of some recent tactical application of bioisosteres in drug design. J. Med. Chem 2011, 54, 2529–2591. [PubMed: 21413808]

(51). Nordqvist A; O'Mahony G; Friden-Saxin M; Fredenwall M; Hogner A; Granberg KL; Aagaard A; Backstrom S; Gunnarsson A; Kaminski T; Xue Y; Dellsen A; Hansson E; Hansson P; Ivarsson I; Karlsson U; Bamberg K; Hermansson M; Georgsson J; Lindmark B; Edman K Structure-based drug design of mineralocorticoid receptor antagonists to explore oxosteroid receptor selectivity. ChemMedChem 2017, 12, 50–65. [PubMed: 27897427]

(52). Le HT; Jang JG; Park JY; Lim CW; Kim TW Antibody functionalization with a dual reactive hydrazide/click crosslinker. Anal. Biochem 2013, 435, 68–73. [PubMed: 23313755]

(53). Lahasky SH; Serem WK; Guo L; Garno JC; Zhang D Synthesis and characterization of cyclic brush-like polymers by N-heterocyclic carbene-mediated zwitterionic polymerization of N-propargyl N-carboxyanhydride and the grafting-to approach. Macromolecules 2011, 44, 9063–9074.

(54). Krishnamoorthy G; Wolloscheck D; Weeks JW; Croft C; Rybenkov VV; Zgurskaya HI Breaking the permeability barrier of *Escherichia coli* by controlled hyperporination of the outer membrane. Antimicrob. Agents Chemother 2016, 60, 7372–7381. [PubMed: 27697764]

(55). Wolloscheck D; Krishnamoorthy G; Nguyen J; Zgurskaya HI Kinetic control of quorum sensing in *Pseudomonas aeruginosa* by multidrug efflux pumps. ACS Infect. Dis 2018, 4, 185–195. [PubMed: 29115136]

(56). Richmond GE; Evans LP; Anderson MJ; Wand ME; Bonney LC; Ivens A; Chua KL; Webber MA; Sutton JM; Peterson ML; Piddock LJ The *Acinetobacter baumannii* two-component system AdeRS regulates genes required for multidrug efflux, biofilm formation, and virulence in a strain-specific manner. mBio 2016, 7, e00430–16. [PubMed: 27094331]

(57). Gallagher LA; Ramage E; Weiss EJ; Radey M; Hayden HS; Held KG; Huse HK; Zurawski DV; Brittnacher MJ; Manoil C Resources for genetic and genomic analysis of emerging pathogen *Acinetobacter baumannii*. J. Bacteriol 2015, 197, 2027–2035. [PubMed: 25845845]

(58). Mehla J; Malloci G; Mansbach R; Lopez CA; Tsivkovski R; Haynes K; Leus IV; Grindstaff SB; Cascella RH; D'Cunha N; Herndon L; Hengartner NW; Margiotta E; Atzori A; Vargiu AV; Manrique PD; Walker JK; Lomovskaya O; Ruggerone P; Gnanakaran S; Rybenkov VV; Zgurskaya HI Predictive rules of efflux inhibition and avoidance in *Pseudomonas aeruginosa*. mBio 2021, 12, No. e02785–20. [PubMed: 33468691]

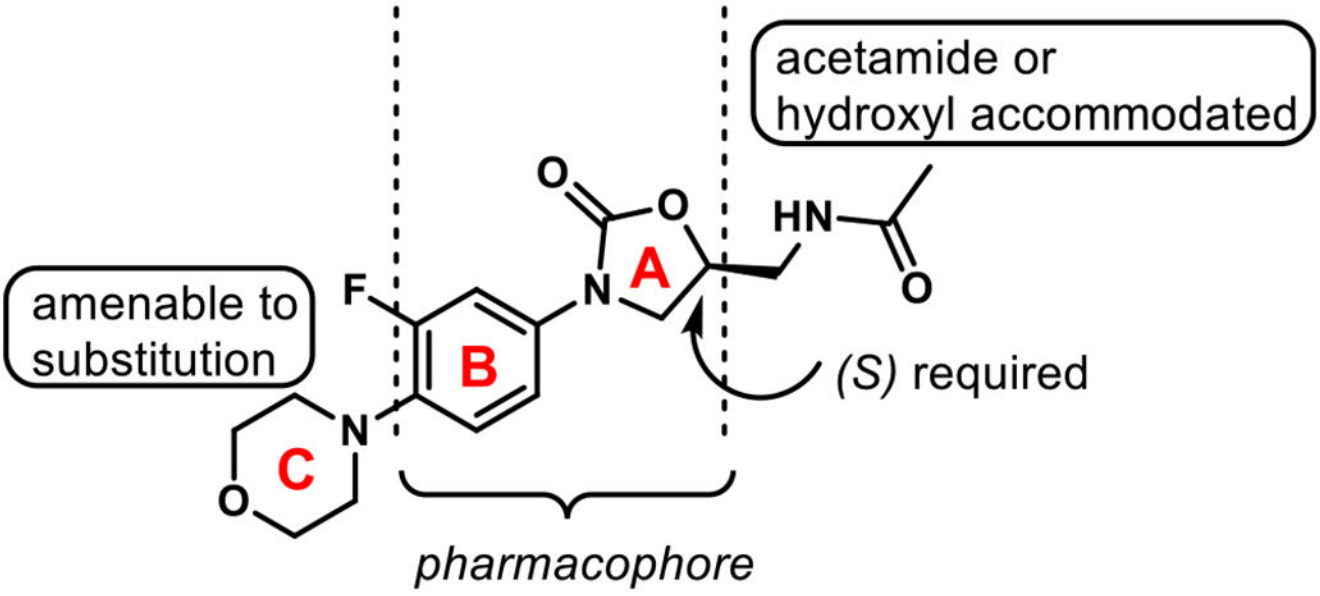

Figure 1.
Structure of linezolid and general SAR features of the oxazolidinone chemotype.

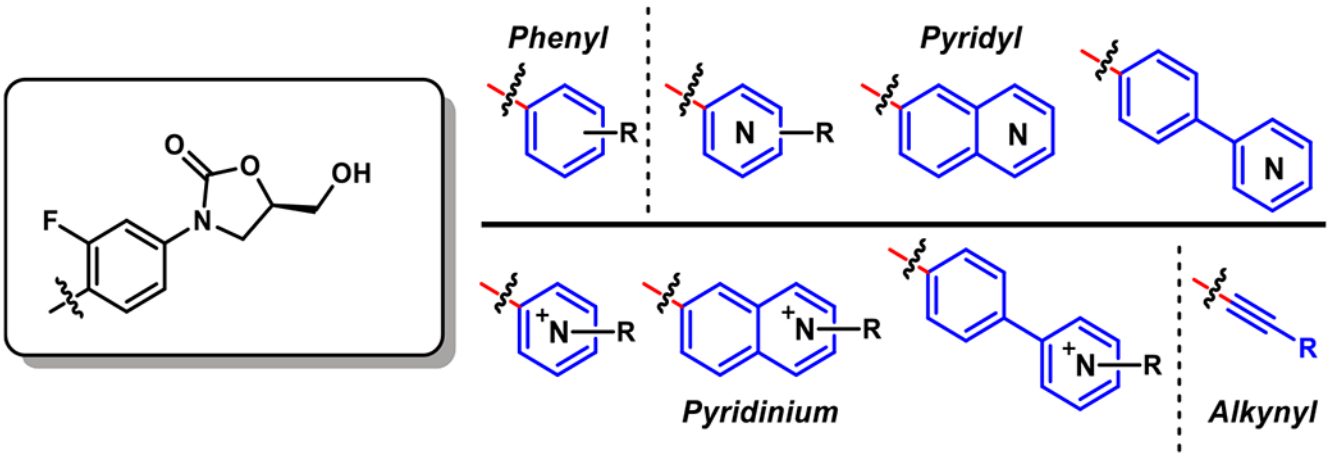

Figure 2.
Subgroups represented within the library.

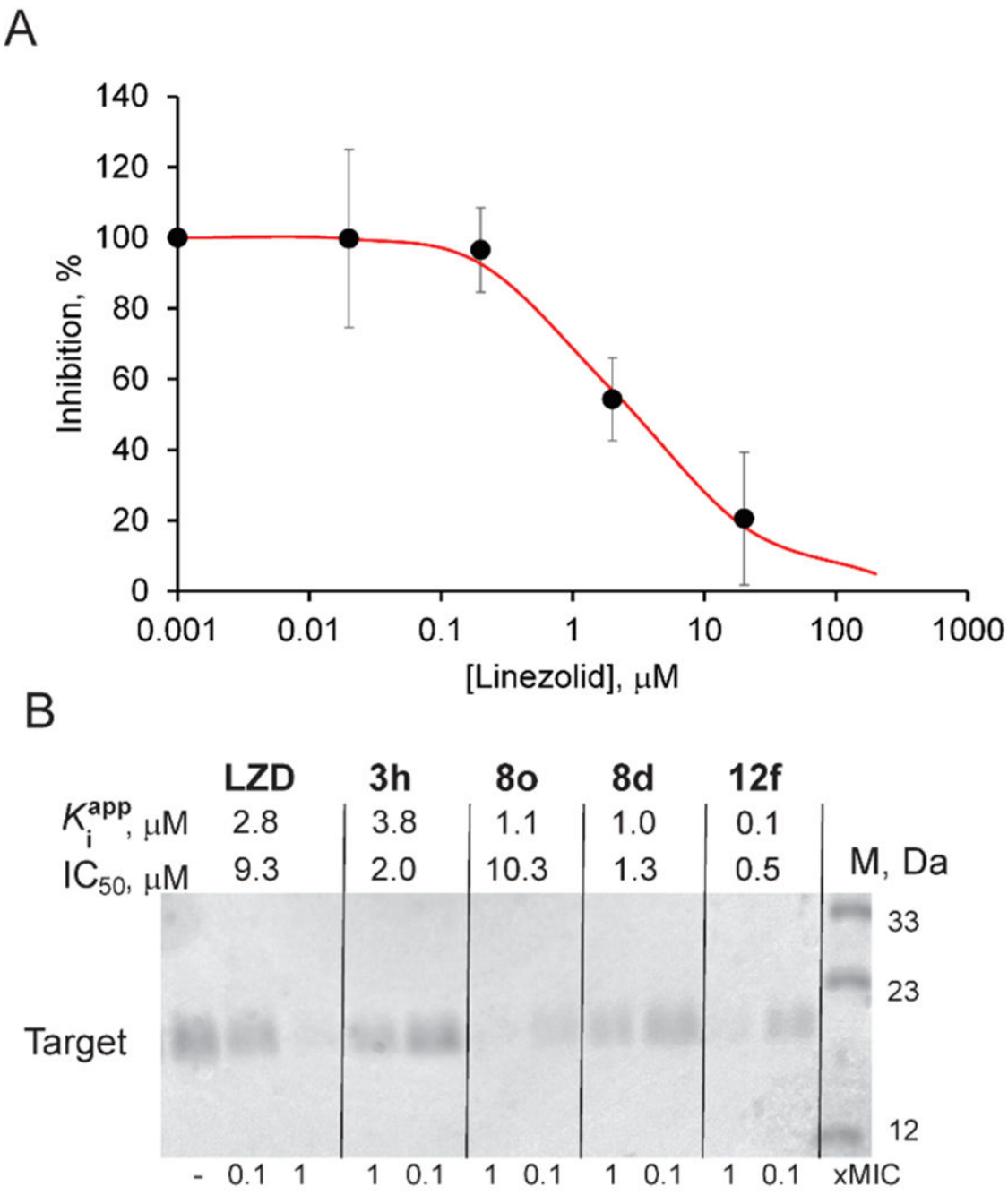

Figure 3.

Effects of oxazolidinones on cell-free coupled transcription–translation in *E. coli*. A. Increasing concentrations of linezolid were added to transcription–translation reaction mixtures, and reactions were allowed to proceed for 5 h. To quantify the amounts of the synthesized protein, the reactions were treated with the Lumio reagent and were resolved on 16% sodium dodecyl sulfate polyacrylamide gel electrophoresis (SDS-PAGE). Fluorescent bands corresponding to the target protein were quantified, normalized to the reaction that lacked the antibiotic, and plotted as a function of the antibiotic concentration. Error bars:

standard deviation (SD) ($n = 3$). B. The same as in panel A but reactions were set with the indicated compounds at concentrations corresponding to their 1× and 0.1× MICs. The K_I^{app} values were calculated as in panel A and shown on top of the gel image along with IC_{50} values, as determined in bacterial growth inhibition assays. M, protein size marker in kDa.

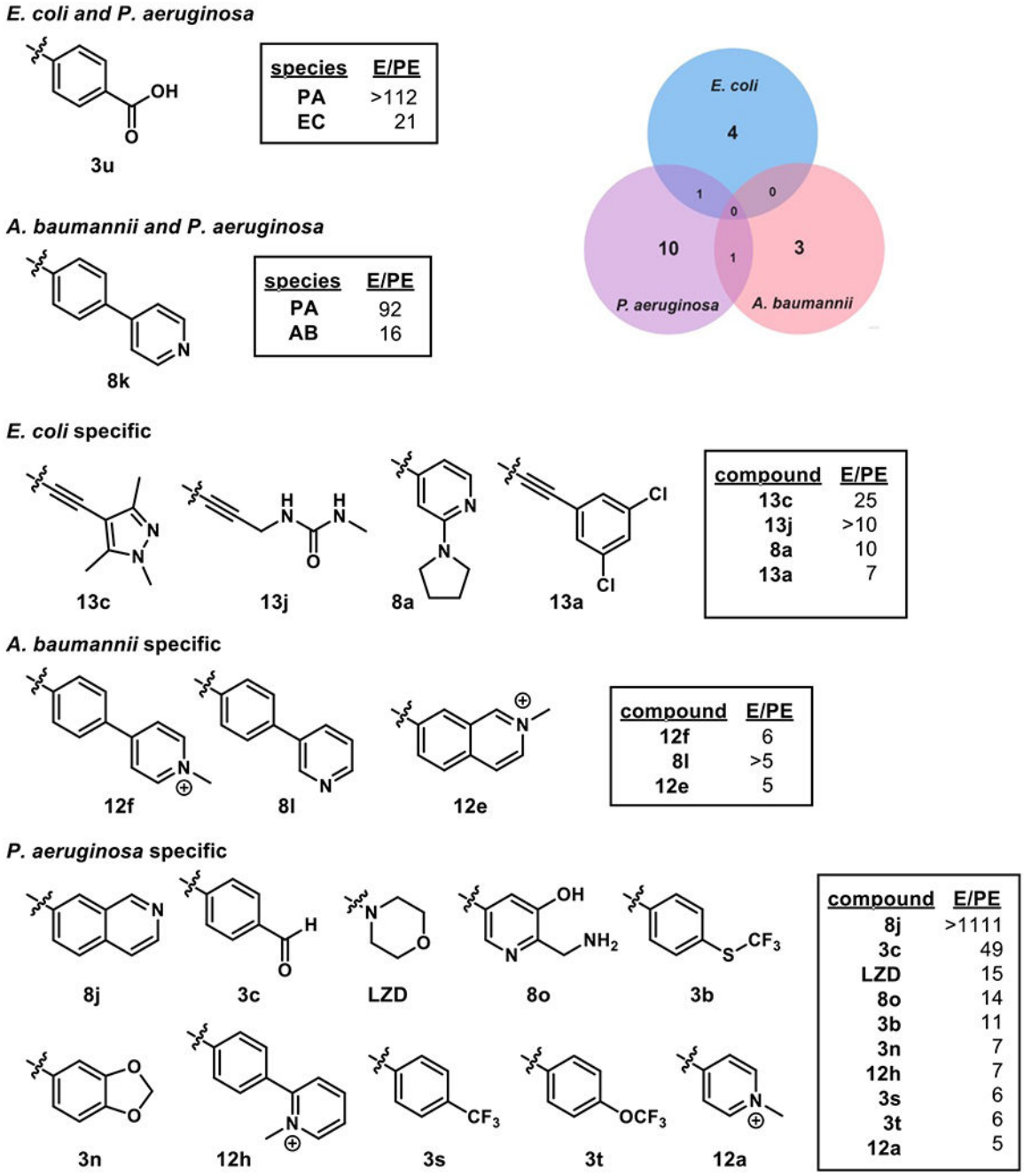

Figure 4.

Motifs identified as liabilities to OM permeation. *E*/PE = Δ/ΔPore IC_{50} ratio for the indicated species.

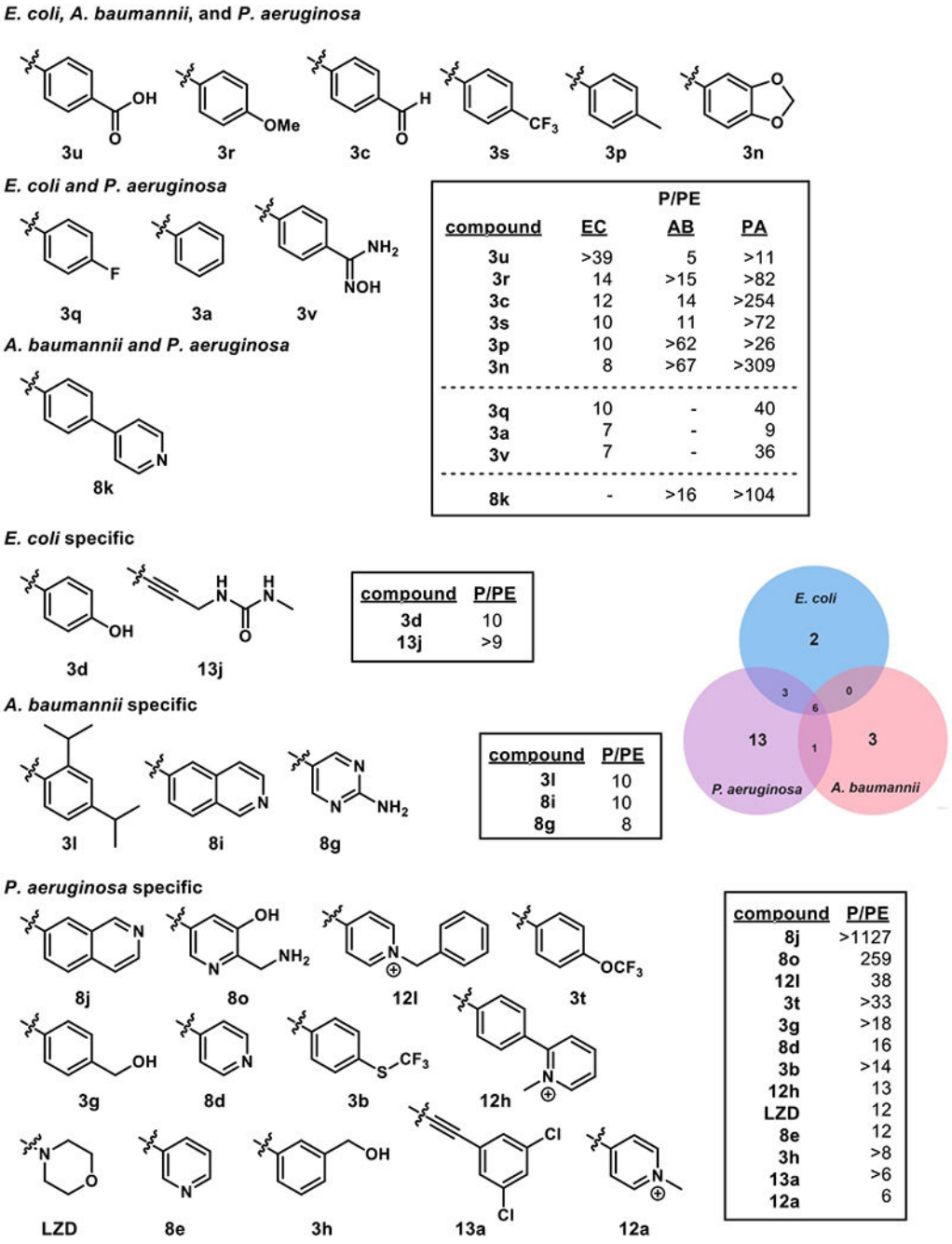

compound	P/PE EC	AB	PA
3u	>39	5	>11
3r	14	>15	>82
3c	12	14	>254
3s	10	11	>72
3p	10	>62	>26
3n	8	>67	>309
3q	10	-	40
3a	7	-	9
3v	7	-	36
8k	-	>16	>104

compound	P/PE
3d	10
13j	>9

compound	P/PE
3l	10
8i	10
8g	8

compound	P/PE
8j	>1127
8o	259
12l	38
3t	>33
3g	>18
8d	16
3b	>14
12h	13
LZD	12
8e	12
3h	>8
13a	>6
12a	6

Figure 5.

Motifs identified as liabilities to efflux susceptibility. *P*/PE = Pore/ΔPore IC_{50} ratio for the indicated species.

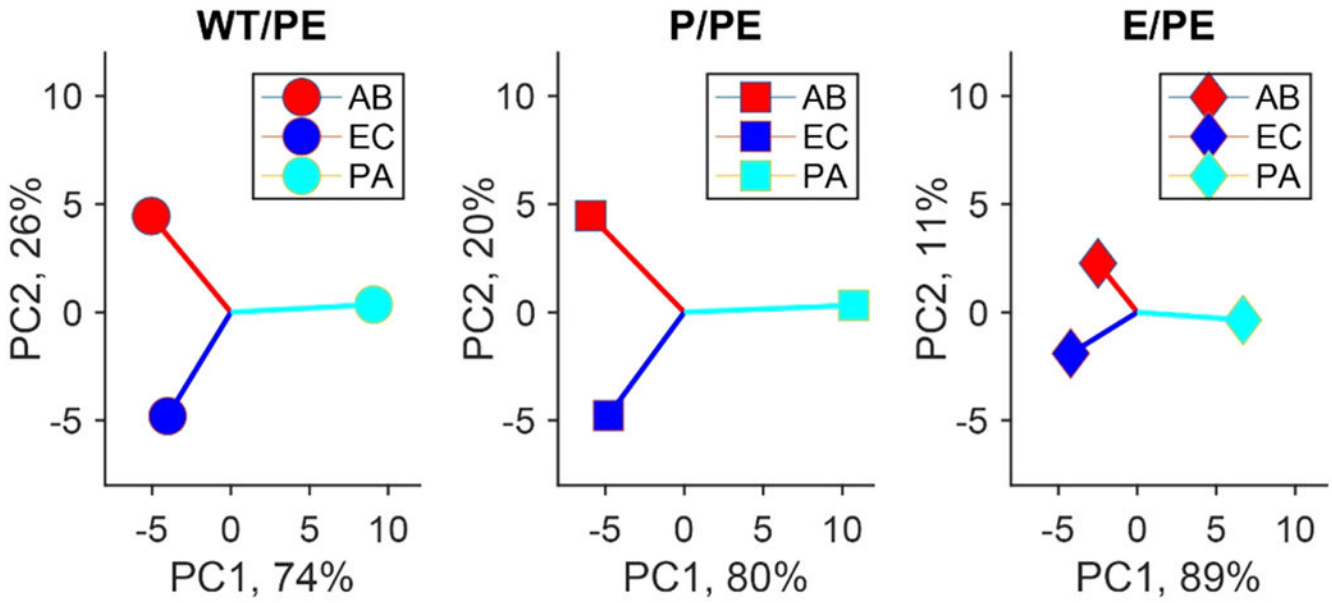

Figure 6.

Principal component analysis of the three permeation ratios in *A. baumannii* (AB), *E. coli* (EC), and *P. aeruginosa* (PA).

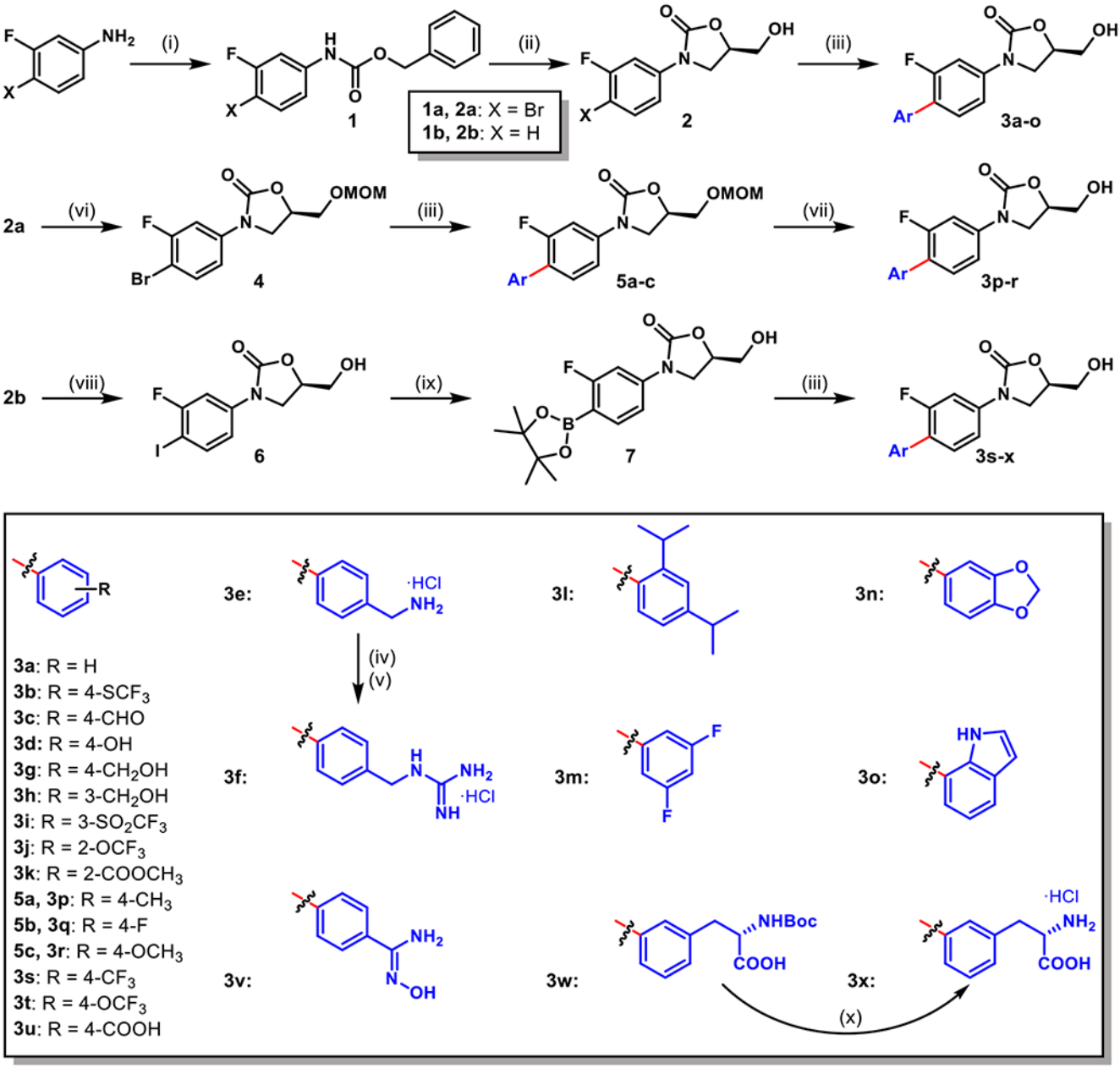

Scheme 1. General Synthetic Approach for Substituted Phenyl C-Ring Derivatives 3a–x[a]

*a*Reagents and reaction conditions: (i) for **1a**: benzyl chloroformate, $NaHCO_3$, tetrahydrofuran (THF), 25 °C, 16 h, 91%; for **1b**: benzyl chloroformate, $NaHCO_3$, THF, 0 °C, 3 h, 99%; (ii) (*R*)-(–)-glycidyl butyrate, LHMDS (1 M in THF), THF, −78 °C to 25 °C, N_2, 16–20 h, 70–76%; (iii) aryl boronic acid/ester or aryl bromide, Pd(dppf)CI_2·dichloromethane (DCM), K_2CO_3, dioxane/H_2O (v/v = 9:1), 90 °C, N_2, 3 h, 11–98%; (iv) *N,N*′-di-Boc-1*H*-pyrazole-1-carboxamidine, *N,N*-diisopropylethylamine (DIPEA), THF, 60 °C, 3 h, 26%; (v) HCI/dioxane (4 M), 50 °C, 30 min, 56%; (vi) methyl chloromethyl ether, DIPEA, DCM, 25 °C, 5 h, 85%; (vii) HCI/dioxane (4 M), 25 °C, 1 h, 50–100%; (viii) *N*-iodosuccinimide, trifluoroacetic acid (TFA), 25 °C, 2 h, 77%; (ix)

bis(pinacolato)diboron, Pd(dppf)CI_2·DCM, KOAc, DMSO, 80 °C, N_2,16 h, 49%; and (x) HCI/dioxane (4 M), 25 °C, 30 min, 91%.

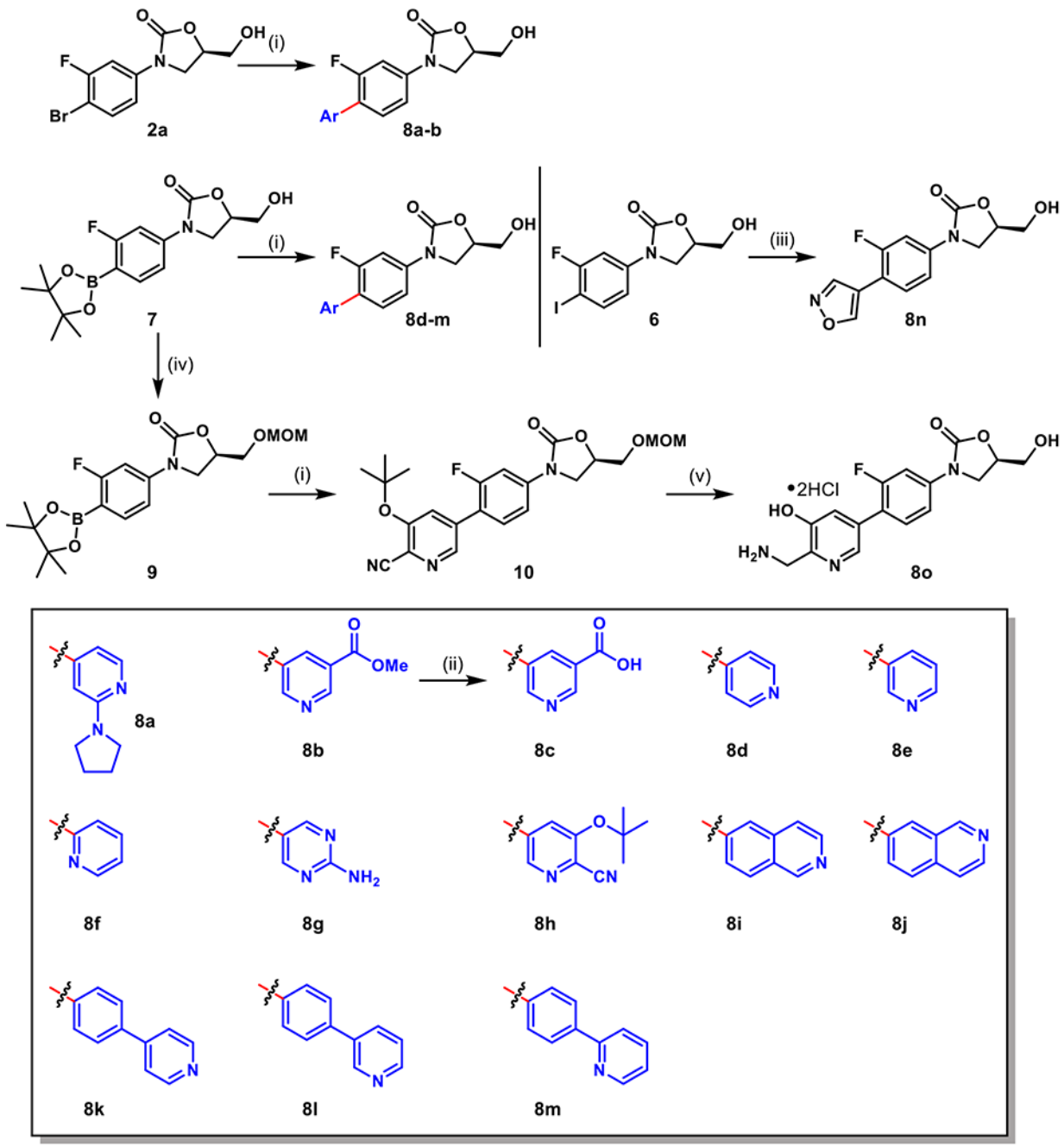

Scheme 2. General Synthetic Approach for Substituted Pyridyl C-Ring Derivatives 8a–o[a]

*a*Reagents and reaction conditions: (i) aryl boronic acid/ester or aryl bromide, Pd(dppf)CI_2·DCM, K_2CO_3, dioxane/H_2O (v/v = 9:1), 90 °C, N_2, 3 h, 38–90%; for compound **8g**, 2-amino-5-iodopyrimidine, Pd(dppf)CI_2·DCM, Na_2CO_3, dioxane/H_2O (v/v = 9:1), 130 °C, N_2, 2.5 h, 20%; (ii) LiOH·H_2O, THF/MeOH/H_2O (v/v/v = 3:1:1), 25 °C, 1 h, 56%; (iii) isoxazole-4-ylboronic acid, Pd(dppf)CI_2·DCM, K_3PO_4·H_2O, THF/H_2O (v/v = 4:1), 80 °C, 16 h, 50%; (iv) methyl chloromethyl ether, DIPEA, DCM, 25 °C, 1 h, 58%; (v)

(a) $NiCI_2 \cdot 6H_2O$, $NaBH_4$, Boc_2O, MeOH, 25 °C, 16 h, 52%; and (b) TFA, DCM, 40 °C, 1 h, 66%.

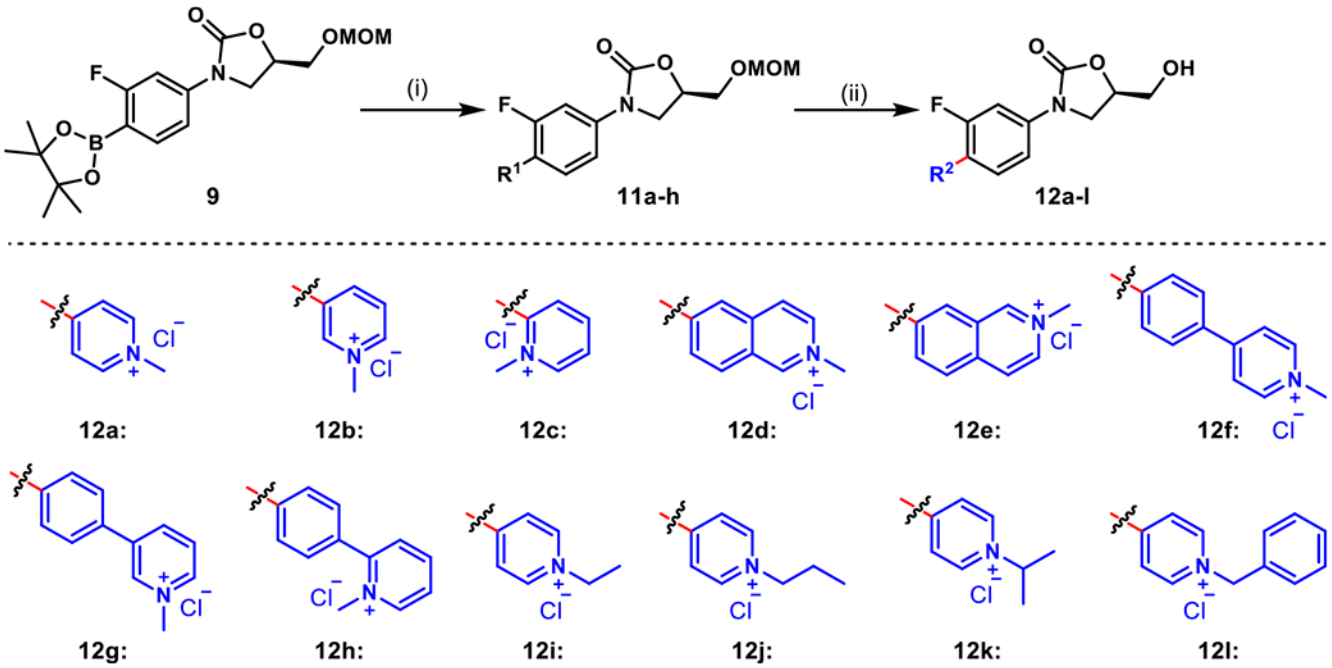

Scheme 3. General Synthetic Approach for Substituted Pyridinium C-Ring Derivatives 12a–l[a]

*a*Reagents and reaction conditions: (i) aryl bromide, Pd(dppf)CI_2·DCM, K_2CO_3, dioxane/H_2O (v/v = 9:1), 90 °C, N_2, 3 h, 73–90%; (ii) (a) haloalkane, CH_3CN, 80 °C, 24 h; and (b) HCI/dioxane (4 M), 25 °C, 1 h, 14–65%.

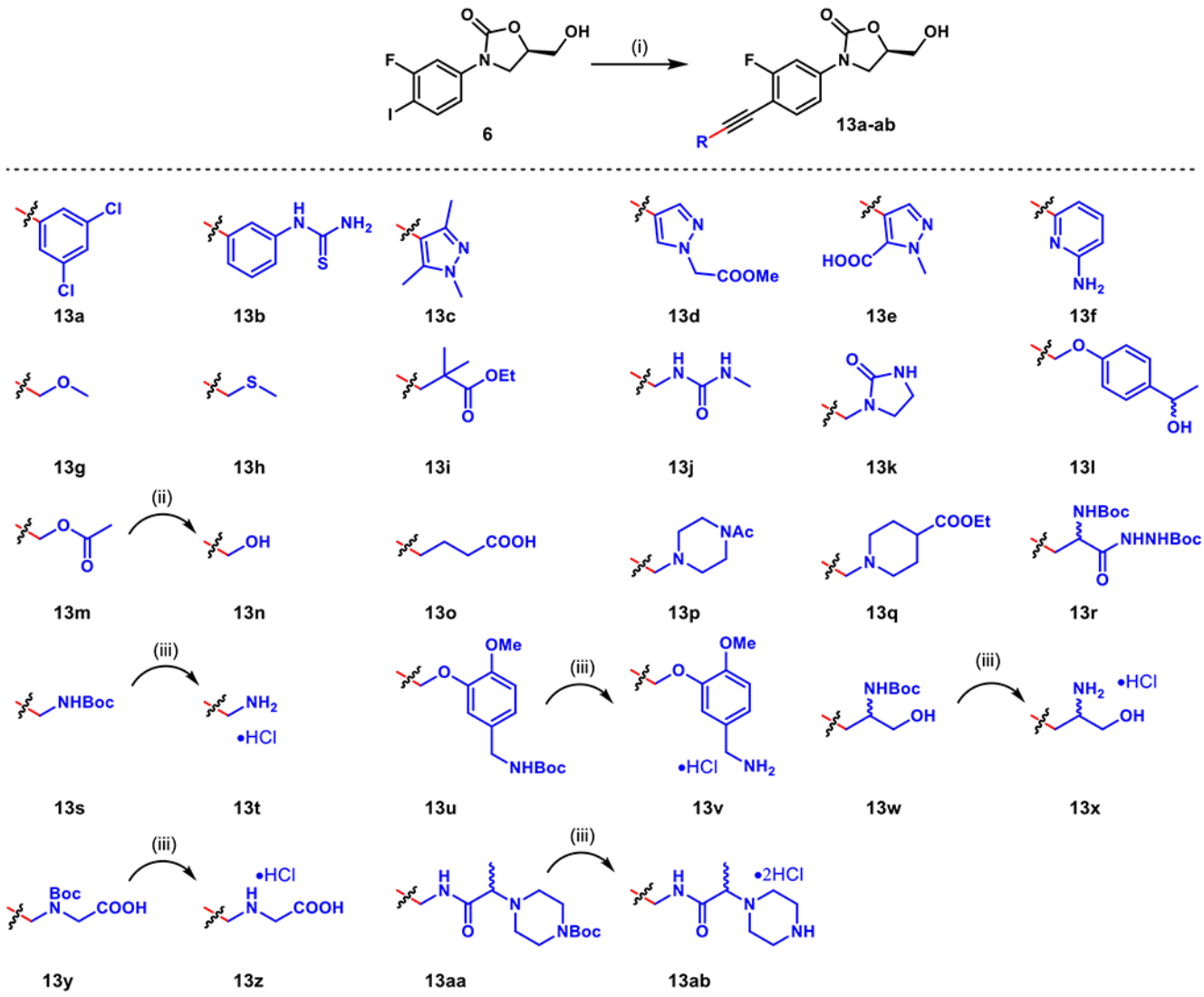

Scheme 4. General Synthetic Approach for Substituted Akynyl Derivatives 13a–ab[a]

*a*Reagents and reaction conditions: (i) alkyne, $Pd(PPh_3)_4$, Cul, DIPEA, *N,N*-dimethyl formamide (DMF), N_2, 25 °C, 16 h, 22–89%; (ii) $LiOH{\cdot}H_2O$, THF/MeOH/H_2O (v/v/v = 3:1:1), 25 °C, 1 h, 47%; and (iii) TFA, DCM, 25 °C, 1 h, 40–91%.

Table 1.

IC_{50} Values of Substituted Phenyl C-Ring Derivatives in the M9-MOPS Medium[a]

compound	ABWT	AB Pore	AB Δ	AB ΔPore	ECWT	EC Pore	EC Δ	EC ΔPore	PAWT	PA Pore	PA Δ	PA ΔPore
3e	54.5	14.3	17.7	8.2	18.1	2.6	1.7	2.6	23.0	26.3	3.3	8.1
3a	18.4	5.5	2.3	1.9	18.4	2.0	0.4	0.3	>100	13.1	2.3	1.4
3n	>100	>100	2.4	1.5	23.0	2.4	0.3	0.3	>100	>100	2.4	0.3
3r	>100	>100	0.7	0.6	23.3	3.4	0.2	0.3	>100	>100	0.7	1.2
3p	>100	>100	2.3	1.6	28.0	3.2	0.3	0.3	>100	>100	2.3	3.8
3b	63.5	23.5	9.1	8.1	35.1	9.4	6.9	4.9	>100	>100	78.2	6.9
3j	>100	59.1	33.2	24.8	42.6	46.3	9.3	21.9	>100	>100	75.6	29.9
3v	22.1	2.8	1.2	0.9	55.9	7.5	0.6	1.0	>100	63.6	5.1	1.8
3c	18.4	16.9	1.1	1.2	66.8	5.0	0.6	0.5	>100	5.9	1.1	0.02
3h	45.8	10.8	5.4	7.6	66.9	1.5	1.5	2.0	>100	>100	15.5	13.0
3g	45.3	5.7	4.4	4.6	67.9	17.6	3.9	3.7	>100	>100	5.3	5.5
3o	>100	>100	64.4	62.1	77.0	19.5	21.6	7.2	>100	>100	>100	>100
3s	>100	41.1	8.0	3.9	88.8	35.3	4.1	2.9	>100	>100	8.0	1.4
3q	>100	89.8	8.8	9.7	89.1	22.8	4.3	2.3	>100	89.8	8.8	2.2
3k	>100	>100	>100	>100	96.0	61.5	64.6	39.7	>100	>100	>100	>100
3l	>100	77.9	17.3	8.2	99.1	20.4	15.9	6.6	>100	>100	49.0	22.3
3d	>100	12.9	8.4	7.3	>100	22.1	2.0	2.3	>100	27.7	8.4	5.8
3u	>100	55.5	12.8	10.2	>100	>100	54.0	2.6	>100	>100	>100	8.9
3i	>100	>100	48.8	38.5	>100	21.2	19.3	12.5	>100	>100	>100	>100
3t	>100	25.6	16.3	6.4	>100	76.9	17.2	18.8	>100	>100	18.6	3.1
3f	>100	65.9	67.8	32.5	>100	56.1	63.8	55.7	>100	>100	12.0	25.7
3m	>100	>100	>100	>100	>100	>100	>100	>100	>100	>100	>100	>100
3w	>100	>100	>100	>100	>100	>100	>100	>100	>100	>100	>100	>100
3x	>100	>100	>100	>100	>100	>100	>100	>100	>100	>100	>100	>100
Linezolid	33.4	9.2	4.9	4.0	>100	18.0	8.7	9.3	>100	19.8	24.7	1.7

[a]Arranged in order of potency against ECWT. All values are reported in μM.

Table 2.

IC_{50} Values of Substituted Pyridyl C-Ring Derivatives in the M9-MOPS Medium[a]

compound	ABWT	AB Pore	AB Δ	AB ΔPore	ECWT	EC Pore	EC Δ	EC ΔPore	PAWT	PA Pore	PA Δ	PA ΔPore
8d	16.5	4.1	1.4	2.2	44.3	5.6	0.8	1.3	44.2	48.2	8.1	2.9
8o	37.6	5.8	15.4	6.3	66.1	23.3	10.0	10.3	55.9	40.8	2.2	0.2
8m	35.3	15.8	21.5	22.6	76.2	47.2	55.6	55.2	>100	>100	>100	>100
8g	>100	>100	53.0	13.6	>100	2.0	5.9	1.5	>100	>100	>100	33.0
8a	71.9	40.4	72.4	49.1	>100	4.0	15.4	1.5	>100	>100	>100	>100
8b	83.2	28.1	12.1	11.3	>100	4.7	2.7	2.2	>100	>100	32.9	38.7
8e	19.0	5.2	4.3	3.5	>100	14.5	2.8	3.2	>100	75.3	4.7	6.0
8n	>100	39.0	83.4	73.1	>100	56.1	23.6	30.6	>100	>100	22.7	32.9
8c	>100	>100	>100	>100	>100	>100	>100	42.2	>100	>100	>100	>100
8k	>100	>100	>100	6.2	>100	>100	>100	75.2	>100	>100	92.1	1.0
8f	>100	>100	>100	>100	>100	>100	76.8	79.6	>100	>100	64.2	47.4
8i	>100	35.3	5.6	3.4	>100	>100	>100	>100	>100	>100	67.7	37.9
8j	>100	>100	>100	>100	>100	>100	>100	>100	>100	>100	>100	0.1
8l	>100	59.4	>100	20.4	>100	>100	>100	>100	>100	>100	>100	>100
8h	>100	>100	>100	>100	>100	>100	>100	>100	>100	>100	>100	>100
Linezolid	33.4	9.2	4.9	4.0	>100	18.0	8.7	9.3	>100	19.8	24.7	1.7

[a]Arranged in order of potency against ECWT. All values are reported in μM.

Table 3.

IC_{50} Values of Substituted Pyridinium C-Ring Derivatives in the M9-MOPS Medium[a]

compound	ABWT	AB Pore	AB Δ	AB Δ Pore	ECWT	EC Pore	EC Δ	EC ΔPore	PAWT	PA Pore	PA Δ	PA ΔPore
12a	59.4	13.8	23.3	13.8	13.5	12.3	10.0	11.0	>100	59.7	48.8	9.4
12f	>100	10.0	64.0	10.8	15.4	1.7	0.5	0.5	>100	>100	>100	>100
12i	>100	>100	>100	38.5	43.8	36.0	13.7	15.9	>100	>100	57.4	42.3
12j	>100	19.8	89.7	19.8	43.9	28.3	12.7	16.6	>100	>100	>100	>100
12l	>100	15.6	23.4	13.0	51.6	23.3	15.5	15.6	>100	41.7	4.6	1.1
12d	>100	20.1	29.7	27.9	63.6	30.0	4.0	11.4	>100	>100	>100	>100
12h	>100	13.3	20.4	10.2	72.6	13.2	3.1	4.4	>100	15.9	8.4	1.2
12k	89.5	22.0	34.5	22.3	81.6	42.8	16.9	16.6	>100	>100	35.1	36.6
12g	>100	13.9	29.7	12.6	98.4	7.8	1.2	2.1	>100	28.1	29.7	18.1
12e	>100	27.4	48.6	9.4	>100	21.0	5.6	9.6	>100	>100	>100	>100
12c	>100	>100	>100	33.3	>100	>100	72.3	60.4	>100	>100	>100	40.4
12b	>100	>100	>100	>100	>100	>100	70.6	88.8	>100	>100	>100	>100
Linezolid	33.4	9.2	4.9	4.0	>100	18.0	8.7	9.3	>100	19.8	24.7	1.7

[a]Arranged in order of potency against ECWT. All values are reported in μM.

Table 4.

IC_{50} Values of Substituted Alkynyl Derivatives in the M9-MOPS Medium[a]

compound	ABWT	AB Pore	AB Δ	AB ΔPore	ECWT	EC Pore	EC Δ	EC ΔPore	PAWT	PA Pore	PA Δ	PA ΔPore
13f	>100	49.8	83.9	76.7	59.0	19.2	34.2	20.5	>100	>100	>100	>100
13l	>100	>100	61.9	34.7	62.4	24.7	30.2	13.5	>100	>100	>100	91.3
13a	>100	>100	>100	>100	74.8	12.8	26.1	3.6	>100	>100	64.9	16.2
13g	>100	>100	>100	>100	74.9	36.3	80.3	44.0	>100	>100	>100	>100
13h	>100	>100	>100	>100	94.9	35.1	65.9	47.8	>100	>100	>100	>100
13c	>100	>100	>100	>100	>100	1.2	86.3	3.4	>100	>100	>100	>100
13j	>100	>100	>100	>100	>100	>100	>100	11.2	>100	>100	>100	>100
13i	>100	60.3	44.0	30.3	>100	65.3	17.8	21.9	>100	>100	>100	30.1
13d	>100	>100	>100	62.0	>100	52.3	88.7	36.6	>100	>100	>100	>100
13k	>100	>100	>100	>100	>100	>100	64.3	39.0	>100	>100	>100	>100
13m	>100	>100	>100	>100	>100	44.4	72.4	39.7	>100	>100	>100	>100
13n	>100	>100	>100	>100	>100	>100	84.0	43.6	>100	>100	>100	>100
13u	>100	42.4	72.2	28.7	>100	>100	42.9	44.4	>100	>100	>100	46.9
13r	>100	>100	>100	>100	>100	51.4	13.3	56.1	>100	>100	>100	>100
13aa	>100	>100	>100	>100	>100	>100	50.9	62.6	>100	>100	>100	>100
13b	>100	>100	>100	>100	>100	>100	85.0	64.5	>100	>100	>100	>100
13s	>100	>100	>100	>100	>100	74.3	83.4	64.7	>100	>100	>100	>100
13w	>100	>100	>100	>100	>100	97.3	72.6	67.8	>100	>100	>100	>100
13e	>100	61.3	88.2	89.5	>100	>100	>100	>100	>100	>100	>100	>100
13p	>100	>100	>100	>100	>100	>100	>100	>100	>100	>100	>100	>100
13q	>100	>100	>100	>100	>100	>100	>100	>100	>100	>100	>100	>100
13o	>100	>100	>100	>100	>100	>100	>100	>100	>100	>100	>100	>100
13ab	>100	>100	>100	>100	>100	>100	>100	>100	>100	>100	>100	>100
13x	>100	>100	>100	>100	>100	>100	>100	>100	>100	>100	>100	>100
13y	> >100	>100	>100	>100	>100	>100	>100	>100	>100	>100	>100	>100
13z	>100	>100	>100	>100	>100	>100	>100	>100	>100	>100	>100	>100
13t	>100	>100	>100	>100	>100	>100	>100	>100	>100	>100	>100	>100
13v	>100	>100	>100	>100	>100	>100	>100	>100	>100	>100	>100	>100

J Med Chem. Author manuscript; available in PMC 2023 October 27.

compound	ABWT	AB Pore	AB Δ	AB ΔPore	ECWT	EC Pore	EC Δ	EC ΔPore	PAWT	PA Pore	PA Δ	PA ΔPore
Linezolid	33.4	9.2	4.9	4.0	>100	18.0	8.7	9.3	>100	19.8	24.7	1.7

[a] Arranged in order of potency against ECWT. All values are reported in μM.

Table 5.

MICs of Select Oxazolidinone Analogues in LB Medium[a]

compound	AB ΔPore	EC ΔPore	PA ΔPore	*S. aureus* ATCC 25923	SQ110	SQ110 DTC	SQ110 DTC G2032A	SQ110 DTC C2610A
8o	25	50	6.25	12.5	>100	25	100	50
3s	6.25	>100	100	3.12	>100	25	>100	>100
3t	25	>100	100	6.25	>100	100	>100	>100
3u	50	12.5	>100	6.25	>100	25	50	25
8d	6.25	6.25	3.125	1.56	>100	6.25	25	6.25
8e	12.5	25	6.25	1.56	>100	12.5	50	25
8g	50	100	12.5	6.25	>100	25	100	50
12a	100	100	100	>100	100	50	>100	100
12f	50	12.5	12.5	12.5	>100	3.12	25	12.5
12g	25	25	25	12.5	>100	12.5	50	25
3e	25	100	12.5	6.25	>100	50	100	50
3g	12.5	25	6.25	1.56	>100	12.5	50	25
Linezolid	25	25	12.5	6.25	>100	25	>100	50

[a]All values are reported in μM.

Table 6.

MICs of Select Oxazolidinone Analogues in MHI and M9-MOPS Media[a]

strain	medium	LZD	3h	3e	8o	8e	8d	12f
AB AYE	MHI	>200	>200	>200	>200	>200	>200	>200
	M9-MOPS	**200**	**200**	>200	>200	**100**	**100**	>200
AB Ab5075	MHI	>200	>200	>200	>200	>200	>200	>200
	M9-MOPS	≥200	**200**	>200	>200	**100**	**100**	**200**
PA BAA 2108	MHI	>200	>200	>200	>200	>200	>200	>200
	M9-MOPS	>200	>200	>200	>200	>200	≥200	>200
PA BAA 2109	MHI	>200	>200	>200	>200	>200	>200	>200
	M9-MOPS	>200	>200	>200	>200	>200	>200	>200
K. pneumoniae ATCC13883	MHI	>200	>200	>200	>200	>200	200	>200
	M9-MOPS	≥200	**200**	**100–200**	**50–100**	**200**	**100–200**	**100**
K. pneumoniae ATCC43816	MHI	>200	>200	>200	>200	>200	>200	>200
	M9-MOPS	>200	>200	**200**	**100**	>200	**200**	>200
K. aerogenes ATCC13048	MHI	>200	>200	>200	**200**	>200	**200**	>200
	M9-MOPS	>200	>200	**100**	**12.5**	**200**	**200**	**50**

[a]All values are reported in μM.